

STATUS OF THESIS

Title of thesis

THE DEVELOPMENT OF CYLINDRICAL DIELECTRIC
RESONATOR ANTENNA ARRAY

I, AFFAN AZIZ BABA

hereby allow my thesis to be placed at the Information Resource Center (IRC) of
Universiti Teknologi PETRONAS (UTP) with the following conditions:

1. The thesis becomes the property of UTP
2. The IRC of UTP may make copies of the thesis for academic purposes only.
3. This thesis is classified as

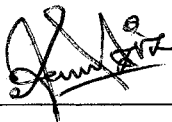
☐ Confidential

☒ Non-confidential

If this thesis is confidential, please state the reason:

The contents of the thesis will remain confidential for _____ years.

Remarks on disclosure:



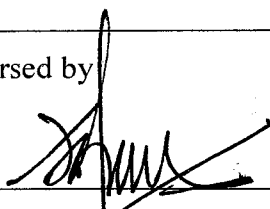
Signature of Author

Permanent address:

House # 150, Mohalla Pakistani Jalal Pur
Jattan, Gujrat, Pakistan

Date : 30/9/13

Endorsed by



Signature of Supervisor

Name of Supervisor

Mr. Mohd. Azman B. Zakariya

Department of Electrical And
Electronics Engineering.

Universiti Teknologi PETRONAS.

Date: 30/9/13

UNIVERSITI TEKNOLOGI PETRONAS

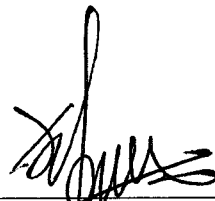
THE DEVELOPMENT OF CYLINDRICAL DIELECTRIC RESONATOR ANTENNA
ARRAY

by

AFFAN AZIZ BABA

The undersigned certify that they have read, and recommend to the Postgraduate Studies Program for acceptance this thesis for the fulfillment of the requirements for the degree stated.

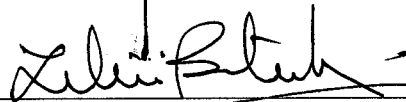
Signature:



Main Supervisor:

Mr Mohd. Azman B. Zakariya


Signature:



Co-Supervisor:

Dr. Zuhairi B Hj Baharudin


Signature:



Co-Supervisor:

Dr. M. Haris B Md Khis Assoc Prof Dr Fawnizu Azmadi B Hussin

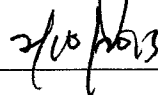
Signature:

 Deputy Head
Electrical & Electronic Engineering Department
Universiti Teknologi PETRONAS

Head of Department:

 Assoc. Prof. Dr. Rosdiazli B Ibrahim

Date:



THE DEVELOPMENT OF CYLINDRICAL DIELECTRIC RESONATOR
ANTENNA ARRAY

by

AFFAN AZIZ BABA

A Thesis

Submitted to the Postgraduate Studies Program
as a Requirement for the Degree of

MASTERS BY RESEARCH
ELECTRICAL AND ELECTRONIC ENGINEERING
UNIVERSITI TEKNOLOGI PETRONAS
BANDAR SERI ISKANDAR
PERAK, MALAYSIA

SEPTEMBER 2013

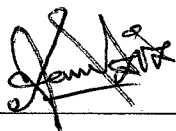
DECLARATION OF THESIS

Title of thesis

THE DEVELOPMENT OF CYLINDRICAL DIELECTRIC
RESONATOR ANTENNA ARRAY

I, AFFAN AZIZ BABA
hereby declare that the thesis is based on my original work except for quotations and citations which have been duly acknowledged. I also declare that it has not been previously or concurrently submitted for any other degree at UTP or other institutions.

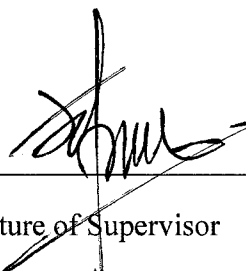
Witnessed by



Signature of Author

Permanent address:

House # 150, Mohalla Pakistani Jalal Pur ,
Jattan, Gujrat Pakistan.



Signature of Supervisor

Mr. Mohd Azman B Zakariya

Date : 30/9/13

Date : 30/9/13

DEDICATION

This thesis is dedicated to my parents, teachers and friends.

ACKNOWLEDGEMENT

All praise is due to ALLAH (SWT), who created a man and taught him what he knew not “Who has taught (the writing) by pen”, and taught man which was not possible without ALLAH’s guidance. May ALLAH grant peace and honor to messenger of Islam Muhammad (PBUH) and his family. I would like to thank Almighty Allah for successful completion of my degree. I express my deep gratitude to my parents for their prayers and moral support.

I would like to thank my supervisor Mr. Azman B Zakariya for his encouragement, kind support and creative suggestion throughout the research work especially during the design selection and preparation of this thesis.

Secondly I specially express my gratitude to my co-supervisor Dr. Zuhairi B Hj Baharudin for sparing his precious time during my publications and thesis writing stage.

Many thanks must go to my co-advisor Dr. Mohd Hairs Md Khir and Mr Adz for his kind support during experiments. Last but not least, I would like to thank all my lab fellows for their continuous support during my master research work. I would also like to thank Universiti Teknologi PETRONAS for their financial support and providing internal grants for smooth running of my activity.

ABSTRACT

In today's communication era, small size, wideband and high gain antennas are the requirement to meet high capacity and efficient long distance communication. In this thesis, experimental study on linear aperture and mutual coupled cylindrical dielectric resonator antenna (CDRA) arrays for ISM band has been presented. The antennas presented possess properties of small size, wideband, high gain, low back side radiation and good front to back ratio.

The three antenna arrays presented in the thesis are single band, dual band and small size high gain CDRA arrays. The antenna arrays have been designed on the basis of a single element aperture coupled CDRA. In all proposed designs, use similar CDRA's of Calcium Copper Titanium Oxide (CCTO- $\text{CaCu}_3\text{Ti}_4\text{O}_{12}$) material with $\epsilon_r = 55$. The aperture and mutual coupling mechanisms are used to excite the radiating elements. The top and bottom radiating elements are excited through coupling slots etched on the ground plane, while the middle radiating element is excited through the two elements by its side. The 50Ω microstrip feed line is used to excite the coupling slots. Computer Simulation Technology (CST) microwave studio is used for the array antenna simulation.

The single band array antenna is excited through the microstrip line of width 2.33 mm, designed on Rogers RT/Duroid 5880 substrate with $\epsilon_{s1} = 2.2$. The corresponding achieved bandwidth and gain are 1.023 GHz from 4.6-5.623 GHz and 9.4 dBi respectively. Secondly, dual band and small size array antennas are excited through the microstrip line of width 2.6 mm, designed on an Flame Retardant (FR4) substrate with $\epsilon_{s2} = 4.9$. The dual band design achieved bandwidths of 2.48-2.51 GHz for lower band and 5.0-5.21 GHz for upper band with gains of 5.7 and 9.6 dBi respectively. Finally, the small size antenna array obtained bandwidth of 1.076 GHz from 4.536-5.612 GHz with 10.5 dBi gain. In addition to CST design, the equivalent lumped element circuit of the small size array antenna is modeled to verify the antenna feasibility by using Advanced Design System (ADS) software. The impedance bandwidths obtained through the CST (i.e., 1.076 GHz) and ADS (i.e., 1.0 GHz) are in good agreement. The advantages of using two slots and mutual coupling to excite three elements in terms of improvement in the impedance bandwidth and the reduction in the back side radiation are also presented.

The three designed array antennas: single band, dual band and small size high gain are fabricated. Their corresponding achieved impedance bandwidths are 1.08 GHz (4.75-5.83 GHz, for single band array), 0.1 GHz (2.42-2.52 GHz, lower band of the dual band array), 1.04 GHz (4.40- 5.44 GHz, upper band of the dual band array) and 1.2 GHz (4.9-6.0 GHz, for small size) respectively. The measured gain of the fabricated antenna prototypes is around 10.0 dBi, fulfilled the requirement for indoor and outdoor wireless local area network (WLAN) application.

ABSTRAK

Pada era komunikasi semasa, antenna bersaiz kecil, jalur lebar dan antenna kuasa tinggi merupakan satu keperluan untuk mencapai komunikasi jarak jauh yang efektif dan berkapasiti tinggi. Di dalam kertas kerja ini, kajian terhadap aperture linear dan ditambah bersama susunan antenna resonator dielektrik berbentuk silinder untuk 'ISM band' telah dilakukan. Antenna yang di gunakan terdiri dari saiz kecil, jalur lebar, kuasa tinggi, sisi belakang radiasi yang rendah dan baik untuk nisbah hadapan dengan belakang.

Susunan tiga antenna yang dibincangkan di dalam kertas kerja ini merupakan satu jalur, dua jalur dan susunan antenna resonator dielektrik berbentuk silinder kecil yang berkuasa tinggi. Susunan antenna ini direka berdasarkan unsur tunggal aperture yang ditambah antenna resonator dielektrik berbentuk silinder. Semua cadangan yang diberikan menggunakan antenna resonator dielektrik berbentuk silinder yang sama daripada bahan 'Calcium Copper Titanium Oxide' (CCTO- $\text{CaCu}_3\text{Ti}_4\text{O}_{12}$) iaitu $\epsilon_r = 55$. Gandingan aperture dan mutual digunakan untuk merangsang unsur radiasi. Unsur radiasi di bahagian atas dan bawah terangsang melalui gandingan slot yang di sambung pada plat tanah di mana di bahagian tengah pula unsur radiasi dirangsang melalui dua unsur yang terletak di lokasi berkenaan. $50\ \Omega$ talian suapan mikrostrip yang di gunakan untuk merangsang gandingan slot. Studio gelombang mikro "Computer Simulation Technology" (CST) digunakan untuk simulasi susunan antenna.

Antenna satu jalur terangsang melalui talian mikrostrip yang lebarnya 2.33 mm, dimana ia direka di "Rogers RT/Duroid 5880 substrate" dengan $\epsilon_{s1} = 2.2$. Jalur lebar dan gandaan yang perlu di perolehi adalah 1.023 GHz iaitu daripada 4.6-5.623 GHz dan 9.4 dBi. Seterusnya, dua jalur dan susunan saiz kecil antenna juga dirangsang melalui talian mikrostrip iaitu lebarnya 2.6 mm yang direka bentuk di "Flame Retardant (FR4) substrate" dengan $\epsilon_{s2} = 4.9$. Rekaan dua jalur mencapai jalur lebar di antara 2.48-2.51 GHz untuk jalur rendah dan 5.0-5.21 GHz untuk jalur tinggi dengan gandaan 5.7 dan 9.6 dBi masing-masing. Susunan antenna bersaiz kecil pula mencapai jalur lebar 1.076 GHz dimana dari 4.536-5.612 GHz dengan gandaan 10.5 dBi. Sebagai penambahan rekaan CST, unsur litar setara sekaligus dengan susunan antenna bersaiz kecil di reka untuk

menguji keberkesanan antenna dengan menggunakan perisian “Advanced Design System” (ADS). Rintangan jalur lebar di perolehi melalui CST (cth : 1.076 GHz) dan ADS (cth: 1.0 GHz) berada dalam keadaan yang baik. Kelebihan menggunakan dua slot gandingan bersama adalah untuk merangsang tiga unsur dimana untuk memperbaiki rintangan jalur lebar dan pengurangan radiasi pada bahagian belakang antenna turut di bincangkan.

Tiga susunan antenna yang direka: satu jalur, dua jalur dan juga antenna kecil yang mempunyai gandaan tinggi di pasang pada litar. Rintangan jalur lebar masing-masing adalah 1.08 GHz (4.75-5.83 GHz, untuk susunan satu jalur), 0.1 GHz (2.42-2.52 GHz, susunan dua jalur) yang mempunyai jalur rendah 1.04 GHz (4.40-5.44 GHz, susunan dua jalur yang mempunyai jalur tinggi) dan 1.2 GHz (4.9-6.0 GHz, untuk saiz kecil). Gandaan yang dikira dari pasangan prototaip antenna dalam lingkungan 10.0 dBi, dimana ia memenuhi keperluan aplikasi rangkaian kawasan tempatan wayarles di dalam bangunan dan luar bangunan.

In compliance with the terms of the Copyright Act 1987 and the IP Policy of the university, the copyright of this thesis has been reassigned by the author to the legal entity of the university,

Institute of Technology PETRONAS Sdn Bhd.

Due acknowledgement shall always be made of the use of any material contained in, or

derived from, this thesis.

© Affan Aziz Baba, 2013

Institute of Technology PETRONAS Sdn Bhd

All rights reserved.

TABLE OF CONTENTS

STATUS OF THESIS	i
DECLARATION OF THESIS	iv
DEDICATION	v
ACKNOWLEDGEMENT	vi
ABSTRACT	vii
ABSTRAK	ix
CHAPTER 1	1
INTRODUCTION.....	1
Importance of Antenna Array in Wireless Communication.....	1
Problem Statement	2
Objectives	3
Scope of Research	4
Thesis Layout	5
CHAPTER 2	6
BACKGROUND THEORY AND LITERATURE REVIEW	6
2.1 Background study of Dielectric Resonator Antenna (DRA)	6
2.2 Types of DRA	8
2.2.1 Rectangular DRA	8
2.2.2 Cylindrical DRA	9
2.3 Coupling Techniques	12
2.3.1 Aperture Coupling	12
2.3.2 Direct Coupling.....	14
2.4 DRA Arrays.....	15
2.4.1 Compact Size and Low Profile DRA Array	15
2.4.2 Linear DRA Array	17
2.4.3 DRA Planar Array.....	19
2.4.4 DRA Reflect Array	21
2.5 Main Array Parameters.....	23
2.5.1 Two Element Antenna Array	24
2.5.2 Effect of Variation in Inter-Element Spacing (d)	26

2.5.3 Effect of Variation in Relative Amplitude of Current Distribution (I_2/I_1)	27
2.5.4 Effect of the Variation of Phase Difference Between the Elements of Antenna Array	28
2.6 Lumped Element Modeling of DRA	30
2.7 Conclusion	34
CHAPTER 3	36
METHODOLOGY	36
3.1 Introduction.....	36
3.2 Array Design Methodology	36
3.3 Characterization of the Single Element CDRA with Aperture Couple Technique	38
3.3.1 Development of Equivalent Lumped Element Circuit for Single Element CDRA.....	41
3.3.2 Fabrication and Measurements of Single Element CDRA	42
3.4 Characterization of the Single Band CDRA Array.....	43
3.4.1 Fabrication and Measurements of Single Band CDRA Array	46
3.5 Characterization of Dual Band CDRA Array	48
3.5.1 Fabrication and Measurements of Dual Band CDRA Array	50
3.6 Characterization of the Small size, Wide Band and High Gain CDRA Array	51
3.6.1 Development of Equivalent Lumped Element Circuit for Small Size CDRA Array	53
3.6.2 Fabrication and Measurements of Small Size CDRA Array	55
3.7 Summary.....	56
CHAPTER 4	57
RESULTS AND DISCUSSION.....	57
4.1 Introduction.....	57
4.2 Results and Discussion of Single Element CDRA	57
4.2.1 Design Verification	58
4.2.2 Parametric Study	59
4.2.2.1 Effects of Slot Length.....	59
4.2.2.2 Effects of Slot Position	60
4.2.3 Antenna Radiation Pattern	62
4.3 Results and Discussion of Single Band CDRA Array	65
4.3.1 Design Verification	65
4.3.2 Parametric Study	66

4.3.2.1 Effects of Inter-slot Distance	66
4.3.2.2 Effects of Slots Length	67
4.3.2.3 Effects of Slots Widths	68
4.3.3 Antenna Radiation Pattern	69
4.3.4 Antenna Gain and Efficiency	72
4.4 Results and Discussion of Dual Band CDRA Array	73
4.4.1 Design Verification	74
4.4.2 Parametric Study	75
4.4.2.1 Effects of Diameter of Top-Loaded Metallic Sheet	75
4.4.2.2 Effects of Slot Width	76
4.4.3 Antenna Radiation Pattern	77
4.4.4 Antenna Gain and Efficiency	80
4.5 Results and Discussion of Small Size CDRA Array	81
4.5.1 Design Verification	81
4.5.2 Parametric study	83
4.5.2.1 Effects of Aperture Slot Length on the Top Radiating Element of Small Size CDRA Array	83
4.5.2.2 Effects of Aperture Slot Length on the Bottom Radiating Element of Small Size CDRA Array	85
4.5.2.3 Effects of Two Slots Lengths on the Bandwidth of Small Size CDRA Array	88
4.5.2.4 Effects of Inter-Slot Distance	91
4.5.2.5 Effects of Inter-element Distance	92
4.5.3 Antenna Radiation Patterns	93
4.5.4 Antenna Gain and Efficiency	97
4.5.5 Advantages and Comparison of Proposed Technique with Literature Work	97
4.6 Summary	99
CHAPTER 5	101
CONCLUSION AND CONTRIBUTION	101
5.1 Conclusion	101
5.2 Contribution	103
5.3 Recommendation and Future Work	104
REFERENCES	106
ACHIVEMENTS	116
Appendix A	118

Appendix B.....	120
Appendix C.....	122
Appendix D.....	128

LIST OF FIGURES

Figure 2.1 Directional radiation pattern	7
Figure 2.2 Omnidirectional radiation pattern	7
Figure 2.3 The geometry of the rectangular shaped dielectric resonator	9
Figure 2.4 The geometry of the cylindrical shaped dielectric resonator	9
Figure 2.5 Geometry of aperture coupled cylindrical DRA	12
Figure 2.6 Microstrip Line Coupled DRA	14
Figure 2.7 Examples of (a) Low profile DRAs (b) Compact size top loaded and sectored DRAs	16
Figure 2.8 Configuration of top-loaded CDRA.....	17
Figure 2.9 Configuration of nine elements aperture coupled linear DRA array	18
Figure 2.10 Configuration of 15 elements linear DRA array.....	18
Figure 2.11 The geometry of triangular shaped DRA array.....	20
Figure 2.12 Example of reflect- array fed by horn antenna	21
Figure 2.13 Configuration of duaband DRA reflect array	22
Figure 2.14 Configuration of two element antenna array.....	24
Figure 2.15 Electrical model of rectangular patch antenna.....	31
Figure 2.16 Equivalent circuit of aperture coupled DRA.....	31
Figure 3.1 Flow chart of methodology	37
Figure 3.2 Antenna designs presented in the proposed work.....	38
Figure 3.3 The geometry of single element aperture coupled cylindrical DRA	39
Figure 3.4 Equivalent circuit of single element aperture coupled CDRA.....	41
Figure 3.5 Fabricated prototype of single element aperture coupled CDRA	43
Figure 3.6 The geometry of the single band aperture-coupled CDRA array (a) Rectangular slots and (b) Front view.....	45
Figure 3.7 Fabricated prototype of the single band CDRA array (a) Rectangular slots (b) Front view	47
Figure 3.8 The geometry of the dual band CDRA array (a) Rectangular slots and (b) Front view	48
Figure 3.9 Fabricated prototype of the dual band CDRA array	50
Figure 3.10 The geometry of the small size CDRA array (a) Rectangular slots and (b) Front view	52
Figure 3.11 Proposed equivalent lumped element circuit of the small size CDRA array	54

Figure 3.12 Fabricated design of the small size CDRA array	55
Figure 4.1 Comparison between return losses (S_{11}) of single element aperture coupled CDRA.....	59
Figure 4.2 Slot position analysis of single element cylindrical DRA (a) CST (b) ADS.....	61
Figure 4.3 Effects of slot offset on R_r , L_r and C_r	62
Figure 4.4 The radiation pattern of single element aperture coupled CDRA at 5.2 GHz (a) E- plane (b).H-plane	63
Figure 4.5 The comparison between simulated and measured return loss (S_{11}) of single band CDRA array.....	66
Figure 4.6 E-plane radiation patterns of single band CDRA array at (a) 4.8 GHz (b) 5.1 GHz (c) 5.6 GHz.....	70
Figure 4.7 H-plane radiation patterns of single band CDRA array at (a) 4.8 GHz (b) 5.1 GHz (c) 5.6 GHz.....	71
Figure 4.8 Return loss results of with and without top-loaded CDRA array	74
Figure 4.9 Comparison between fabricated and simulated return loss of top-loaded CDRA array	75
Figure 4.10 Effects of slot dimensions on lower frequency band	77
Figure 4.11 Effects of slot dimensions on upper frequency band	77
Figure 4.12 Radiation pattern of dual band CDRA array at 2.47 GHz (a) E-plane ($\theta = 0^\circ$) (b) H-plane (90°)	78
Figure 4.13 Radiation pattern dual band CDRA array at 5.0 GHz (a) E-plane ($\theta = 0^\circ$) (b) H-plane (90°)	79
Figure 4.14 The comparison between the simulated and measured return loss (S_{11}) of small size CDRA array.....	82
Figure 4.15 Slot length analysis on a first radiating element using (a) CST (b) ADS	84
Figure 4.16 Slot length analysis on a last radiating element using (a) CST (b) ADS	85
Figure 4.17 Slot length analysis on three element array using (a) CST (b) ADS	86
Figure 4.18 Relation between slot length, resonance frequency and R_r , C_r and L_r of bottom radiating element of small size CDRA array	88
Figure 4.19 Slot length analysis on three element array using (a) CST (b) ADS.....	90
Figure 4.20 Relation between slots lengths, resonance frequency and R_r , C_r and L_r of middle radiating element of small size CDRA array	91
Figure 4.21 E-plane radiation patterns of small size CDRA array at (a) 5.0 GHz (b) 5.6 GHz (c) 5.8 GHz.....	94

Figure 4.22 H-plane radiation patterns of small size CDRA array at (a) 5.0 GHz (b) 5.6 GHz (c) 5.8 GHz	95
Figure 4.23 Back side radiation comparison using two and three aperture slots	98

LIST of TABLES

Table 2.1 Previous work on aperture coupled DRAs	14
Table 2.2 Previous work on microstrip line coupled DRA	15
Table 2.3 Previous work on planar DRA arrays	20
Table 2.4 Previous work on reflect array.....	23
Table 3.1 Dimensions of single element aperture coupled CDRA.....	40
Table 3.2 Parameters of equivalent lumped element circuit of single element CDRA	41
Table 3.3 The dimensions of single band CDRA array	46
Table 3.4 Dimensions of dual band CDRA array	49
Table 3.5 Dimensions of small size CDRA array.....	53
Table 4.1 The slot length analysis of the single element CDRA.....	60
Table 4.2 Effects of slot position under CDRA on R_r , C_r , and L_r	62
Table 4.3 Signal strength of single element aperture coupled CDRA at different distances	64
Table 4.4 Effects of changing the distance between the slots	67
Table 4.5 Effects of changing the length of slots on the central frequency and bandwidth	68
Table 4.6 Effects of changing the width of slots on central frequency and bandwidth	69
Table 4.7 Signal strength of single band CDRA array at different distances	72
Table 4.8 The efficiency and gain of single band CDRA array antenna	73
Table 4.9 Top-loaded sheet analysis on lower band.....	76
Table 4.10 Signal strength of dual band CDRA array at different distances	80
Table 4.11 The efficiency and gain of dual band CDRA array	81
Table 4.12 Effect of slot length on the R_r , L_r and C_r of the first radiating element.....	85
Table 4.13 Effect of slot length on the R_r , L_r and C_r of the last radiating element.....	87
Table 4.14 Slot length analysis on the bandwidth	89
Table 4.15 Effect of slot length on the R_r , L_r and C_r of the middle radiating element	91
Table 4.16 Effect of inter-slot distance on bandwidth.....	92
Table 4.17 Effect of inter-element distance on antenna array bandwidth	93
Table 4.18 Signal strength of small size CDRA array at different distances.	96
Table 4.19 The efficiency and gain of the small size CDRA array	97
Table 4.20 Comparison between the previous literatures on aperture coupled array antenna and the proposed array antenna	99

LIST OF ABBREVIATIONS

CDRA	Cylindrical dielectric resonator antenna
CCTO- $\text{CaCu}_3\text{Ti}_4\text{O}_{12}$	Calcium Copper Titanium Oxide
CST	Computer Simulation Technology
FR4	Flame Retardant
ADS	Advanced Design System
WLAN	Wireless local area network
EM	Electromagnetic
DRA	Dielectric resonator antenna
ISM	Industrial, Scientific and Medical
RFID	Radio frequency identification
DIL	Dielectric Image Line
USM	Universiti Sains Malaysia
VNA	Voltage Network Analyzer

CHAPTER 1

INTRODUCTION

1.1 Importance of Antenna Array in Wireless Communication

The great demand and revolution in the world of wireless communication, makes the communication devices part and parcel of the human life. Wireless communication can be defined as conveying useful information between two or more devices that are not physically connected. Wireless communication usually comprises the transfer of information over large distances by using antennas. For the last decade, a number of wireless technologies are being developed and adopted by the communication industry to remove the wire-link between the commercial products such as digital TVs, computers, high video cameras and digital cameras. Compact, high gain, highly integrated and highly efficient antennas are the requirement for these applications. The major phase of wireless communication is that it requires electromagnetic (EM) waves for conveying the information. The information to be conveyed is modulated on EM waves at the source end and the information is retrieved at the destination by demodulating the electromagnetic signal.

The transfer of information in wireless communication is related to the use of proficient antenna systems which are the major component of a communication link. Subsequently, many research works are being carried out to achieve the efficient communication in antenna designs. The antenna communication is being applied in many applications in wireless communication. However, with the advent of small size communication devices, the antennas possesses properties for compact size, wide band, high gain with a good front to back ratio are required. The characteristics or the techniques of the antenna, gain the attraction from many researchers over the previous few years.

Single element antenna has broad and less directive radiation pattern. Antenna possess narrow band and low gain is not suitable for efficient long distance communications. Antenna performance (i.e., bandwidth and gain) can be enhanced by using it in array configuration. Antenna array is a configuration of individual elements which are configured in such a way that they are able to produce directional radiation pattern. Antenna array has the capability of producing radiation pattern in the desired direction without changing the terminal characteristics of the antenna. The simplest and one of the most practical arrays are formed by placing the elements of the array in a single line which constitutes a linear array.

Recently, dielectric resonator antenna (DRA) has become the main priority of the researchers due to its many attractive features as compared to conventional low gain antennas. The small size and low cost of the DRA maintain the compactness and cost of the communication system. In addition to these advantages, DRA is easy to manufacture and has low conductor and surface wave losses.

Single element DRA is a low gain antenna of about ~ 5.0 dBi. For certain WLAN applications, there is a requirement of high gain greater than 10 dBi (for indoor and outdoor wireless communication) [1]. Single element DRA is not capable of producing a required high gain. Like other conventional low gain antennas, DRA elements with the proper feed arrangement can be used to configure the DRA array to achieve high gain. The similarity between DRA and conventional low gain micro-strip antenna is that mostly all the excitation methods used for micro-strip can also be used for DRA [2]. The motivation for the DRA array is to eliminate the losses at millimeter frequencies and to achieve the wideband with high gain without affecting the profile of the compact microwave devices.

1.2 Problem Statement

In today's communications era, communication industry is progressing toward the availability of system possessing features such as low cost, small size, wide band and high gain. The main challenges in the expansion of wireless communication are the cost and the losses of the microstrip patch antennas. To maintain the communication system profile and to reduce its cost, microstrip patch antenna technology is widely used in the industry. However, the microstrip patch antennas have some limitations which affect the communication system performance i.e., it has low gain, narrow bandwidth (1%), high conductor and surface wave losses [3]. Although in most of the ISM (Industrial, Scientific

and Medical) band applications (6.765 MHz – 246.0 GHz), there are the requirements that the system should be compact in size, wideband ($> 10\%$), low cost and possess higher gain more than 10 dBi. Recently, various efforts have been made to design the antenna which can efficiently fulfill the requirements of modern wireless applications. However, antenna parameters such as radiation pattern, gain and operating bandwidth may be affected by miniaturizing antenna size.

Dielectric resonator antenna (DRA) technology is showing a good potential for replacement of the conventional costly and large size antennas. Subsequently DRA offered low conductor and surface wave losses as compared to conventional low gain patch antenna technology. DRAs possess the advantages over traditional technologies, i.e., small size, can be fabricated in different shapes, can cover the frequency band 0.7-35 GHz and different kinds of noisy objects like human bodies are less effective on the performance of DRAs as compared to the conventional conductor antennas [4-5]. Due to these advantages, ~~DRA has received good attention in today's wireless communication industry.~~

Single element DRA has some limitations i.e., gain of about 5.0 dBi and bandwidth of about 10%. The performance of DRA can be enhanced (in terms of gain and bandwidth) by using it in an array configuration. The performance of the array depends on the geometry and dimension of the DRA, spacing between the elements, the number of elements and feed arrangement. In the proposed work, to improve the single DRA performance and to enhance the bandwidth of aperture coupled array, the aperture and mutual coupled three element cylindrical dielectric resonator antenna (CDRA) arrays are designed, simulated and fabricated.

1.3 Objectives

The research work embarks on the following objectives:

1. To design and simulate a single band, dual band and compact size cylindrical dielectric resonator antenna (CDRA) arrays for ISM (Industrial, Scientific and Medical) band applications.
2. To characterize and validate the impedance behavior (RLC characteristic) for the CDRA array design parameter such as the distance between the array elements, distance between the slots and dimensions of the slots. Characterize the tuning parameter to optimize the CDRA array design.
3. To produce equivalent lumped element circuit which represents the characteristic of 3D structure of DRA array using Matlab programs and ADS simulator.

1.4 Scope of Research

The following points characterize the scope of the proposed work.

1. In the research work, cylindrical DRs are used to design the antenna arrays. The attractive features of CDRA include: directional as compared to annular and rectangular DR, dielectric material can be easily molded into a cylindrical shape, possess simple field structure and its geometry involves less edges as compared to rectangular DR. The CST microwave studio is used to design and simulate the antenna structures prior to the fabrication.
2. The proposed work covers the designs of antenna arrays for ISM (Industrial, Scientific and Medical) band applications. The selected operating frequency is between 4.915 GHz to 5.825 GHz.
3. The characteristics of designing antenna arrays in terms of inter-element distance, the distance between the coupling slots and the number of elements are also evaluated. The equivalent lumped element circuit of CDRA array is modeled by using the Advanced Digital System (ADS) software and the Matlab programs to verify the antenna feasibility. The effects of slot length and inter-slot distance on the bandwidth and central frequency are analyzed using a CST

microwave studio. The slot length effects on the RLC values of different antenna components is analyzed by using the equivalent RLC model.

4. The prototypes for the designed antenna arrays are fabricated by using Roges's and FR4 substrates with permittivity of 2.2 (0.787 mm thickness) and 4.9 (1.565 mm thickness) respectively. The proposed antenna arrays are suitable for IEEE 802.11a/b/g applications.

1.5 Thesis Layout

The remaining parts of the thesis are structured as follows.

Chapter 2: reviews the theoretical background of the dielectric resonator antenna (DRA). The advantages of the cylindrical dielectric resonator antenna (CDRA) are also discussed.

Reviews on microstrip line feeding mechanism are also the part of Chapter 2. Different DRA arrays that have been proposed in the literature are also introduced. The previous work on the equivalent lumped element circuit of DRA is also presented. The theoretical work needs to model the equivalent lumped element circuit of aperture coupled DRA is also the part of Chapter 2.

Chapter 3: covers the research methodology and the antenna design procedure followed throughout the research work. The simulated geometries of single element CDRA and three proposed CDRA arrays: single band, dual band and small size three element CDRA arrays are presented. The steps involved in obtaining the equivalent lumped element RLC circuits of the single element CDRA and small size cylindrical dielectric resonator antenna (CDRA) array are discussed. In addition to the CST and ADS design, the procedure followed to build the proposed antenna array prototypes is also presented.

Chapter 4: is devoted for the results of proposed single element CDRA and CDRA arrays in terms of return loss (S_{11}), bandwidth, directivity and radiation pattern. The comparison between the return loss (S_{11}) results obtained through the CST microwave studio, ADS and fabricated design are part of Chapter 4.

Chapter 5: concludes the thesis and highlights the major contributions, in addition to suggestions for future work.

CHAPTER 2

BACKGROUND THEORY AND LITERATURE REVIEW

Chapter two reviews the theoretical background and characteristics of the DRA. A brief review of a microstrip transmission line feeding techniques used to excite the antenna array is discussed. It presents a detailed literature works on different configurations of DRA arrays, such as compact size and low profile DRA arrays, linear DRA arrays, planar DRA arrays and high gain reflect array. Finally, design structures about the equivalent lumped element circuits of microstrip patch and DR antennas are reviewed in detail.

2.1 Background study of Dielectric Resonator Antenna (DRA)

In the late 1960's, advancements in research led to reduction in losses of ceramic materials, hence allowing dielectric resonators to be employed in circuit applications as a high quality factor element. In circuit applications these materials possessing high permittivity dielectric resonators contribute in making the system compact. In early times, the DR was encapsulated in metal cavities in order to fulfill filter and oscillator requirements; i.e., maintained high quality factor and minimal radiation. Hence the DRs present to be an alternative to the waveguide cavity resonator, and comparatively exhibit better response in a printed-circuit combination. Although the advent of open DR had taken place very earlier, but it got recognition as an antenna only after the publication of cylindrical DRA by Long in 1983 [6].

The microstrip patch antenna has high conductor and surface wave losses at millimetre wave frequencies which degrade the antenna performance in terms of gain. Whereas DRA is the best alternative to low gain conventional patch antennas due to its attractive features such as low conductor losses, wide impedance bandwidth ($\sim 10\%$ for $\epsilon_r \sim 10$) [7] and high radiation efficiency ($> 98\%$) at millimetre wave frequencies.

The advancement in compact size wireless devices has eventually led to miniaturization of system components. Due to many attractive properties, DRAs attains the attraction of researcher and communication industry. An antenna designed for any system depends upon the nature and requirement of the system, some system operates only in certain direction which requires a directional antenna as depicted in Figure 2.1, and some transmit radio waves in all directions by using omni-directional antennas as depicted in Figure 2.2.

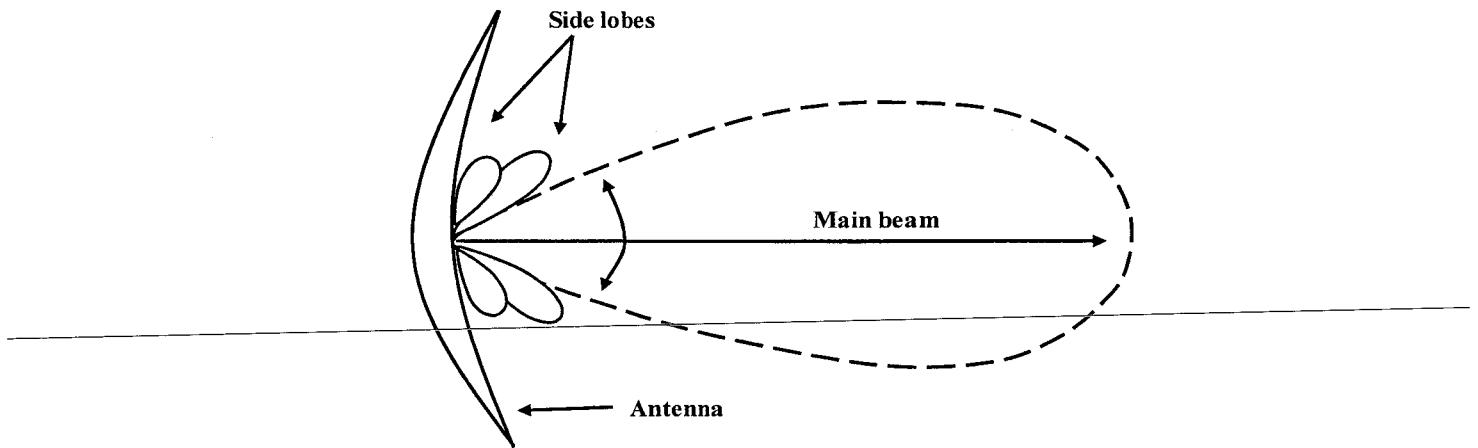


Figure 2.1. Directional radiation pattern.

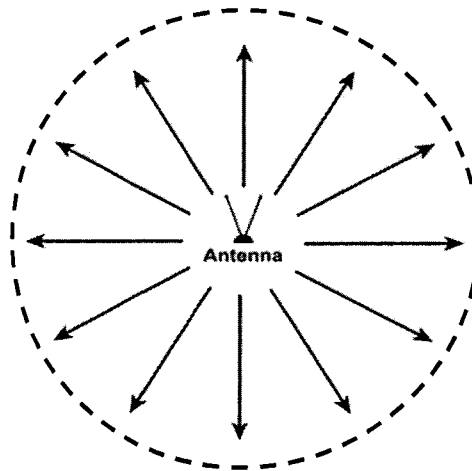


Figure 2.2. Omni-directional radiation pattern.

DRA has become a popular antenna as compare to the conventional patch antennas due to its following attractive features:

- It can be fabricated using a high dielectric constant material.
- covers wide range of frequency band: $f = 0.7\text{-}35\text{ GHz}$.
- exhibits a high radiation efficiency (95%); due to low conductor and surface wave losses.
- excitable through from different transmission lines i.e., microstrip feed line, dielectric image line, coaxial probe.
- can be fabricated in different shapes i.e., cylindrical, rectangular, hemispherical.
- the performance of DRAs is minimally effected by the presence of nearby noisy objects (such as human bodies).

These attractive characteristics of DRA make it a very versatile radiating element in various communication applications such as radars, satellite communication, wireless local area network (WLAN) and radio frequency identification (RFID). Due to the remarkable research in the field of DRAs, it has resolved prominent disadvantages of conventional patch antennas. Since 1983, DR of different shapes like spherical, cylindrical, triangular, rectangular has been used as an antenna in different applications [2].

2.2 Types of DRA

Different shapes of DRs are found in the literatures. In this section, a brief introduction and comparison between the two basic and most widely used shapes of DR such as rectangular and cylindrical are discussed.

2.2.1 Rectangular DRA

Rectangular shaped DR is characterized by dielectric material permittivity ϵ_r , its height h , width w and depth d as depicted in the Figure 2.3. By changing the (w/h) and (w/d) of rectangular DRA, the resonance frequency, input impedance and radiation pattern will change. Rectangular DRA with different feeding mechanisms has been presented in the literatures [8-11]. The equation for resonance frequency of rectangular DR is given as [2]

$$f_{GHz} = \frac{15F}{w_{cm}\pi\sqrt{\epsilon_r}} \quad (2.1)$$

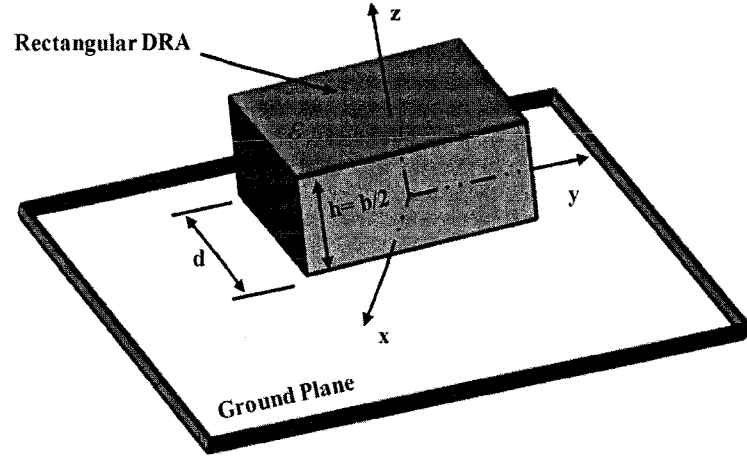


Figure 2.3. The geometry of the rectangular shaped dielectric resonator [2]

where

$$F = \frac{2\pi w f_0 \sqrt{\epsilon_r}}{c} \quad (2.2)$$

where ϵ_r is the dielectric material permittivity, f_0 is the resonance frequency, c is the speed of light and w is the width of the rectangular DRA.

2.2.2 Cylindrical DRA

Cylindrical shaped DR is characterized by its dielectric material permittivity ϵ_r , height h and radius a as depicted in Figure 2.4.

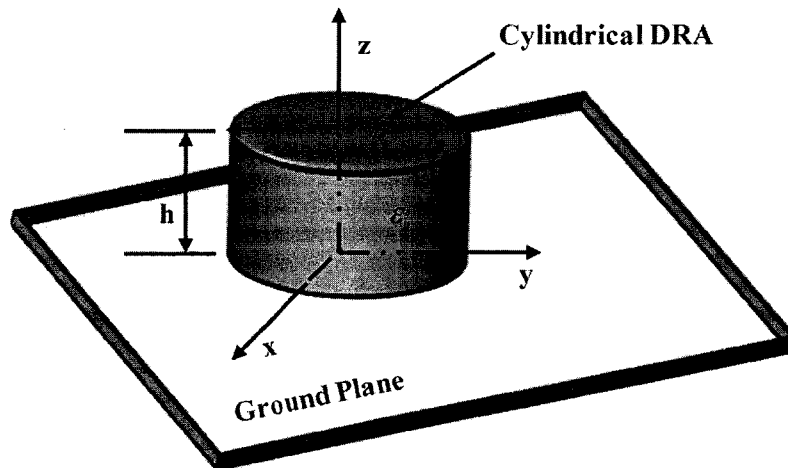


Figure 2.4. The geometry of the cylindrical shaped dielectric resonator [2].

Cylindrical DRA with different feeding mechanisms has been presented in the literature [12-19]. In 1983, cylindrical DRA was first time examined by Long and [6] showed that cylindrical DRA operating in $HE_{11\delta}$ mode provide efficient radiation. The resonance frequency, input impedance and radiation pattern can be controlled by changing the radius of cylindrical DR [20]. The cylindrical DRA is a suitable for directional wireless application. It is more directional and has a low resonance frequency as compared to the rectangular and annular DRA [21]. In addition to this, dielectric material can be easily molded into cylindrical shaped by utilizing commercially existing dielectric rod [22]. The cylindrical DRA is easy to analyze as compared to rectangular DRA. Rectangular DRA contains more edges and has a complex field structure as compared to cylindrical DRA [23-24].

Before using CDRA for any particular application, it is required to calculate the relation between its height, radius and resonance frequency. The equation to calculate the resonance frequency of cylindrical DR for different modes is calculated by using the expressions found in [25].

The resonance frequency for $HE_{11\delta}$ mode is given as

$$k_0 a = \frac{6.324}{\sqrt{\epsilon_r + 2}} \left[0.27 + 0.36 \left(\frac{a}{2h} \right) + 0.02 \left(\frac{a}{2h} \right)^2 \right] \quad (2.3)$$

Or equivalently

$$f_{0(HE_{11\delta})} = \frac{c \cdot 6.324}{2\pi a \sqrt{\epsilon_r + 2}} \left[0.27 + 0.36 \left(\frac{a}{2h} \right) + 0.02 \left(\frac{a}{2h} \right)^2 \right] \quad (2.4)$$

The resonance frequency for $TE_{01\delta}$ mode is given as

$$k_0 a = \frac{2.327}{\sqrt{\epsilon_r + 1}} \left[1 + 0.2123 \left(\frac{a}{h} \right) - 0.00898 \left(\frac{a}{h} \right)^2 \right] \quad (2.5)$$

Or equivalently

$$f_{0(TE_{01\delta})} = \frac{c \cdot 2.327}{2\pi a \sqrt{\epsilon_r + 1}} \left[1 + 0.2123 \left(\frac{a}{h} \right) - 0.00898 \left(\frac{a}{h} \right)^2 \right] \quad (2.6)$$

The resonance frequency for $TM_{01\delta}$ mode can is given as

$$k_0 a = \frac{\sqrt{3.83^2 + \left(\frac{\pi a}{2h}\right)^2}}{\sqrt{\epsilon_r + 2}} \quad (2.7)$$

Or equivalently

$$f_{0(TM01\delta)} = \frac{c \sqrt{3.83^2 + \left(\frac{\pi a}{2h}\right)^2}}{2\pi a \sqrt{\epsilon_r + 2}} \quad (2.8)$$

The resonance frequency for $TE_{011+\delta}$ mode is given as

$$k_0 a(\epsilon_r) = \frac{2.208}{\sqrt{\epsilon_r + 1}} \left[1.0 + 0.7013 \left(\frac{a}{h}\right) - 0.002713 \left(\frac{a}{h}\right)^2 \right] \quad (2.9)$$

Or equivalently

$$f_{0(TE011+\delta)} = \frac{c 2.208}{2\pi a \sqrt{\epsilon_r + 1}} \left[1.0 + 0.7013 \left(\frac{a}{h}\right) - 0.002713 \left(\frac{a}{h}\right)^2 \right] \quad (2.10)$$

where

a = radius of CDRA;

h = height of CDRA;

ϵ_r = dielectric constant of CDRA;

c = speed of light;

k_0 = free space wave number.

The relation between the resonance frequency f_0 and free space wave number k_0 is given as

$$k_0 = \frac{2\pi f_0}{c} \quad (2.11)$$

Different modes of CDRA can be excited by adjusting the slot position under the CDRA. By placing aperture slot in the middle of DR only hybrid modes are excited and by moving slot away from the centre TE and TM modes can be excited. In the proposed research work, CDRA's are designed for WLAN applications. The design procedure and results of three linear CDRA arrays are presented in Chapter 4.

2.3 Coupling Techniques

In antenna structure, the feeder is one of the basic and important components. In transmitting side feed line transfer the radio waves to the rest of the antenna structure meanwhile in receiving side, it collects the radio waves and converts them to electric current. Different feeding techniques have been developed to excite the DRA such as aperture coupling, microstrip feed, probe feed and dielectric image line [26-27]. This section highlights the most commonly use microstrip line coupling to excites the DRAs.

2.3.1 Aperture Coupling

One of the common feeding techniques to be used with DRA is the aperture coupling. In this technique, there is no direct contact between the feed line and the radiating element. The coupling slot etched on the ground plane is used to excite the radiating element from the transmission line. The coupling slot is characterized by it length, l_s and width, w_s as depicted in the Figure 2.5. The equation to calculate the initial slot length is given as [2]

$$l_s = \frac{0.04\lambda_0}{\sqrt{\epsilon_e}} \quad (2.12)$$

and

$$\epsilon_e = \frac{\epsilon_e + \epsilon_s}{2} \quad (2.13)$$

where ϵ_s and ϵ_r are the permittivity of the substrate and dielectric resonator respectively. To avoid the large back lobe level the equation to calculate the slot width is given as

$$w_s = 0.2l_s \quad (2.14)$$

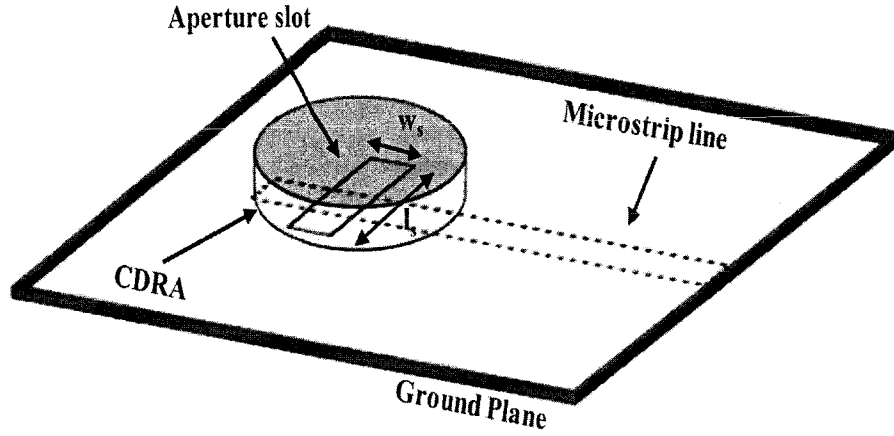


Figure 2.5. Geometry of aperture coupled cylindrical DRA.

where w_s and l_s are the width and length of the slot. The placement of transmission line under the ground plane gives the advantage of the aperture coupling mechanism which reduces the unwanted coupling and superior radiation from the feed line. The maximum coupling between the radiating element and transmission line can be achieved by placing the slot width w_s and length l_s at the centre of the DRA [23]. The amount of coupling can also be improved by slightly offsetting the DRA from the slot. Different shapes of coupling slots such as circular, rectangular, stair shaped, H shaped, C shaped and E shaped are used to excite the radiating elements. The rectangular coupling slot is most commonly used to excite the microstrip patch and dielectric resonator antennas [28-31]. The Raggad proposed stair shape coupling slot use to excite the DRA has been presented in [32]. The objectives of using the novel technique are to maximize the coupling, enhance the gain, reduce the antenna size and achieve the resonance at the required frequency. The corresponding achieved gain is 5.45 dBi at 3.5 GHz.

Aperture coupled technique has been widely used to excite DRA for different applications as tabulated in Table 2.1. It is clear that the bandwidth from 0.007 to 0.120 GHz with a corresponding gain of 5.1 to 9.0 dBi has been achieved. Various shapes of aperture slot (i.e., rectangular, long rectangular, wider rectangular, H-shape, Dog-bone shape, etc.) for the microstrip slot antenna has also been presented in [33].

Table 2.1. Previous work on aperture coupled DRAs.

Authors and Years	f_o (GHz)	Gain (dBi)	Bandwidth (GHz)	Feeding method	References
M. F. Ain, Y. M. Qasaymeh, Z. A. Ahmad, M. A. Zakariya, and Ubaid Ullah, 2012	5.8	6.0	0.080	Microstrip	[34]
M. F. Ain, Y. M. Qasaymeh, Z. A. Ahmad, M. A. Zakariya, and U. Ullah, 2012	2.45 and 5.0	5.78 and 5.1	0.007 and 0.035	Microstrip	[35]
M. F. Ain, Y. M. Qasaymeh, Z. A. Ahmad, M. A. Zakariya, M. A. Othman, and M. Z. Abdullah, 2012	8.5	9.0	0.120	Microstrip	[36]

2.3.2 Direct Coupling

Secondly another important coupling technique to excite the DR is a microstrip line coupling [37-39]. In this technique, transmission line and DRA are placed on the back side of the ground plane as depicted in the Figure 2.6. The amount of coupling depends upon the permittivity of the dielectric resonator, distance between the microstrip line and dielectric resonators. The $HE_{11\delta}$ mode of the cylindrical DRA is excite by using the microstrip coupling [2].

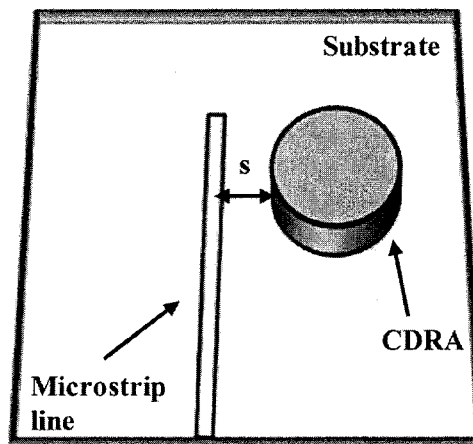


Figure 2.6: Microstrip line coupled DRA [2].

The main disadvantage of this coupling technique is that it produces cross polarization. In addition to this it generates the magnetic field inside the resonator parallel to the transmission line [23]. The findings from literatures works regarding the microstrip line coupling are reviewed in Table 2.2.

Table 2.2. Previous work on microstrip line coupled DRA.

Authors and Years	f_o (GHz)	Gain (dBi)	Bandwidth (GHz)	References
P. Rezaei, Mohd Hakkak and K. Forooraghi, 2006	5.5	Not mentioned	0.98	[40]
M. F. Ain, S. I. S. Hassan, J. S. Mandeep, M. A. Othman and B. M. Nawang, 2007	2.5	5.1	Not mentioned	[41]
A. A. H. Azremi, N. A. Saidatul, P. J. Soh, M. A. Idris and N. Mahmed, 2008	5.0	5.27	0.328	[39]

2.4 DRA Arrays

Generally, single element DRA has a low gain of about 5.0 dBi with broad radiation pattern. The wideband and high gain antennas are essential components required for long distance communication. Like other conventional low gain antennas, DRA gain can be improved by forming an assembly of DRAs in geometrical and electrical configuration. This antenna configuration designed by placing a number of elements is called an array. A brief review on previous work and recent developments on DRA array structures, designed for millimetre wave applications are presented in this section. It includes:

- compact size and low profile DRA array;
- linear DRA arrays;
- planar DRA arrays;
- high gain DRA reflect-arrays.

2.4.1 Compact Size and Low Profile DRA Array

In today's modern era, the customers are attracted towards low profile portable devices such as laptops, mobiles, notebooks and other handheld devices. In order to maintain the device compactness, communication devices require a small profile, high gain and

wideband antenna array. The use of DRA is not suitable at low frequencies because its size increases [42]. One method to reduce the size of DR is by using high dielectric constant at the cost of reduction in bandwidth. Alternative methods to miniaturize the volume of DRAs include: electrical monopole DRA, top-loaded DRA and sector DRA [12]. Examples of low profile and compact size DRs are depicted in Figure 2.7.

Recently, in [43] uses E-shaped coupling slot to excite the cylindrical CDRA for 2.45 GHz band as depicted in Figure 2.8. By using metallic-sheet on the top of cylindrical DRA, the frequency band shifts down from 2.71-2.73 GHz to 2.44-2.46 GHz. Similarly, the four elements DRA array using metallic strip loaded technique to reduce the volume of the elements with 18% bandwidth is presented in [44].

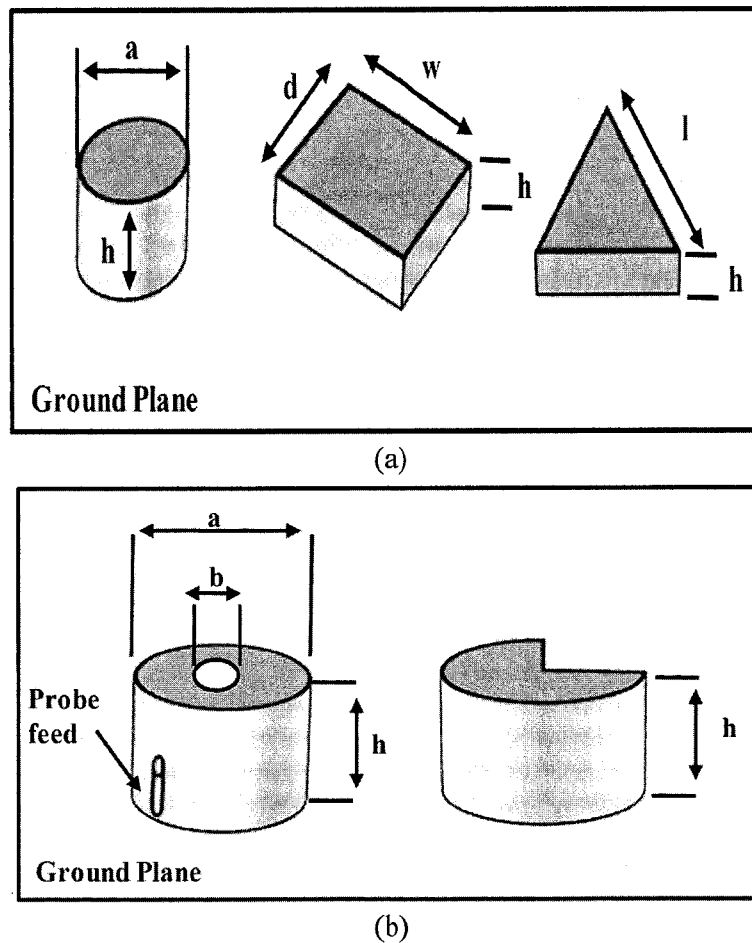


Figure 2.7. Examples of (a) Low profile DRs (b) Compact size top loaded and sector DRs.

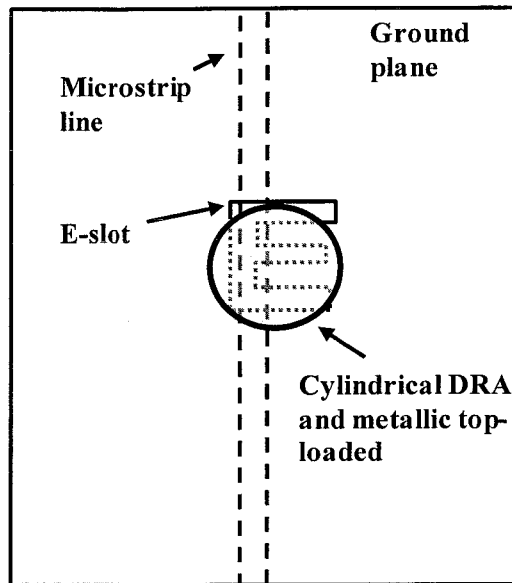


Figure 2.8. Configuration of top-loaded CDRA.

2.4.2 Linear DRA Array

In linear array, the elements are placed along a line at some distance from each other [1]. Linear arrays are used to create a fan shaped radiation pattern with broad beam along the orthogonal plane and narrow beam in the direction of plane corresponding to the axis of the array [41]. Different feeding techniques have been used to excite the linear array elements such as aperture coupled micro-strip line [42], dielectric image line [29] and coaxial probe feed [20].

A linear array using nine rectangular DRAs designed at 5.8 GHz is depicted in Figure 2.9. In this linear array [45], the aperture coupled microstrip line is applied to excite the radiating elements. The gain of 10 dBi with an impedance bandwidth of 60 MHz is achieved. Various linear DRA arrays by using different feeding techniques have been investigated at 20 GHz in [46]. By using microstrip feed, slot coupling technique and dielectric image line feed, the achieved gains are 13.8, 4.83 and 13.2 dB respectively. A log periodic linear array using 9 DRAs designed for K- (18.5-26 GHz) and Ka (26.5-40 GHz) bands has been introduced in [47]. The spacing, width and length of the DRAs increase nonlinearly from one side of the antenna to the other. Recently, the four element rectangular DRA array using coupling slot with microstrip feed has been presented in [36]. The characteristics of standing wave ratio are used to determine the positions of coupling slots. The corresponding achieved gain and bandwidth are 9.0 dBi and 0.08 GHz respectively at 8.5 GHz.

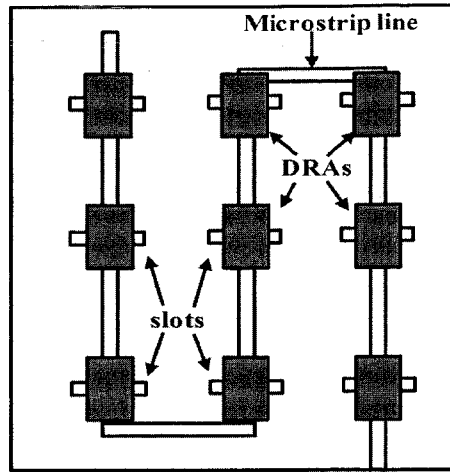


Figure 2.9. Configuration of nine elements aperture coupled linear DRA array [45].

Dielectric image line (DIL) is another feeding mechanism used to excite the radiating elements placed in a linear configuration. Example of DRA array using a DIL is depicted in Figure 2.10. In the proposed array, the direct coupling technique is used to excite the radiating element. The power coupled to each radiating element is controlled by adjusting the distance between the DRA and DIL. The corresponding achieved gain is 10.22 dBi at 10.5 GHz by using 15 DRAs [48]. A single element antenna and an three element linear array using aperture coupled dielectric image line has been proposed in [49]. For array structure, the achieved gain is 10.2 dB with -8 dB back lobes. Then furthermore by using a back reflector and four side walls around the antenna structure,

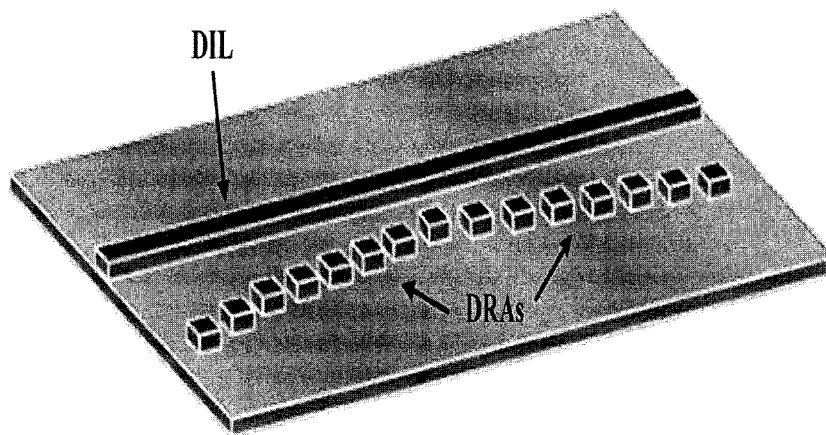


Figure 2.10. Configuration of 15 elements linear DRA arrays [48].

the obtained gain and back lobes are 11 dB and -12 dB respectively. By using the same aperture coupling technique, three element rectangular DRA array has been presented in [50]. The achieved gain and backward radiation with side wall and back reflector are 11 dB and -12 dB. Subsequently by replacing back reflector with metallic box the achieved gain and backward radiation are 11.5 dB and -22 dB. The circular polarized linear array using 3 elliptical DRA with aperture coupled dielectric image line has been introduced in [51]. Additionally, through the use of back reflector, a 5.3% improvement in the bandwidth is obtained.

Various other linear DRA arrays using different feeding configuration have been reported in the literatures [52-73]. There are a number of advantages of the linear array design. The side lobes levels can be reduced by controlling the amplitude and direction of main beam can be tuned by controlling the phase between the elements of linear array [5].

2.4.3 DRA Planar Array

The planar arrays are used to control the main beam in two planes while linear arrays are used to scan the main beam in one plane [74]. Linear arrays can be extended into a planar arrangement to achieve the narrow beam pattern in two planes. In planar array, the distance between the elements is fixed and main beam can be controlled by changing the phase and wavelength [75]. Planar arrays are commonly designed for applications demanding pencil beam like radiation pattern with high gain [76]. Mostly planar array depends upon the ground plane and element radiation pattern to reduce the back lobes on the other side of the plane. The design of the planar array is almost same as linear array but their grating lobe has unique properties, they sometimes lie outside the desired scan plane.

A dual band triangular shaped DRA array for WLAN/WIMAX applications has been introduced as depicted in Figure 2.11. The triangular shaped DRA array, used microstrip feed line to excite the radiating elements. The bandwidths of 3.35 to 3.70 GHz and 4.52 to 5.34 GHz are achieved by adjusting the height of dielectric resonators for WLAN and WiMAX band respectively. The corresponding achieved gains are 7.02 and 8.02 dB at 3.5 and 5.2 GHz respectively [77]. The 4 x 4 element DRA array using a microstrip corporate feed has been reported in [78]. The proposed array designed over a ground plane and showed that microstrip corporate feed is responsible for losses instead of DRAs. The comparison between the planar 64 elements perforated DRA array and microstrip patch antenna has been presented in [79]. The perforated DRA array achieved

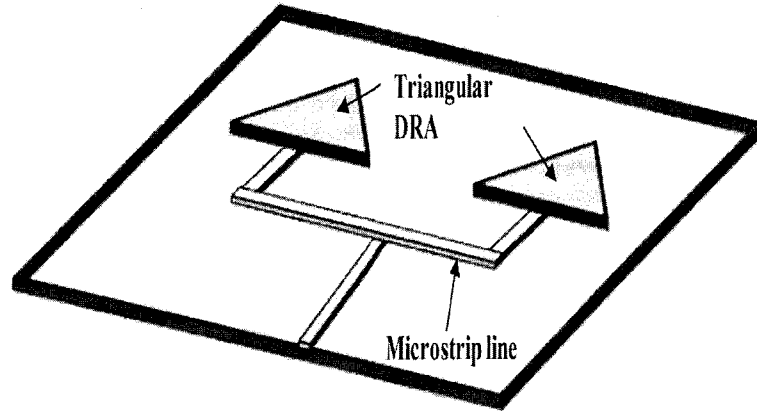


Figure 2.11. The geometry of triangular shaped DRA array.

1 dB improvement in gain with better gain bandwidth as compared to the microstrip patch antenna. The perforated DRA technique eliminates the requirement to place individual DRA on the fabrication board.

Some planar DRA arrays along with their characteristics designed for different applications are depicted in Table 2.3. It is apparent that a 43.9% bandwidth and 16.50 dB gain has been achieved by using DRA in planar configuration. Several other planar arrays using different shapes of DRAs have been reported in the literatures [80-83].

Table 2.3. Previous work on planar DRA arrays.

Authors and Years	f_o (GHz)	Gain	Bandwidth	Array Feed	References
S. L. Steven Yang Ricky Chair, A. A. Kishk, K. F. Lee and K. M. Luk 2006	10.00	Not available	43.9%	Microstrip	[84]
Yizhe Zhang, A. A. Kishk and A.B. Yakovlev 2007	X-band	Not available	15.0%	Waveguide Horn	[85]
J. Svedin, L.-G. Huss', D. Karlen, P. Enoksson, and, C. Rusu 2007	94.00	10.00 dB	Not available	Microstrip	[86]
Runa Kumari, Kapil Parmar and S K Behera 2011	3.50 and 5.20	7.02 and 8.90 dBi	Not available	Microstrip	[77]
Robab Kazemi, Aly E. Fathy and Ramezan Ali Sadeghzadeh 2012	11.00	16.50 dBi	Not available	Substrate integrated waveguide	[87]

2.4.4 DRA Reflect Array

An alternative technique for further enhancement of antenna gain is by using radiating elements in a reflect-array configuration. In this method, array elements are placed on a surface and excites through a primary feed antenna, which is placed at a particular distance from the array. The elements in the reflect-array are designed and placed in such a way that they reflect the incident rays in the desired direction as depicted in Figure 2.12.

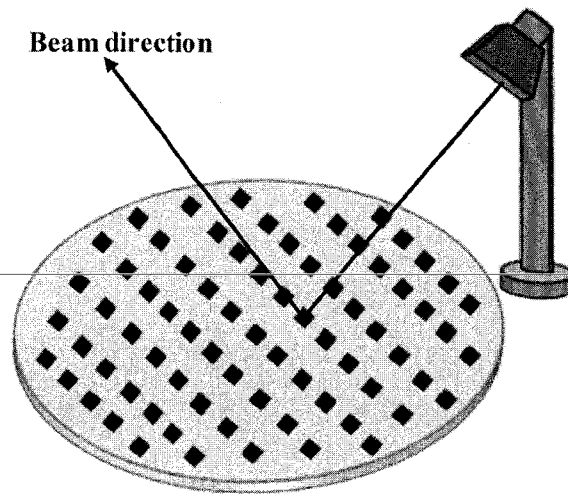


Figure 2.12. Example of reflect-array fed by horn antenna.

Reflect-array is basically another mechanism to achieve a high gain as compared to bulky size reflector antennas [88]. Some attractive features of reflect-array includes: low cost, easy to manufacture and can be integrated with communication devices in contrast to the reflector antennas [89]. DRA reflect-arrays possess different advantages as compared to other low profile phase array antennas and classical high gain antennas (parabolic reflector antennas). DRA reflect-array is a low profile and low cost in contrast to the parabolic reflector [89-91] and has less ohmic losses at millimetre frequencies which are the main limitation of the micro-strip antenna array technology [92].

A high gain dual reflect-array antenna for W- and Ku-bands is proposed as depicted in Figure 2.13 [93]. The dual reflect-array consists of a main reflect-array fed by a sub-reflect-array, while the sub-reflect-array is fed by the horn antenna. The achieved gain for W- and Ku bands are 38.7 dBi and 42.75 dB respectively. A high gain reflect-array using

dielectric resonators as radiators has been presented in [94]. The required phase shift from each element is tuned by using different dimensions of DRAs. The corresponding achieved gain for Ka-band is 27.40 dB by using a horn feed. The 23 x 23 DRA reflect-array designed for X-band has been introduced in [95]. The reflect-array elements are fed by the pyramidal horn antenna and obtained 28.77 dB gain with an impedance bandwidth of 1.8 GHz.

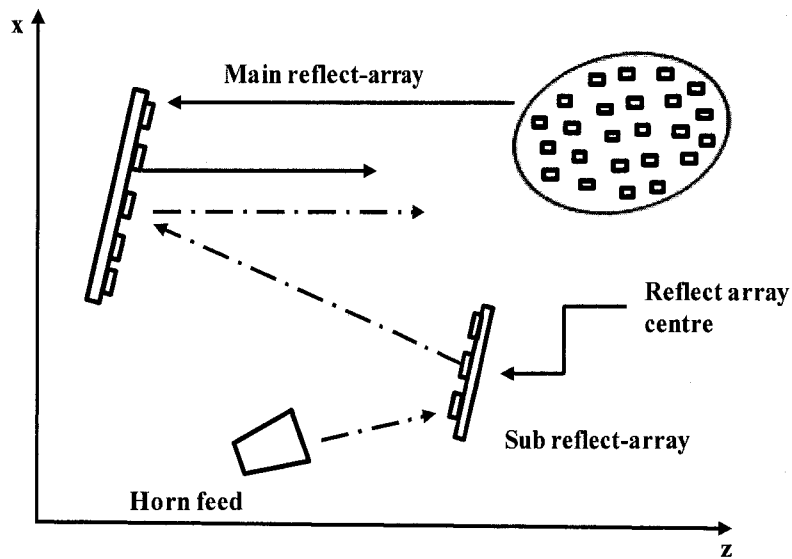


Figure 2.13. Configuration of dualband DRA reflect-array [93].

Various designed DRA reflect-arrays for different applications (satellite communications, radar system, remote sensing and radio astronomy) along with their characteristics are depicted in Table 2.4. It is clear that the bandwidth from 7.0 % to 13 % has been reported by using a horn feed. The corresponding maximum achieved gain is 28.77 dB.

Table 2.4. Previous work on reflect array.

Authors and Years	f_o (GHz)	Gain	Bandwidth	Array Feed	References
A.Elhady. M., S.H. Zainud-Deen, A.A. Mitkees, and A.A. Kishk 2010	10.00	28.00 dBi	13.0%	Horn Feed	[96]
S.H. Zainud-Deen, Abd-Elhady, A.A. Mitkees and A.A. Kishk 2010	X-band	28.77 dB	18.0%	Pyramidal Horn	[97]
M. Moeini-Fard and M. Amirhosseini 2010	30.00	26.50 dB	16.3%	Horn Feed	[98]
Mojtaba Moeini-Fard, and Mohd Amirhosseini 2011	30.00	25.40 dB	7.0%	Horn Feed	[99]

2.5 Main Array Parameters

The antenna array configuration depends upon three main design parameters such as the number of elements, operating frequency and inter-element distance as discussed in Chapter 1.

The most important phenomenon in antenna array design is to rotate the main beam in the specified direction. The radiation pattern of an array can be controlled by adjusting the following design parameters [100].

- Configuration of antenna elements (circular, linear, rectangular, etc.).
- Distance between the consecutive elements.
- Relative amplitude of the individual elements.
- Phase of the individual elements
- Relative pattern of the individual element.

Suppose the spatial configuration and antenna type in the array are fixed. Then by using following parameters, antenna radiation pattern can be controlled.

- Inter-element distance (N-1)

- Relative amplitude (N-1)
- Phase of elements (N-1)

Therefore, by changing $3(N-1)$ degrees of freedom the radiation pattern can be controlled. It is clear that degree of freedom is proportional to the number of elements in the array. For proper understanding how an array works, the investigation of the simplest possible array which consists of two elements is presented.

2.5.1 Two Element Antenna Array

To investigate the effects of inter-element distance, relative amplitude and phase of array elements on the radiation pattern, suppose two element array. The parameters to control the radiation pattern includes the spacing between the consecutive elements (d), the relative phase difference between the consecutive elements ($\delta_2 - \delta_1$) and the amplitude of currents between the elements of antenna array ($I_2 - I_1$). The configuration of two elements antenna array is depicted in the Figure 2.14.

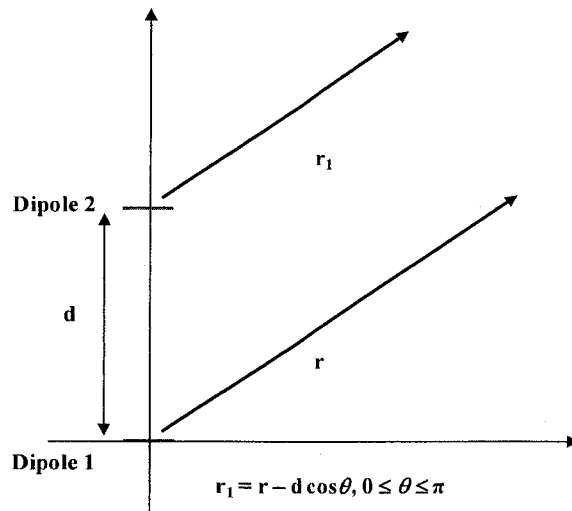


Figure 2.14. Configuration of two element antenna array.

To calculate the total electric field, the equation of electric field from first element is given as

$$E_1 = \frac{kI_1 e^{j\delta_1}}{r} e^{-j\beta r} \quad (2.15)$$

Similarly, as the distance between the two consecutive elements is ' $d \cos \varphi$ ', the equation of electric field for the second element of antenna array is given as

$$E_2 = \frac{kI_2 e^{j\delta_2}}{r - d \cos \varphi} e^{-j\beta(r - d \cos \varphi)} \quad (2.16)$$

As the point of interest is very far away, the above expression is written as

$$E_2 = \frac{kI_2 e^{j\delta_2}}{r} e^{-j\beta r} e^{j\beta d \cos \varphi} \quad (2.17)$$

The total electric field at the point of interest is the summation of fields due to the both elements. The equation of total electric at the point of interest is given as

$$E = \frac{kI_1 e^{j\delta_1}}{r} e^{-j\beta r} + \frac{kI_2 e^{j\delta_2}}{r} e^{-j\beta r} e^{j\beta d \cos \varphi} \quad (2.18)$$

For the simplicity of the above relation, suppose $k_0 = k e^{-j\beta r}/r$. The equation of the total electric field is given as

$$E = k_0 [I_1 e^{j\delta_1} + I_2 e^{j(\delta_2 + \beta d \cos \varphi)}] \quad (2.19)$$

By taking some terms common, the equation of total electric field is given as

$$E = k_0 I_1 e^{j\delta_1} [1 + (I_2/I_1) e^{j(\delta_2 - \delta_1)} e^{j\beta d \cos \varphi}] \quad (2.20)$$

Now, it's clear from the above expression that, the radiation pattern of the antenna can be controlled by changing three parameters which are the relative amplitude of currents (I_2/I_1), the phase difference between the elements ($\delta_2 - \delta_1$) and the inter-element spacing (d). Now the effects of these three parameters are discussed in the following subsections.

2.5.2 Effect of Variation in Inter-Element Spacing (d)

To investigate the effects of inter-element spacing on the radiation pattern, the first step is to fix the phase difference ($\delta_2 - \delta_1$) and current ratio (I_2/I_1). Then by changing the distance between elements, analyzing the effects on the radiation pattern.

Suppose that the relation between the currents of two elements ($\frac{I_2}{I_1} = 1$) i.e., both the elements has the same current amplitudes. Secondly the phase difference between the elements of the array is zero ($\delta_2 - \delta_1 = 0$) i.e., this means that current reaches both the elements at the same time. Now, by using these values, the equation for electric field is given as

$$E = k_0 I_1 e^{j\delta_1} [1 + e^{j\beta d \cos \varphi}] \quad (2.21)$$

After certain mathematical manipulation on equation 2.21, the equation of the electric field is given as

$$E = k_0 e^{j\frac{\beta d}{2} \cos \varphi} + e^{-j(\frac{\beta d}{2}) \cos \varphi} \quad (2.22)$$

It is know that $e^{j(\frac{\beta d}{2}) \cos \varphi} + e^{-j(\frac{\beta d}{2}) \cos \varphi} = 2 \cos[(\beta d/2) \cos \varphi]$, by using this, the equation 2.22 is written as

$$E = k_0 e^{j(\frac{\beta d}{2}) \cos \varphi} 2 \cos[(\beta d/2) \cos \varphi] \quad (2.23)$$

The equation 2.23 is divided by maximum radiation to eliminate the constant terms. The equation for normalized radiation pattern of two element antenna array is given as

$$E_{normalized} = \cos[(\beta d/2) \cos \varphi] \quad (2.24)$$

From equation 2.24, it is clear that when $\varphi = 90^\circ$, the normalized pattern would have maximum value i.e., one. It is also observed that the nulls will be between the two maxima's. To analyze the null's in the radiation pattern, it is observed that the nulls will expose when

$$\left(\beta d/2\right) \cos \varphi = \pm \frac{\pi}{2}, \pm \frac{3\pi}{2}, \dots \quad (2.25)$$

As $\beta = 2\pi/\lambda$, so above expression is written as

$$\cos \varphi = \pm \frac{\lambda}{2d}, \pm \frac{3\lambda}{2d}, \dots \quad (2.26)$$

As the cosine function value lies between 1 and -1, so if the above expression value exceeds 1 or below the -1, the term is ignored. From the above discussion, it is concluded that by changing the inter-element spacing, the depth of nulls in the radiation pattern can be controlled.

2.5.3 Effect of Variation in Relative Amplitude of Current Distribution (I_2/I_1)

To investigate the effects of relative amplitude of currents ($\frac{I_2}{I_1}$) on the radiation pattern, the first step is to fix the phase difference and spacing between the elements. Then by changing the current ratio, analyzing its effects on the radiation pattern.

Let us suppose that phase difference between the consecutive elements of array is zero (i.e., $\delta_2 - \delta_1 = 0$), and the distance between the elements of the array is $d = \lambda$. After using these values in the expression of total electric field and assuming $\delta_1 = 0$, $I_1 = 1$, we have

$$E = k_0 [1 + (I_2/I_1) e^{j2\pi \cos \varphi}] \quad (2.27)$$

By using $\varphi = 0$ and $\varphi = 90$, the equations to find the maximum and minimum value of radiation pattern are given as $E = k_0[1 + (I_2/I_1)]$ and $E = k_0[1 - (I_2/I_1)]$ respectively.

From the above calculation, it is clear that if the value of (I_2/I_1) is equal to one, nulls will appear in the radiation pattern and if this ratio is not equal to one then there will be no null in the radiation pattern. Therefore, it is concluded that the depth of the nulls in radiation pattern can be controlled by the relative amplitude of the current. If the ratio (I_2/I_1) is close to one the nulls will be deeper and if this ratio is less than one the depth of the nulls is not very deep.

2.5.4 Effect of the Variation of Phase Difference Between the Elements of Antenna Array

To investigate the effects of changing the phase difference between the array elements, the first step is to fix the relative amplitude of current (I_2/I_1) and spacing (d) between the consecutive elements and then observe the effect on the radiation pattern. Now, let us assume that the current ratio (I_2/I_1) is equal to one and the phase of the first element (δ_1) is set to zero. After using these values in the expression of total electric field, we have

$$E = k_0[1 + e^{j\beta d \cos^{-1} \varphi}] \quad (2.28)$$

After taking $e^{j\beta d/2 \cos \varphi}$ common from the above expression, the equation for electric field is given as

$$E = [\cos(\beta d \cos \varphi + \delta/2)] \quad (2.29)$$

From the equation 2.29, it is examined that by taking value of cosine equal to zero or a multiple of pi, the normalized radiation pattern gives the maximum value. So, this can be written as

$$(\beta d \cos \varphi + \delta)/2 = 0, \pi, 2\pi, \dots \quad (2.30)$$

Now let us assume the case when

$$(\beta d \cos \varphi + \delta)/2 = 0 \quad (2.31)$$

After simplification the above expression is written as

$$\cos \varphi = -\delta/\beta d \quad (2.32)$$

From the above expression, it is clear that $\varphi = \varphi_{max}$, because this gives the maximum tilt of the radiation pattern.

$$\cos \varphi_{max} = -\delta/\beta d \quad (2.33)$$

Therefore, from the above discussion it is clear that by changing the phase difference between the elements of array, the direction of main beam can be controlled.

Now let us assume the following examples to understand the phase difference effects on radiation pattern. Suppose the phase difference between the two consecutive elements of the array is zero i.e., all antenna array elements are excited with the same phase.

$$\varphi_{max} = \cos^{-1}(-0/\beta d) = \cos^{-1}(0) \quad (2.34)$$

Thus, the direction of a main beam is at

$$\varphi_{max} = \pi/2 \quad (2.35)$$

Now let us assume another example in which the phase difference is set to be $-\beta d$. The equation of the φ_{max} is given as

$$\varphi_{max} = \cos^{-1}(-(-\beta d)/\beta d) = \cos^{-1}(1) \quad (2.36)$$

Thus, the direction of a main beam is

$$\varphi_{max} = \pi, 0 \quad (2.37)$$

As a result, it is clear that by changing the phase difference between the two elements of the antenna array, direction of main beam can be changed.

2.6 Lumped Element Modeling of DRA

Modeling of an equivalent lumped element circuit of antennas has become an attraction for designers; it validates the antenna's feasibility. The lumped element circuit for any antenna can be modeled by replacing all antenna components by their equivalent RLC blocks. Over the past several years, several circuits of microstrip patch antennas and dielectric resonator antennas have been assembled to validate the CST or HFSS software's designs such as microstrip fed slot antenna [101-102], probe fed circular patch antenna [103], conical DRA [104], cylindrical DRA [105-106] and aperture coupled rectangular DRA [35].

The equivalent lumped model circuit of microstrip patch antenna array is presented in [107]. The electrical model of single element microstrip patch antenna is depicted in Figure 2.15. The electric model is used to validate the microstrip patch antenna, designed using HFSS at 2.4 GHz band.

The novel four elements aperture coupled rectangular shaped DRA array has been introduced to check the antenna array feasibility for X-band [36]. The equivalent lumped element circuit of single element aperture coupled DRA is depicted in Figure 2.16, where A represents the microstrip transmission line RLC block, B represents the aperture slot RLC block and C represents the equivalent circuit of DRA.

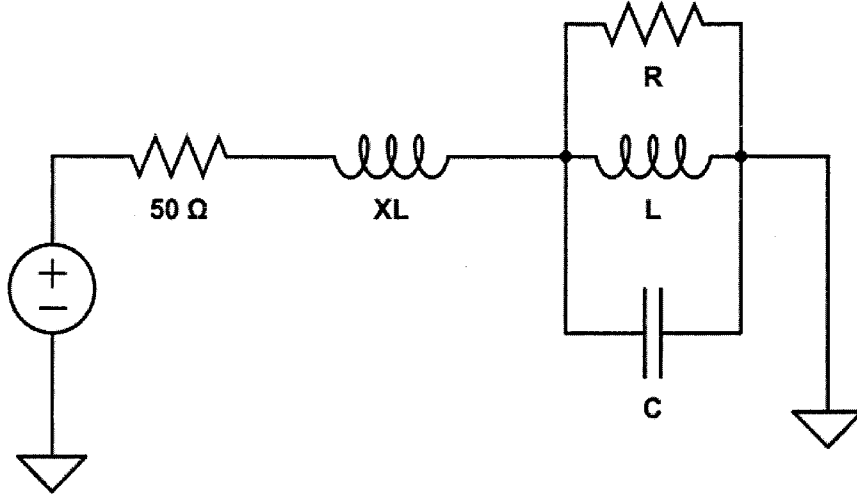


Figure 2.15. The electrical model of rectangular patch antenna.

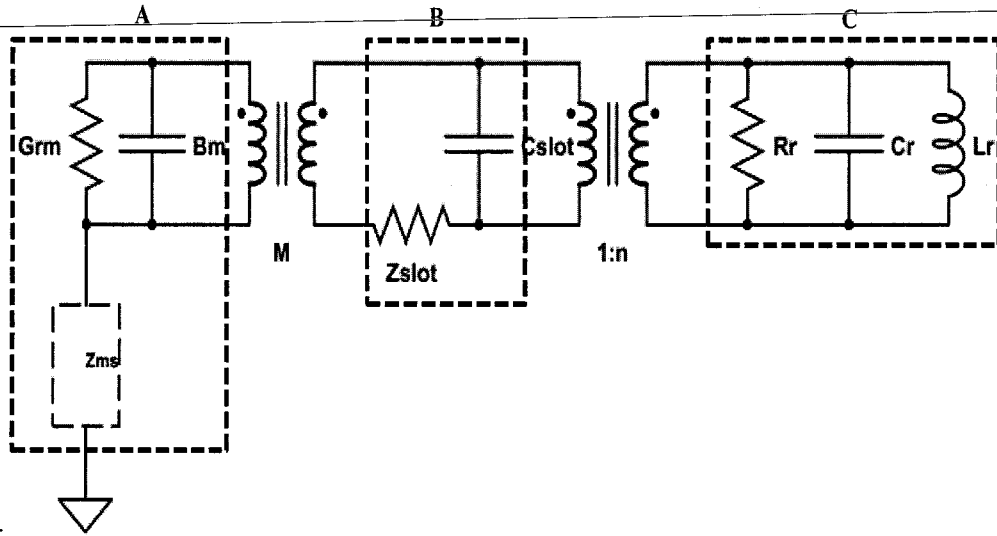


Figure 2.16. Equivalent circuit of aperture coupled DRA.

The equations for resonant resistance R_r , inductance L_r and capacitance C_r for the dielectric resonator are given as [108].

$$R_r = \frac{2n^2 z_0 s_{11}}{1 - s_{11}} \quad (2.38)$$

$$C_r = \frac{Q_0}{\omega_0 R_r} \quad (2.39)$$

$$L_r = \frac{1}{C_r \omega_0^2} \quad (2.40)$$

where S_{11} is the reflection coefficient, z_0 is the characteristic impedance, Q_0 is the quality factor and n is the coupling magnitude between excitation source and dielectric resonator. It is mentioned in [108], that the value of R_r is to be chosen properly because it plays an important contribution in determining the value of L_r and C_r .

The equation for Z_{slot} is given as

$$Z_{slot} = Z_c \frac{2R}{1-R} + jZ_c \cot(\beta_f L_t) \quad (2.41)$$

where Z_c is the characteristic impedance of transmission line, R is the voltage reflection coefficient, β_f is the propagation constant and L_t is the stub length.

The next step is to find the input impedance of the transmission line [101]. The input admittance Y_m is equal to $G_{rm} + jB_m$ where G_{rm} is the equivalent radiation conductance and B_m is the susceptance of the fringing capacitance of the microstrip. The expressions of G_{rm} and B_m are:

$$G_m = \frac{160\pi^2 h^2}{Z_{cm}^2 \lambda_0^2 \epsilon_{cm}} \quad (2.42)$$

$$B_m = \frac{wl_{eq}\sqrt{\epsilon_{cm}}}{cZ_{cm}} \quad (2.43)$$

where h is the substrate height, Z_{cm} is the characteristic impedance of the microstrip, ϵ_{cm} is the effective dielectric constant, l_{eq} is the equivalent extra length of microstrip and c is the velocity of light.

The equivalent lumped element circuit of mutual coupled rectangular shaped patched antenna array has been introduced in [107]. In this array, the mutual coupling between the rectangular shaped patch antennas are represented by coupling capacitor C_c . The equation of the coupling capacitance is given as

$$C_c = C_{air} + C_{gd} \quad (2.44)$$

where C_{air} and C_{gd} represents the coupling between the elements in the air and in the dielectric material. For radiating elements placed on the ground plane, the total coupling capacitance is the summation of gap capacitance in air (C_{air}), fringe capacitance (C_{fringe}) and overlapped capacitance ($C_{overlapped}$). The C_{fringe} is the capacitance from the edges of the radiating elements, while the overlapped capacitance ($C_{overlapped}$) is formed in the overlapped area of radiating element and ground plane.

The equation for air gap capacitance between the array elements is given as

$$C_{air} = \begin{cases} \frac{\epsilon_0}{\pi} \ln \left(2 \frac{1+\sqrt{K'}}{1-\sqrt{K'}} \right), \\ \frac{\pi \epsilon_0}{\ln \left(2 \frac{1+\sqrt{K'}}{1-\sqrt{K'}} \right)} \end{cases} \quad 0 \leq K^2 \leq 0.5 \quad (2.45)$$

where

$$K' = \sqrt{1 - K^2} \quad (2.46)$$

In [107], by using the rectangular patch antenna design, the equation for constant K is given as

$$K = \frac{S}{S+2W} \quad (2.47)$$

where S is the separation between the elements and W is the width of the patch.

In [109], width of the rectangular patch i.e., $W = 2r_0$ for the cylindrical type. Hence the design which applies cylindrical type, the equation for constant K is given as

$$K_c = \frac{S}{S+4r_0} \quad (2.48)$$

where S represents the distance between the elements and r_0 is the radius of the cylindrical type. The equation of fringe capacitance C_{fringe} between the radiating element and ground plane is given as

$$C_f = K_{av} \epsilon_0 \frac{(d+at) \pi r^2}{2d} \quad (2.49)$$

where K_{av} is the average of dielectric relative permittivity between radiating element and ground plane, ϵ_0 is the permittivity of vacuum, d is the gap between radiating element and ground plane, α is the effective area factor, t is the thickness of the radiating element and r is the radius of the radiating element.

The overlapped capacitance $C_{overlapped}$ between the radiating element and ground plane is given as

$$C_{overlapped} = K \epsilon_0 \frac{A}{d} \quad (2.50)$$

where K is relative dielectric coefficient, ϵ_0 is the vacuum permittivity, A is overlap area and d is distance between two radiating element and ground plane.

2.7 Conclusion

The theoretical background and characteristics of single element DRA along with its equivalent circuit modeling has been reviewed. To enhance the performance of single element DRA, linear, planar and reflect array configurations have been implemented. The linear DR antenna array has established itself in various applications at high and low frequencies. Linear arrays with large number of elements has been used, but with limitations in bandwidth for WLAN and X band applications as presented in section 2.4.2.

In the proposed work, the three element cylindrical dielectric resonator antenna arrays are designed to enhance the bandwidth for ISM band applications. The equivalent lumped element circuit of the small size antenna array is designed by using ADS and

Matlab programs. The small size array design methodology and its results are discussed in Chapter 3 and Chapter 4 respectively.

CHAPTER 3

METHODOLOGY

3.1 Introduction

Chapter three presents the design methodology of single element CDRA, single band CDRA array, dual band CDRA array and small size high gain and wide band CDRA array. The design methodology covers the multiple steps taken to achieve the objectives of the proposed work. In this chapter, the design parameters for single element aperture coupled CDRA is being determined before it is proceed to achieve high gain and wide band CDRA array structure. The coupling slot technique embedded under 50 Ω microstrip transmission line is characterized as tuning mechanism towards three array element design. The methodology used in the research work describes the steps taken to accomplish the proposed objectives.

3.2 Array Design Methodology

The following sections describe all the steps taken, related to design methodology; which lead to the research objective. There are four main steps involved in the research work pertaining to design methodology; these include design process, the development of the equivalent lumped model circuit, fabrication process and finally the testing and measurements. The flow chart of the methodology to accomplish the research objective is depicted in Figure 3.1.

As been discussed extensively in the literature reviews, an antenna is the most important component in wireless communication system. In today's modern communication era, highly efficient, small size, high gain and wide bandwidth antennas are required. The communication devices can be miniaturized by using low

profile antenna. Four antennas are being developed and designed on the basis of the design methodology procedure and it is shown in Figure 3.2.

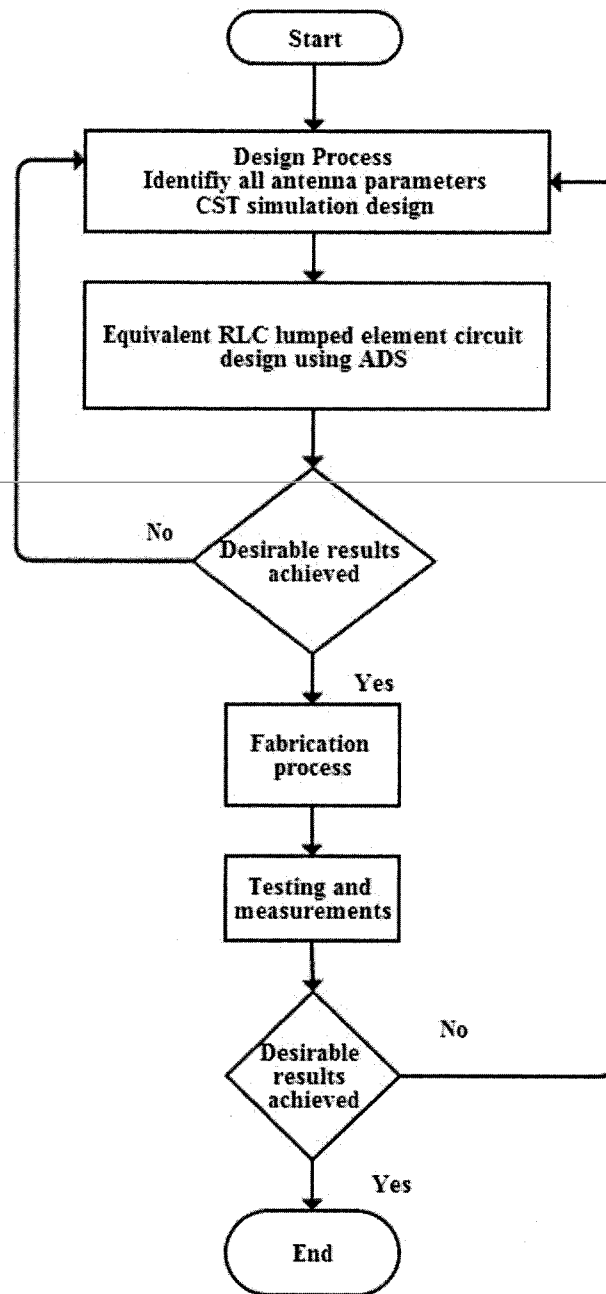


Figure 3.1. Flow chart of the proposed methodology.

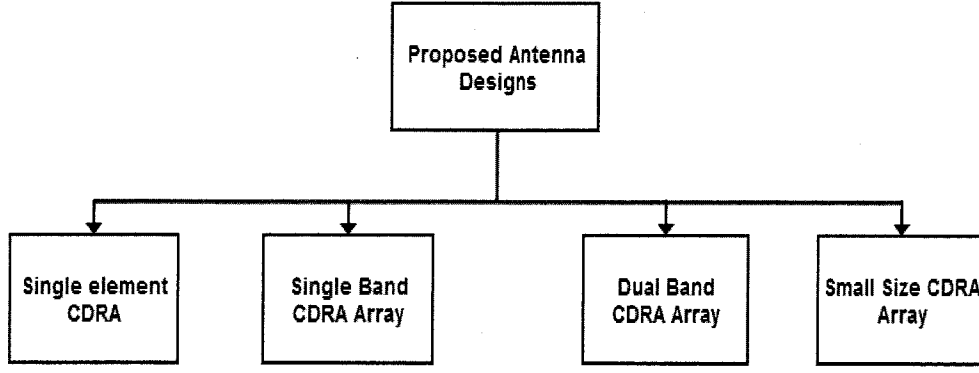
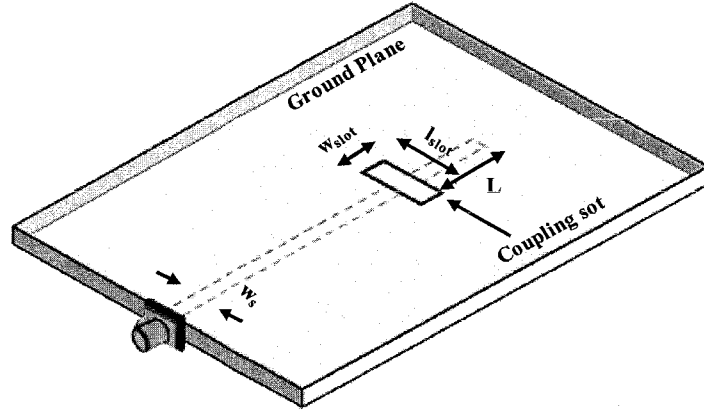


Figure 3.2. Antenna designs presented in the proposed work.

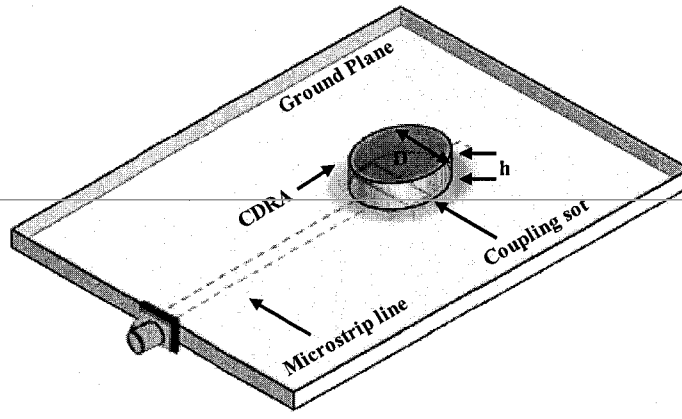
3.3 Characterization of the Single Element CDRA with Aperture Couple Technique

The characteristics of single element CDRA are required to be investigated and studied to proceed toward the designing of CDRA array. The performance of single element CDRA dictates the configuration of array antenna. The CDRA array is the one possible solution to enhance the limited gain of single element CDRA. The important step in the characterization of a single element design is to determine its different design parameters. The width of the microstrip transmission line, w_s , coupling slot dimensions (l_{slot} , w_{slot}), diameter and height of the CDR (D , h) permittivity and thickness of the substrate (ϵ_s , h_{sub}) are the single element CDRA design parameters, that need to be found. The corresponding antenna parameters are derived on the basis of required frequency or for specific application. The Computer Simulation Technology (CST) software is used to design, simulate and analyzed the characteristics of 3D structure of single element CDRA.

The single element CDRA is designed for IEEE 802.11a WLAN application. With CST the design is being simulated and finalized. The proposed geometries of the rectangular aperture slot and single element CDRA are depicted in Figure 3.3. The FR4 substrate with a thickness and permittivity of 1.565 mm and 4.9 respectively is used as a PCB board in the proposed single element CDRA. The $50\ \Omega$ microstrip transmission line of width $w_s = 2.61$ mm is used to excite the coupling slot etched on



(a)



(b)

Figure 3.3. The geometry of single element aperture coupled cylindrical DRA.

the ground plane. The equations used to calculate the width of a microstrip transmission line are given as

$$\epsilon_{eff} = \frac{\epsilon_s + 1}{2} + \frac{\epsilon_s - 1}{2\sqrt{1 + 12(h/w)}} \quad (3.1)$$

$$Z_0 = \frac{120\pi}{\sqrt{\epsilon_{eff}}[(w/h) + 1.393 + 0.667\ln(1.444 + w/h)]} \quad (3.2)$$

where h is the height of the substrate, Z_0 is the impedance of microstrip line and ϵ_s is the permittivity of substrate. The CDRA with diameter $D = 15.5$ mm, height $h = 3.0$ mm and permittivity $\epsilon_r = 55$ is used as a radiating element and it is placed on the top of the coupling slot. The initial slot length and width are determined by using equations (2.12) to

(2.14) which are electrically small in size. Thus the parametric study is carried out to improve the antenna performance and to achieve the optimum results. The coupling slot is placed at a distance $\frac{\lambda_g}{4} = 6.66$ mm from the microstrip line edge. The equation to calculate the value of λ_g is given as [2]

$$\lambda_g = \frac{c}{f\sqrt{\epsilon_s}} \quad (3.3)$$

where ϵ_s is the permittivity of the substrate, c is the speed of light (3×10^8 m) and f is the resonance frequency.

The parametric study of the antenna tuning parameters such as slot length and width, position of CDR on the coupling slot and position of the coupling slot from the microstrip transmission line edge is carried out to improve the antenna performance. The effects of tuning parameters on the central frequency and the bandwidth of antenna are analyzed and investigated. The complete dimensions of single element aperture coupled CDRA are depicted in Table 3.1.

Table 3.1. Dimensions of single element aperture coupled CDRA.

Dimensions	Length (mm)
D	15.50
H	3.00
l_{slot}	14.00
w_{slot}	4.00
w_s	2.61
L	6.67

3.3.1 Development of Equivalent Lumped Element Circuit for Single Element CDRA

An equivalent lumped element circuit of single element CDRA is modeled to validate the antenna's operation, after the preliminary estimation and initial designing using CST Microwave Studio. The Advanced Design System (ADS) software is used to model the equivalent circuit of the antenna design. The equivalent lumped model of proposed antenna is designed by transforming each antenna component into its equivalent RLC block such as microstrip transmission line, coupling slot and DRA. The lumped element circuit of the proposed single element CDRA is depicted in Figure 3.4. The block *A*, *B* and *C* represent the RLC equivalent circuit of a microstrip transmission line, coupling slot and DRA respectively. The Matlab programs of various equations (2.38) to (2.43) are used to determine the RLC parameters of the equivalent lumped model circuit. The Matlab programs used to calculate the electrical circuit parameters are presented in Appendix A. The values of R_r , C_r , L_r , Z_{slot} , C_{slot} , G_{rm} and B_{rm} at the desired frequency for single element CDRA is tabulated in Table 3.2.

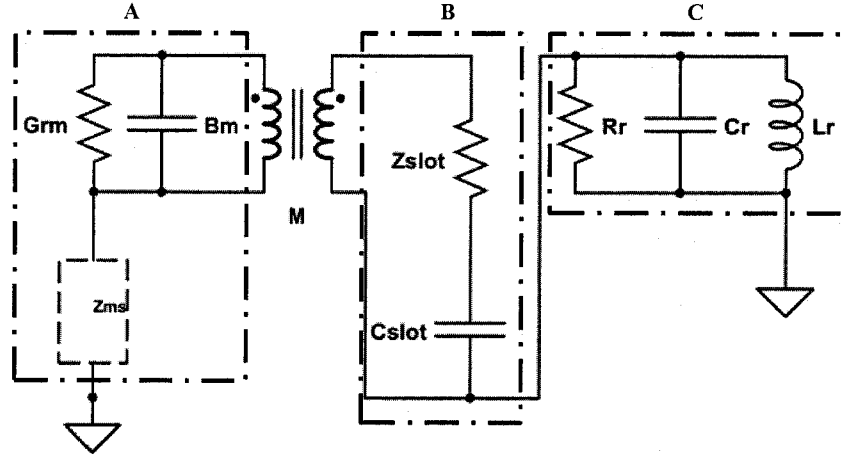


Figure 3.4. Equivalent circuit of single element aperture coupled CDRA.

The effects of parametric study of antenna tuning parameters, on the equivalent lumped circuit RLC values are also investigated by using equations (2.38) to (2.43). The analysis of parametric study using equivalent circuit helps in the understanding of RLC relation with 3D antenna structure and return loss response. The reliability of the proposed antenna equivalent lumped model and its parametric study is verified by comparing its return loss (S_{11}) to those obtained through CST design.

Table 3.2. Parameters of equivalent lumped element circuit of single element CDRA.

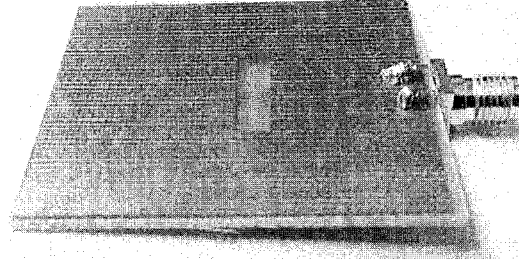
Parameters	Values
$R_r (\Omega)$	90.0000
$L_r (\text{pH})$	103.9400
$C_r (\text{pF})$	8.8400
$Z_{slot} (\Omega)$	33.5100
$C_{slot} (\text{pF})$	0.9349
$B_m (\text{F})$	0.0024
$G_{rm} (\Omega)$	0.0002
$Z_{ms} (\Omega)$	50.0000

3.3.2 Fabrication and Measurements of Single Element CDRA

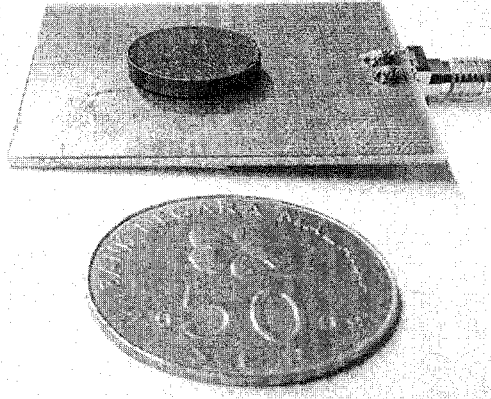
The initial antenna design is fabricated upon achieving satisfactory simulation results by using CST and ADS. The CDR is fabricated at the School of Material and Resources Universiti Sains Malaysia (USM) after the extensive studies. The CCTO ($\text{CaCu}_3\text{Ti}_4\text{O}_{12}$) dielectric material with permittivity of 55 is used to fabricate the CDR. For the substrate, the FR4 board with permittivity $\epsilon_s = 4.9$ and thickness $h_{sub} = 1.565$ mm is being implemented. The final antenna circuit design is fabricated by utilizing the PCB fabrication Lab and Wireless Communication Lab facilities at the Universiti Teknologi PETRONAS, which is carried out by providing the layout of the design to a fabrication Lab in the form of gerber file. The fabricated geometry of the proposed single element CDRA is depicted in Figure 3.5.

The antenna measurements are performed by using Wireless Communication Lab facilities in Universiti Teknologi PETRONAS. The E8363C Voltage Network Analyzer (VNA) is used to measure the return loss (S_{11}) of the fabricated antenna prototype. In addition, the rotator and VNA are used to measure the radiation pattern of the antenna prototype. The validity of fabricated prototype is verified by comparing measured results against those obtained through the CST and ADS results. The signal strength of the proposed design at different distances is also measured by using signal generator and Field-Fox handheld spectrum analyzer. The procedures followed to measure the return loss (S_{11}),

radiation pattern of the proposed antenna and open space signal strength are presented in Appendix B, Appendix C and Appendix D respectively.



(a)



(b)

Figure 3.5. Fabricated prototype of single element aperture coupled CDRA.

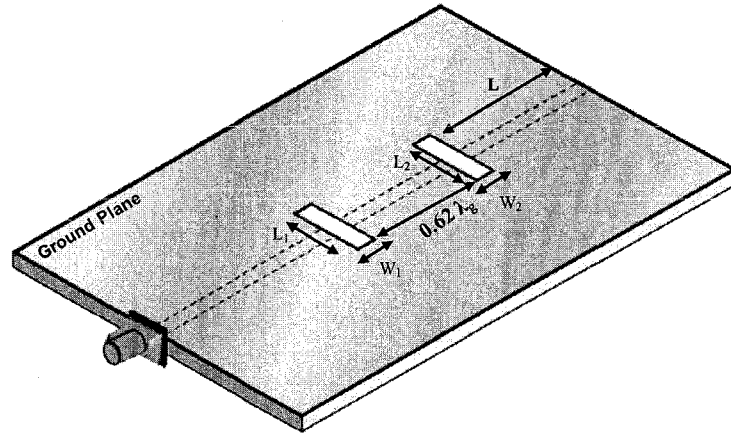
3.4 Characterization of the Single Band CDRA Array

The antenna array configuration is used to enhance the performance of single element antenna. The single band CDRA array is designed to enhance the performance of the single element CDRA presented in section 3.2. The important step in the characterization of the single band CDRA array is to determine its design parameters. The width of the microstrip transmission line, w_s , coupling slot dimensions (l_{slot} , w_{slot}), diameter and height of the CDR (D , h), inter-slot distance (d_{slot}), inter-element distance (d_{DRA}), permittivity and thickness of the substrate (ϵ_s , h_{sub}) are the antenna array design parameters, that have to

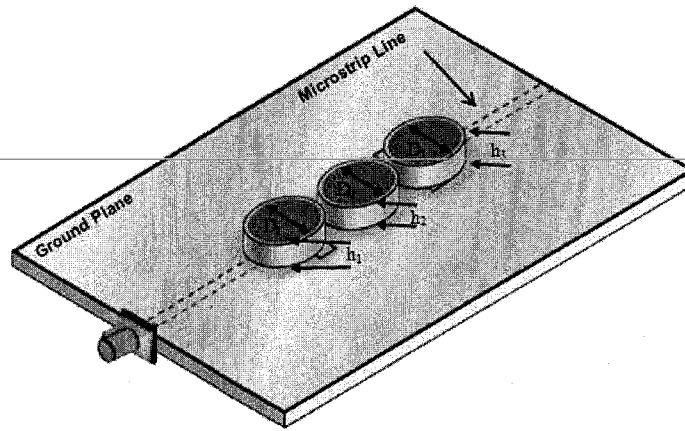
be determine before designing the CDRA array. The CST software is used to design and simulate the 3D structure of the single band CDRA array.

The single band CDRA array is designed to operate for 802.11a WLAN application. With CST the design is being simulated and finalized. The proposed geometries of the single band CDRA array and rectangular aperture slots are depicted in Figure 3.6. The single band CDRA array consists of three CDRs of diameter $D_1 = D_2 = D_3 = 15.5$ mm, height $h_1 = h_2 = h_3 = 3.0$ mm and permittivity of $\epsilon_r = 55$. The two aperture slots etched on the ground plane with thickness and permittivity of 0.787 mm and $\epsilon_s = 2.2$ respectively, are used to excite the CDRs, while 50 Ω microstrip transmission line of width 2.33 mm is used to excite the aperture slots. The dimensions of microstrip transmission line are calculated by using the transmission line equations (3.1) and (3.2). The coupling slots etched on the ground plane are used to excite the top and bottom radiating elements of the CDRA array. The middle radiating element is excited through the mutual coupling of the two neighboring elements. The initial calculated slot length and width are 0.44 mm and 0.088 mm respectively, determine by using equations (2.12) to (2.14) which are electrically small in size. Thus the parametric study on the slot length and width is carried out to find the optimum results.

The distance between the feeding sources is the most important parameter for antenna array design. To avoid the mutual coupling effects between source points, the distance between the exciting sources is kept to be of the order of $0.5\lambda_g$ to λ_g . The value of λ_g is calculated by using the equation (3.3). From inter-slot distance analysis, the optimum distance found between the aperture slots is $0.63\lambda_g$. The distances between the consecutive radiating elements are $0.263\lambda_{air}$ and $0.268\lambda_{air}$.



(a)



(b)

Figure 3.6. The geometry of the single band aperture-coupled CDRA array
(a) Rectangular slots without DRA (b) Complete proposed design.

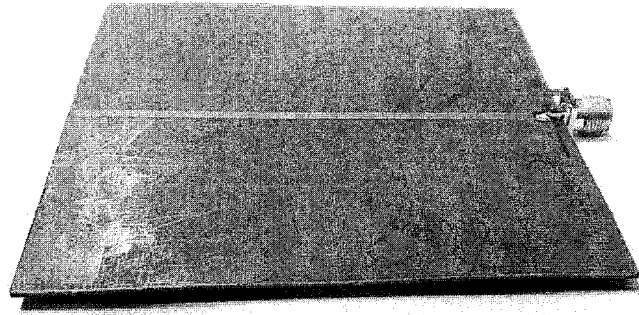
The parametric study of the antenna tuning parameters such as slot length and width, inter-slot distance and inter-element distance is carried out to improve the antenna performance. The effects of tuning parameters on the central frequency and the bandwidth of antenna are analyzed and investigated. The detail dimensions of rectangular shaped slots and antenna elements are depicted in Table 3.3.

Table 3.3. The dimensions of single band CDRA array.

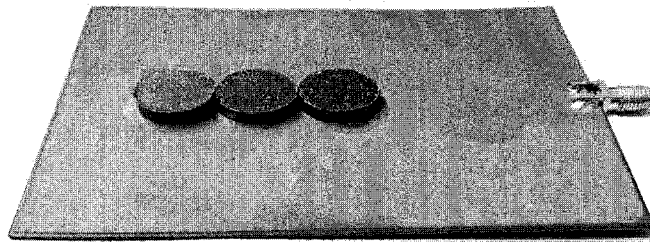
Parameters	Length (mm)
L_1, L_2	14.0
w_1, w_2	4.0
D_1, D_2, D_3	15.5
h_1, h_2, h_3	3.0
$0.62\lambda_g$	25.0
L	$\lambda_g/2$

3.4.1 Fabrication and Measurements of Single Band CDRA Array

The initial single band CDRA array design is fabricated upon achieving satisfactory simulation results by using CST. The fabricated prototype of the single band CDRA array is depicted in Figure 3.7. The CDRs are fabricated at the School of Material and Resources Universiti Sains Malaysia (USM) after the extensive studies. The CCTO ($\text{CaCu}_3\text{Ti}_4\text{O}_{12}$) dielectric material with permittivity of 55 is used to fabricate the CDRs. For the substrate, the Rogers's board with the parameters of permittivity $\epsilon_s = 2.2$ and thickness $h_{sub} = 0.787$ mm is being implemented. The final single band array circuit design is fabricated by utilizing the PCB fabrication Lab and Wireless Communication Lab facilities at the Universiti Teknologi PETRONAS, which is carried out by providing the layout of the design to a fabrication Lab in the form of gerber file.



(a)



(b)

Figure 3.7. Fabricated prototype of the single band CDRA array (a) Back view
(b) Complete proposed design.

The antenna measurements are performed by using Wireless Communication Lab facilities in Universiti Teknologi PETRONAS. The E8363C Voltage Network Analyzer (VNA) is used to measure the return loss (S_{11}) of the fabricated antenna prototype. In addition, the rotator and VNA are used to measure the radiation pattern of the antenna prototype. The validity of fabricated prototype is confirmed by comparing measured results against those obtained through the CST results. The signal strength of the proposed CDRA array at different distances is also measured by using signal generator and Field Fox handheld spectrum analyzer. The procedures followed to measure the return loss (S_{11}), radiation pattern of the proposed antenna and open space signal strength are presented in Appendix B, Appendix C and Appendix D respectively.

3.5 Characterization of Dual Band CDRA Array

The dual band antenna covers the two frequency bands and can be used for different application. When one frequency band is not within range, other frequency band can be used. The important step in the characterization of the proposed dual band CDRA array is to determine the array design parameters. The width of the microstrip transmission line, w_s , coupling slot dimensions (l_{slot} , w_{slot}), diameter and height of the CDR (D , h), inter-slot distance d_{slot} , inter-element distance d_{dra} , permittivity and thickness of the substrate (ϵ_s , h_{sub}). The size of dual band antenna array and technique to excite the radiating elements are same as used for single band CDRA array presented in section 3.4. The CST software is used to design and simulate the 3D structure of the dual band CDRA array. The proposed geometries of the dual band CDRA array and rectangular aperture slots are depicted in Figure 3.8.

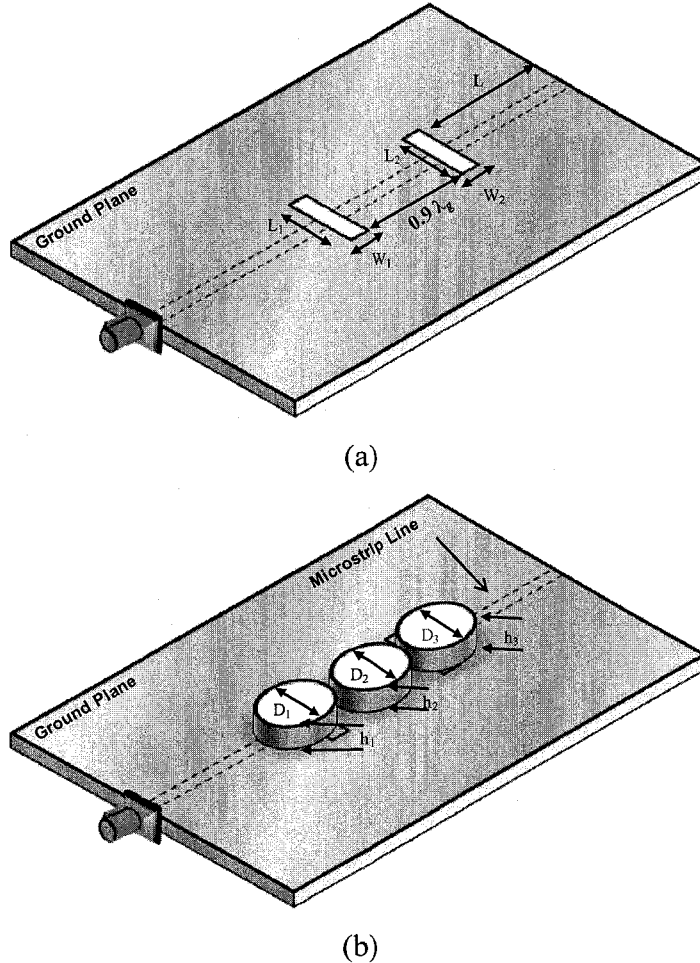


Figure 3.8. The geometry of the dual band CDRA array (a) Rectangular slots and (b) Front view.

The dual band CDRA array is designed for IEEE 802.11 a/b WLAN applications. With CST, the design is being simulated and finalized. The initial important step in the

designing of dual band CDRA array is to design single band array antenna working at 5.0 GHz band, then by using metallic top-loaded mechanism resonance at lower band is achieved. The dual band CDRA array consists of three CDRs of diameter $D_1 = D_2 = D_3 = 15.5$ mm, height $h_1 = h_2 = h_3 = 3.0$ mm and permittivity of $\epsilon_r = 55$. The two aperture slots etched on the ground plane of thickness and permittivity of 1.565 mm and $\epsilon_s = 4.9$ respectively, are used to excite the CDRs, while 50 Ω microstrip transmission line of width 2.61 mm is used to excite the aperture slots. The dimensions of microstrip transmission line are calculated by using the transmission line equations (3.1) and (3.2). The coupling slots etched on the ground plane are used to excite the top and bottom radiating elements of the CDRA array. The separation between the consecutive elements is $0.263\lambda_{air}$ and $0.268\lambda_{air}$ respectively. The middle radiating element is excited through the mutual coupling of the two neighboring elements. The initial slot length and width are determined by using equations (2.12) to (2.14). Thus, the parametric study is carried out to achieve the optimum results. The distance between the coupling slots is $0.9\lambda_g$. The value of λ_g can be calculated by using equation (3.3).

The analysis and characterization of the antenna tuning parameters such as the length and width of the coupling slot, diameters of metallic top-loaded and the distance between the coupling slots are performed to improve the antenna performance. The effects of tuning parameters on the central frequency and the bandwidth of antenna are analyzed and investigated. The complete dimensions of the dual band CDRA array are depicted in Table 3.4.

Table 3.4. Dimensions of dual band CDRA array.

Parameters	Length (mm)
L_1, L_2	14.0
w_1, w_2	4.0
D_1, D_2, D_3	15.5
h_1, h_2, h_3	3.0
$0.9\lambda_g$	25.0
L	$0.95\lambda_g$

3.5.1 Fabrication and Measurements of Dual Band CDRA Array

The antenna circuit of the dual band CDRA array is fabricated after a successful simulation at the 2.4 GHz and 5.0 GHz bands by using CST. The CDRs are fabricated at the School of Material and Resources Universiti Sains Malaysia (USM) after the extensive studies. The CCTO ($\text{CaCu}_3\text{Ti}_4\text{O}_{12}$) dielectric material with permittivity of 55 is used to fabricate the CDRAs. The metal sheets of diameter 15.5 mm are glued on the top of the CDRAs to achieve the resonance of 2.4 GHz band and 5.0 GHz band. For the substrate, the FR4 board with the parameters of permittivity $\epsilon_s = 4.9$ and thickness $h_{sub} = 1.565$ mm is being implemented. The final dual band array circuit design is fabricated by utilizing the PCB fabrication Lab and Wireless Communication Lab facilities at the Universiti Teknologi PETRONAS, which is carried out by providing the layout of the design to a fabrication Lab in the form of gerber file. The fabricated geometry of the proposed single element CDRA is depicted in Figure 3.9.

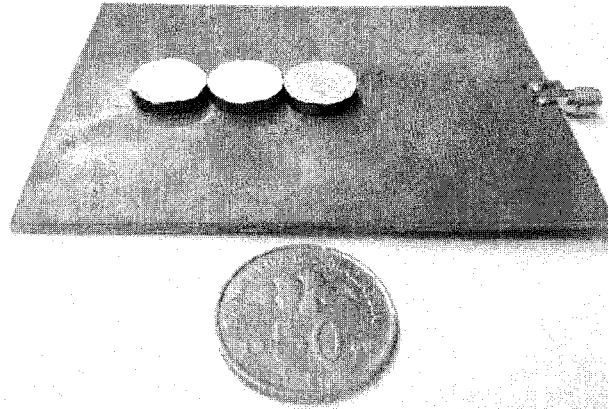


Figure 3.9. Fabricated prototype of the dual band CDRA array.

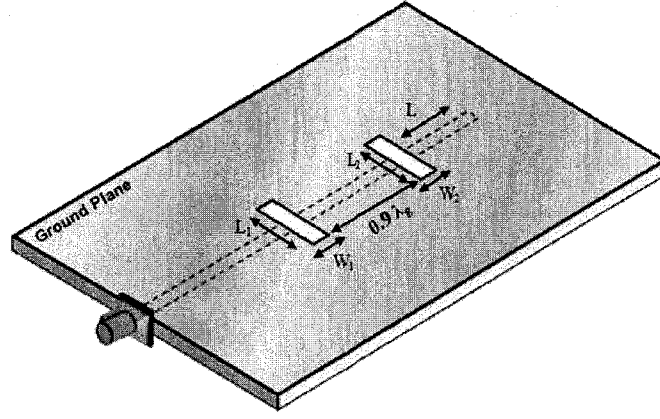
The antenna measurements are performed by using Wireless Communication Lab facilities in Universiti Teknologi PETRONAS. The E8363C Voltage Network Analyzer (VNA) is used to measure the return loss (S_{11}) of the fabricated antenna prototype. In addition, the rotator and VNA are used to measure the radiation pattern of the antenna prototype. The reliability of fabricated prototype is verified by comparing measured results against those obtained through the CST results. The signal strength of the proposed dual band CDRA array at different distances is also measured by using signal generator and Field Fox handheld spectrum analyzer. The procedures followed to measure the return loss

(S_{11}), radiation pattern of the proposed antenna and open space signal strength are presented in Appendix B, Appendix C and Appendix D respectively.

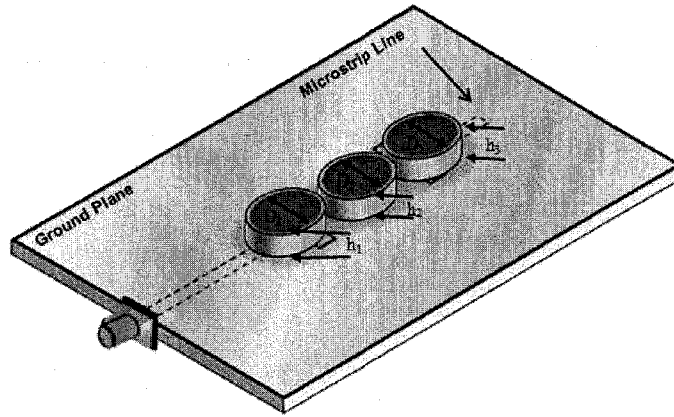
3.6 Characterization of the Small size, Wide Band and High Gain CDRA Array

In modern communication era, communication industry demands small size, wideband, high gain and highly efficient antennas. By using antenna with corresponding properties, communication devices can be miniaturized. The proposed small size CDRA array design possesses the properties of small size, wide band and high gain as compared to the array designs presented in section 3.4 and section 3.5. The important step in the characterization of a small size CDRA array is to determine its different design parameters. The width of the microstrip transmission line, w_s , coupling slot dimensions (l_{slot} , w_{slot}), diameter and height of the CDR (D , h), stub extension length, L , inter-slot distance, d_{slot} , inter-element distance, d_{dra} , permittivity and thickness of the substrate (ϵ_s , h_{sub}) are the small size CDRA array design parameters, that need to be found. The corresponding antenna parameters are derived on the basis of required frequency or for specific application. The Computer Simulation Technology (CST) software is used to design, simulate and analyzed the characteristics of 3D structure of small size CDRA array.

The small size CDRA array is designed for IEEE 802.11a WLAN application. With CST the design is being simulated and finalized. The small size CDRA array consists of three CDRs of diameter $D_1 = D_2 = D_3 = 15.5$ mm, height $h_1 = h_2 = h_3 = 3.0$ mm and permittivity of $\epsilon_r = 55$. The two coupling slots etched on the ground plane of the FR4 substrate with a thickness and permittivity of 1.565 mm and $\epsilon_s = 4.9$. The coupling slots are used to excite the two CDRs (i.e., top and bottom) through 50 Ω microstrip transmission line with width of 2.61 mm, while the middle radiating element is excited through the mutual coupling of the two neighboring elements. The distance between the consecutive array elements is $0.264\lambda_{air}$ and $0.265\lambda_{air}$. The dimensions of microstrip transmission line are calculated by using the transmission line equations (3.1) and (3.2). The initial slot length and width are determined by using equations (2.12) to (2.14) which are electrically small in size. Thus, the parametric study is carried out to find the optimum bandwidth. The two aperture slots are etched at a distance of $0.9\lambda_g$.



(a)



(b)

Figure 3.10. The geometry of the small size CDRA array (a) Rectangular slots and (b) Front view.

The equation used to calculate the stub length L of microstrip line depicted in Figure 3.10 (a) is given as [2]

$$L = \frac{\lambda_g}{4} \quad (3.4)$$

where λ_g can be calculated by using equation (3.3).

The inter-slot spacing is one of the most important parameter during antenna array design. The distance between the coupling slots is $0.9\lambda_g$. The value of λ_g can be calculated by using equation (3.3). The analysis and characterization of the antenna tuning parameters such as slot length and width, position of CDR on the coupling slot and position of the

coupling slot from the microstrip transmission line edge are performed to improve the antenna performance. The effects of tuning parameters on the central frequency and the bandwidth of antenna are analyzed and investigated. The complete dimensions of the small size CDRA array are depicted in Table 3.5.

Table 3.5. Dimensions of small size CDRA array.

Parameters	Length (mm)
L_1, L_2	20.00
w_1, w_2	4.00
d_1, d_2, d_3	15.50
h_1, h_2, h_3	3.00
L	6.67
$0.9\lambda_g$	25.00

3.6.1 Development of Equivalent Lumped Element Circuit for Small Size CDRA Array

An equivalent lumped element circuit of small size aperture and the mutual coupled CDRA array is modeled to validate the antenna's operation, after preliminary estimation and the initial designing using CST Microwave Studio. The Advanced Design System (ADS) software is used to model the equivalent circuit of the antenna design. The equivalent lumped model of proposed antenna is designed by transforming each antenna component into its equivalent RLC block such as microstrip transmission line, coupling slot and DRA. The lumped element circuit of the proposed small size CDRA is depicted in Figure 3.11. The block A , B and C represent the RLC equivalent circuit of a top, middle and bottom radiating elements respectively, while the blocks D and E characterize the coupling between the array elements. The Matlab programs of various equations (2.38) to (2.50) are used to determine the RLC values of the equivalent lumped model circuit. The Matlab programs used to calculate the electrical circuit parameters are presented in Appendix A.

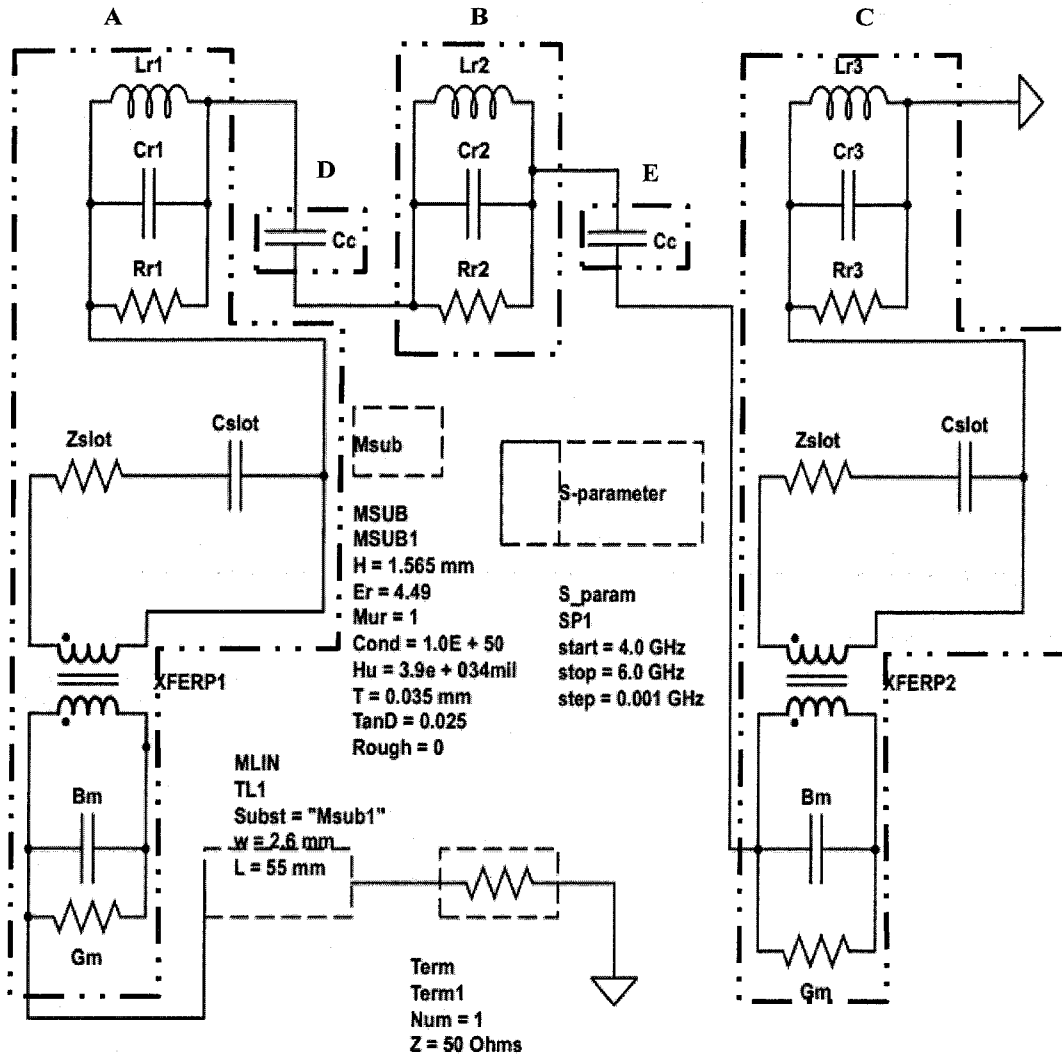
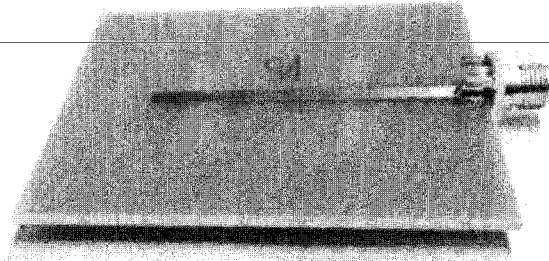


Figure 3.11. Proposed equivalent lumped element circuit of the small size CDRA array.

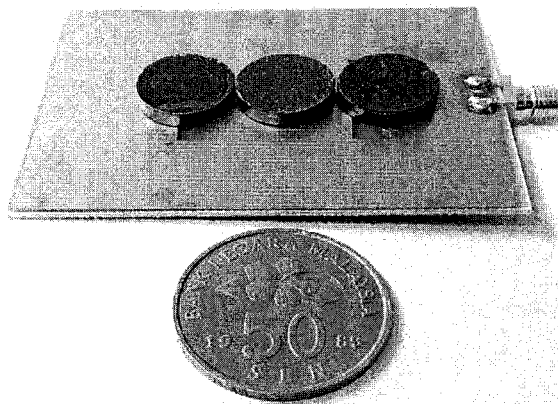
The effects of parametric study of antenna tuning parameters, on the RLC values of equivalent lumped circuit are also investigated by using equations (2.38) to (2.50). The analysis of parametric study using equivalent circuit helps in the understanding of RLC relation with 3D antenna parameters and return loss response. The reliability of the proposed antenna equivalent lumped model and its parametric study is verified by comparing its return loss (S_{11}) to those obtained through CST design.

3.6.2 Fabrication and Measurements of Small Size CDRA Array

The antenna circuit of the small CDRA array is fabricated upon achieving satisfactory simulation results at the 5.0 GHz band by using CST and ADS. The CDRs are fabricated at the School of Material and Resources Universiti Sains Malaysia (USM) after the extensive studies. The CCTO ($\text{CaCu}_3\text{Ti}_4\text{O}_{12}$) dielectric material with permittivity of 55 is used to fabricate the CDRs. For the substrate, the FR4 board with the parameters of permittivity $\epsilon_s = 4.9$ and a thickness $h_{sub} = 1.565$ mm is being implemented. The final antenna circuit design is fabricated by utilizing the PCB fabrication Lab and Wireless Communication Lab facilities at the Universiti Teknologi PETRONAS, which is carried out by providing the layout of the design to a fabrication Lab in the form of gerber file. The fabricated geometry of the proposed single element CDRA is depicted in Figure 3.12.



(a)



(b)

Figure 3.12. Fabricated design of the small size CDRA array.

The antenna measurements are performed by using Wireless Communication Lab facilities in Universiti Teknologi PETRONAS. The E8363C Voltage Network Analyzer (VNA) is used to measure the return loss (S_{11}) of the fabricated antenna prototype. In addition, the rotator and VNA are used to measure the radiation pattern of the antenna prototype. The reliability of fabricated prototype is confirmed by comparing its results against those obtained through the CST and ADS results. The performance of small size high gain CDRA array is also evaluated by discussing its results in term of return loss, bandwidth, radiation pattern and back lobe level. The signal strength of the proposed small size CDRA array at different distances is also measured by using signal generator and Field Fox handheld spectrum analyzer. The procedures followed to measure the return loss (S_{11}), radiation pattern of the proposed antenna and open space signal strength are presented in Appendix B, Appendix C and Appendix D respectively.

3.7 Summary

High gain aperture coupled antenna arrays for various wireless communication systems have been proposed in the literature. In numerous wireless communication applications, antenna possesses wide band along with high gain is required for efficient communication. The IEEE 802.11a WLAN band covers the frequency range from 4.915 GHz to 5.825 GHz. In IEEE 802.11a WLAN, antennas with a gain greater than 10 dBi are used for outdoor wireless communication. The aperture coupled arrays presented in this literature exhibits high gain but is limited in bandwidth.

To overcome the limited bandwidth drawback of aperture coupled antenna array, the design methodology of wideband and high gain antennas are presented. The single element aperture coupled CDRA characteristics are studied in order to design the wide band and a high gain three element CDRA array. The aperture and mutual coupling mechanisms are used to excite the radiating elements of the antenna array. In the proposed three element antenna array, top and bottom radiating elements are excited by using aperture slots, while middle element is excited through the mutual coupling of its neighboring elements. The equivalent lumped model circuits of single element CDRA and small size wide band CDRA array are modeled prior to fabrication. The significant improvement in the bandwidth of CDRA array is achieved as compared to single element CDRA as well as the literature aperture coupled array.

CHAPTER 4

RESULTS AND DISCUSSION

4.1 Introduction

Chapter four presents the results and discussion of single element cylindrical dielectric resonator antenna (CDRA) and three single band, dual band and small size high gain CDRA array designs. The CDRs of same dimensions are used in all the proposed designs.

The aperture coupling technique is used for single element CDRA design, while the aperture and mutual coupling mechanisms are adopted to excite the array elements. The rectangular shape coupling slots etched on the ground plane are used to excite the radiating elements. The 50Ω microstrip transmission line placed under the ground plane is used to excite the coupling slot etched on the ground plane.

The results of all four designs in terms of bandwidth, radiation pattern and antenna gain are presented. The measured results of fabricated antenna design are also reported and verified by comparing with simulation results. The advantages of using two slots in place of three to excite the three radiating elements are also analyzed in the small size antenna array. In addition, the lumped element models for the single element CDRA and small size antenna array are designed to validate the antenna performance. The validity of the equivalent lumped model is confirmed by comparing its results against those obtained through the CST and fabricated prototypes.

4.2 Results and Discussion of Single Element CDRA

The aperture coupled single element CDRA fed by microstrip transmission line is designed and fabricated for IEEE 802.11a WLAN application. With CST the design is being simulated and finalized. The complete dimensions and the proposed geometry of single element CDRA are depicted in Table 3.1 and Figure 3.3 respectively. The

equivalent lumped element circuit of the proposed small size CDRA array is also modeled to validate the antenna's operation. With ADS the equivalent lumped element circuit is being designed and simulated. The equivalent lumped model of single element CDRA is depicted in Figure 3.4. The Matlab programs of various equations (2.38) to (2.43) are used to determine the RLC values of the equivalent lumped element circuit. The results of equivalent lumped element circuit are confirmed by comparing against those obtained through the CST. The fabricated prototype of single element CDRA is depicted in Figure 3.5, which consists of CDR made of CCTO ($\text{CaCu}_3\text{Ti}_4\text{O}_{12}$) dielectric material, whose dielectric constant; height and diameter are 55, 3.0 mm and 15.5 mm respectively. The CDR is placed on the coupling slot which is etched on the ground plane, while the $50\ \Omega$ microstrip transmission line of the width 2.61 mm is used to excite the aperture slot. The reliability of the fabricated prototype of single element CDRA is verified by comparing its results against those obtained through the CST and ADS designs.

4.2.1 Design Verification

The return loss (S_{11}) results of single element CDRA obtained through CST, ADS and fabricated prototype are depicted in Figure 4.1. From the results by using CST and ADS software's, the achieved impedance bandwidths are 0.2 GHz (5.15-5.35 GHz) and 0.2 GHz (5.15-5.35 GHz) respectively. In addition to simulation results, fabricated prototype return loss result measured by using VNA produces the impedance bandwidth of 0.23 GHz (5.14-5.37 GHz). Over the entire frequency band the return losses (S_{11}) coefficients are below -10 dB for both the simulated and measured results. These values show that the antenna works at 5.15–5.35 GHz which is the requirement for IEEE 802.11a WLAN application. The shift in the simulated and measured results is due to fabrication errors (high power loss due to the connector and surface of the CDR is not smooth which create the air gap between the CDR and the ground plane).

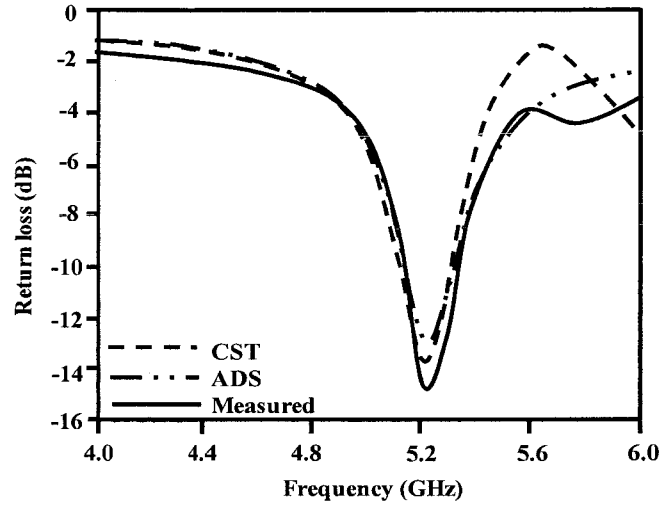


Figure 4.1. Comparison between return losses (S_{11}) of single element aperture coupled CDRA.

4.2.2 Parametric Study

The parametric study of antenna tuning parameters such as slot length and position of slot under CDRA is carried out and investigated to achieve the optimum results. The effects of changing the slot position on resonance frequency f_o and R_r , L_r and C_r of the dielectric resonators are also studied and discussed. The equivalent lumped element circuit of single element CDRA depicted in Figure 3.4 is used to analyze the effects of slot position on R_r , L_r and C_r of the dielectric resonator.

4.2.2.1 Effects of Slot Length

The length of the aperture slot is varied to improve the antenna performance and to analyze its influence on the antenna return loss. The initial aperture slot length, l_s is chosen to be 4.0 mm from equation 2.12 and slot width is chosen to be less than $\frac{\lambda_g}{4}$ to avoid the back radiation. The calculated slot length is electrically small in size, thus the parametric study is carried out to find the optimum antenna performance. The effects of slot length on central frequency and bandwidths are tabulated in Table 4.1. The slot length is increased from 4.0 mm to 16.0 mm with step size of 2.0 mm. It is noticed that antenna gives no resonance for slot length 4.0 mm to 6.0 mm. The antennas return loss below -10 dB when the slot length increased from 8.0 mm to 16.0 mm. It is also observed that, there is also an improvement in the antenna bandwidth from 0.112 GHz to 0.2 GHz by increasing slot

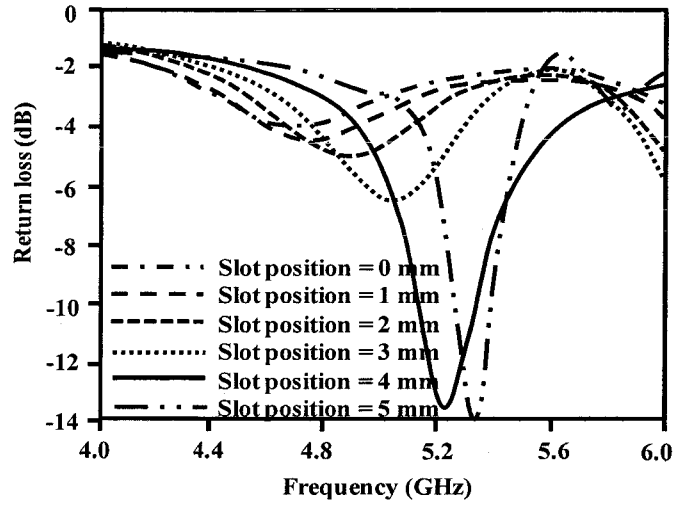
length from 8.0 mm to 14.0 mm. For the slot length of 16.0 mm, the bandwidth reduces to 0.045 GHz. It is depicted that the slot length of 14.0 mm, gives the optimum improvement in the antenna performance with maximum bandwidth of 0.2 GHz.

Table 4.1. The slot length analysis of the single element CDRA.

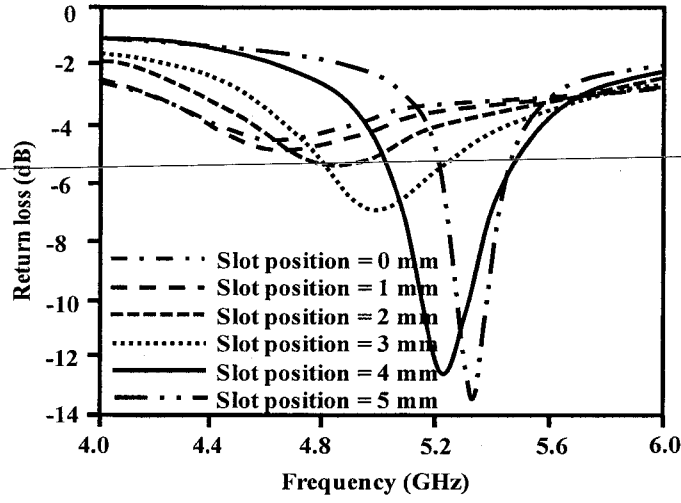
Slot length (mm)	Central frequency (GHz)	Bandwidth (GHz)
4.0	Null	Null
6.0	Null	Null
8.0	5.28	0.112 (5.22-5.332)
10.0	5.26	0.158 (5.172-5.33)
14.0	5.25	0.200 (5.15–5.35)
16.0	5.87	0.045 (5.20-5.245)

4.2.2.2 Effects of Slot Position

The analysis on the position of the aperture slot under CDR is also carried out to improve the coupling to the CDR and to excite the TE mode. The aperture slot moved from the CDR center to 5.0 mm towards its edge. The effects of moving the slot away from the center of the CDR using CST and ADS are depicted in Figure 4.2. It is revealed that by increasing offset distance from the CDR center, there is improvement in the antenna return loss response. From the analysis, it is noticed that the antenna gives no resonance till slot offset distance of 3.0 mm. It is depicted that, the slot offset distance of 4.0 mm from CDR center, gives the optimum performance with bandwidth of 0.5 GHz from 5.15 GHz to 5.35 GHz.



(a)



(b)

Figure 4.2. Slot position analysis of single element cylindrical DRA (a) CST
(b) ADS.

In addition to the return loss response, the effects of slot position on resonance frequency and R_r , C_r , and L_r , are depicted in Figure 4.3 and Table 4.2. From the analysis, it is shown that, till slot offset value of 3.0 mm no resonance below to -10 dB. However when slot offset is adjusted 4.0 mm away from the CDR center, the antenna performance is improved with bandwidth of 0.2 GHz. It is also noticed that the value of R_r decreases from 300 Ω to 83 Ω , by moving slot away from the center of the CDR. The values of C_r and L_r are also affected by the R_r due to the inverse relation between the value of R_r and C_r , and the value of L_r and C_r . Due to the inverse relation of f_o and R_r with C_r , the value of C_r decreased from 432.289 pF to 53.655 pF. Accordingly, the resonance inductance L_r is inversely related to C_r and the square of resonance frequency; hence an increase in the

value of capacitance brings about a decrease in the value of inductance from 2.650 pH to 16.531 pH. The relation between the R_r , C_r and L_r are determine by using equations (2.38) to (2.40). The comparison between S_{11} (Figure 4.2) and the values in Table 4.2, shows that the antenna gives resonance ($S_{11} < -10$ dB) for R_r below 100 Ω .

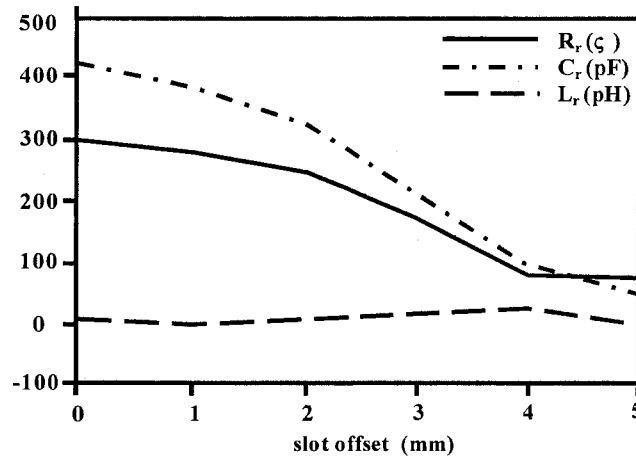


Figure 4.3. Effects of slot offset on R_r , L_r and C_r .

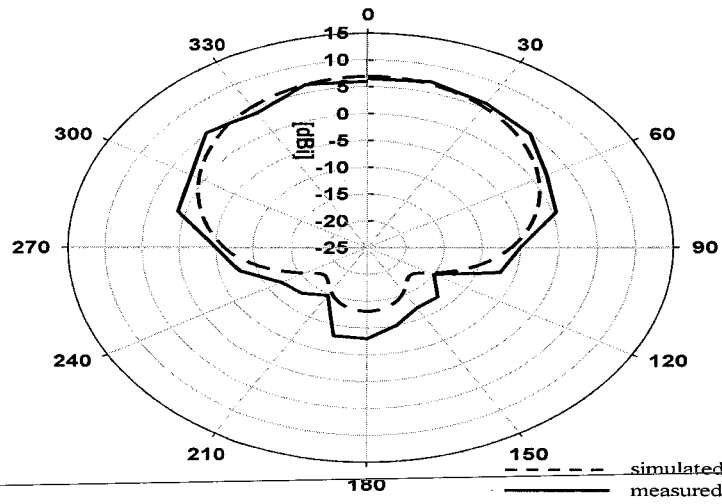
Table 4.2. Effects of slot position under CDR on R_r , C_r , and L_r .

Slot position (mm)	Central Frequency (GHz)	R_r (Ω)	C_r (pF)	L_r (pH)
0	4.70	300	432.289	2.650
1	4.75	280	395.021	2.842
2	4.89	250	332.791	3.183
3	5.05	180	221.249	4.489
4	5.25	90	103.938	8.840
5	5.34	83	53.655	16.556

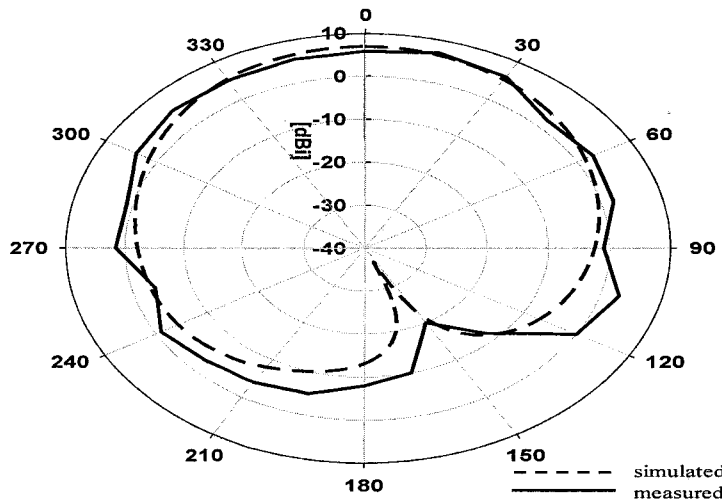
4.2.3 Antenna Radiation Pattern

In general, the single element dielectric resonator is low gain antenna with broad radiation pattern. The simulated and measured E-plane and H-plane radiation patterns of single element CDRA at 5.2 GHz are depicted in Figure 4.4. The magnitude of both E- and H- plane radiation patterns is 6.9 dBi in the direction of 0° and 1° respectively. It is noticed that there is a spillover in the radiation patterns due to the small size ground plane. This kind of spillover in the radiation patterns is due to the electromagnetic scattering from the edges of the small size ground plane. However, simulated and measured results are in good

agreement. The simulated and measured directivity of the antenna at 5.2 GHz is 6.9 dBi and 7.0 dBi respectively. The single element aperture coupled CDRA efficiency at 5.2 GHz is 94.21%. The impedance of the proposed antenna at resonance frequency is $50.56 + j24.64 \Omega$.



(a)



(b)

Figure 4.4. The radiation pattern of single element aperture coupled CDRA at 5.2 GHz
(a) E- plane (b).H-plane.

The signal strength measurements of the single element aperture coupled CDRA and standard monopole antenna of 5.0 dBi gain are performed in open space at different distances. The corresponding signal strength measurements at 5.25 GHz are depicted in Table 4.3. Initially the signal strength is measured at a distance of 2.0 m from the transmitter, then the distance between transmitter and receiver is increased from 5.0 m to

30.0 m with step size of 5.0 m. At 2.0 m, the signal strength of proposed antenna and the monopole antenna is -43.0 dBm and -45.0 dBm respectively. It is noticed that the by increasing distance from 5.0 m to 30.0 m, the signal strength of proposed antenna decreased from -43.0 dBm to -66.0 dBm, while the signal strength of monopole antenna decreased from -45.0 dBm to -70.0 dBm. From the open space measurements depicted in Table 4.3, it is clear that the performance of the proposed antenna is superior as compared to standard monopole antenna.

Table 4.3. Signal strength of single element aperture coupled CDRA at different distances.

Distances (m)	Signal strength of single element CDRA (dBm)	Signal Strength of monopole antenna (dBm)
2.0	-43.0	-45.0
5.0	-51.0	-55.0
10.0	-56.0	-60.0
15.0	-60.0	-65.0
20.0	-63.0	-68.0
25.0	-65.0	-69.0
30.0	-66.0	-70.0

4.3 Results and Discussion of Single Band CDRA Array

The single band CDRA array fed by microstrip transmission line is designed and fabricated for IEEE 802.11a WLAN application. With CST the design is being simulated and finalized. The complete dimensions and the proposed geometry of single band CDRA array are depicted in Table 3.3 and Figure 3.6 respectively. The fabricated prototype of the single band CDRA array is depicted in Figure 3.7, which consists of CDRs made of CCTO ($\text{CaCu}_3\text{Ti}_4\text{O}_{12}$) dielectric material, whose dielectric constant; height and diameter are 55, 3.0 mm and 15.5 mm respectively. The top and bottom CDRs are placed on the coupling slots which are etched on the ground plane, while the $50\ \Omega$ microstrip transmission line of the width 2.33 mm is used to excite the aperture slots. The middle CDR is excited through the mutual coupling of neighboring elements. The reliability of the fabricated prototype of single element CDRA array is verified by comparing its results against those obtained through the CST designs.

4.3.1 Design Verification

The return loss (S_{11}) results of single band CDRA array obtained through CST design and fabricated prototype is depicted in Figure 4.5. The corresponding impedance bandwidths of simulated and fabricated prototype are 1.023 GHz (4.6-5.623 GHz) and 1.08 GHz (4.75-5.83 GHz) respectively. It is clear that return loss coefficients are less than -10 dB over the entire band. By using the mutual coupling mechanism, a significant enhancement in the bandwidth is achieved. It is mentioned in [110], by using mutual coupling antenna performance can be enhanced in terms of bandwidth. Figure 4.5 show that there is a good agreement between the simulated and measured results. The difference between the simulated and measured results is due to the fabrication losses (high power loss due to the connector and surface of the CDR is not smooth which create the air gap between the CDR and the ground plane).

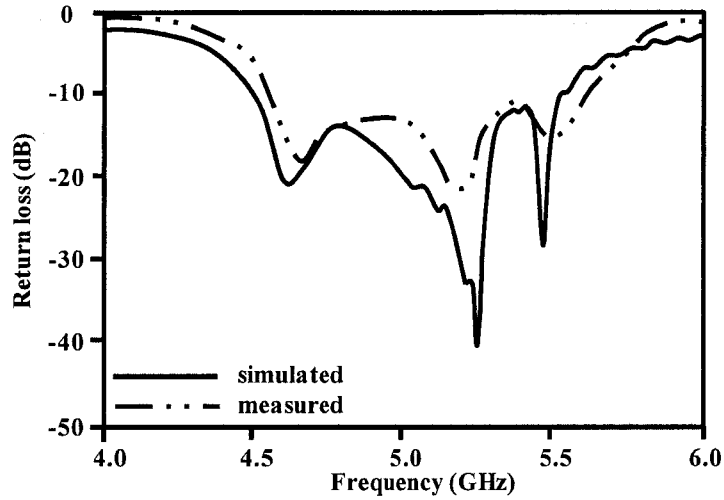


Figure 4.5. The comparison between simulated and measured return loss (S_{11}) of single band CDRA array.

4.3.2 Parametric Study

The parametric study of antenna tuning parameters such as inter-slot distance, slot length and slot width is carried out and investigated to achieve the optimum results.

4.3.2.1 Effects of Inter-slot Distance

The analysis of the antenna tuning parameters such as inter-slot distance, slot length and slot width is carried out to improve the coupling to the CDRs and to enhance the antenna performance. The distance between the feeding sources of radiating element should be between $0.5\lambda_g$ to λ_g to avoid the mutual coupling between the sources. The effects of changing the distance between the coupling slots is depicted in Table 4.4. The distance between coupling slots increased from 23.5 mm to 25.5 mm with step size of 0.5 mm. It is shown that by increasing the inter-slot distance from 23.5 mm to 24.5 mm, there is a decrement in the antenna bandwidth from 0.930 GHz to 0.920 GHz. For the inter-slot distance of 25.0 mm and 25.5 mm, the antenna bandwidths are 1.023 GHz and 0.822 GHz respectively. It is depicted that the inter-slot distance of 25.0 mm gives the optimum improvement in the antenna performance with maximum bandwidth of 1.023 GHz.

Table 4.4. Effects of changing the distance between the slots.

Distance (mm)	Bandwidth (GHz)
23.5	0.930
24.0	0.924
24.5	0.920
25.0	1.203
25.5	0.822

4.3.2.2 Effects of Slots Length

The analysis on the slots lengths are performed to improve the coupling to the CDRs and to find the optimum bandwidth as depicted in Table 4.5. The initial slots lengths are chosen to be 4.0 mm. Thus the parametric study is carried out to improve the antenna performance. The lengths of the coupling slots increased from 4.0 mm to 16.0 mm with step size of 2.0 mm. It is noticed that by increasing the slots lengths from 4.0 mm to 14.0 mm, the antenna bandwidth increased from 0.070 GHz to 1.023 GHz. For the slots lengths of 16.0 mm, the bandwidth reduces to 0.703 GHz. It is depicted that the slots lengths of 14.0 mm, gives the optimum improvement in the antenna performance with bandwidth of 1.023 GHz.

Table 4.5. Effects of slot length on the central frequency and bandwidth.

Slot length (mm)	Central frequency (GHz)	Bandwidth (GHz)
4.0	5.35	0.070
6.0	5.12	0.398
8.0	5.08	0.450
10	5.02	0.517
12	4.98	0.570
14	5.11	1.023
16	5.00	0.703

4.3.2.3 Effects of Slots Widths

The analysis on the slots widths are performed to improve the coupling to the CDRs and to find the optimum antenna performance as depicted in Table 4.6. The initial slots widths are chosen to be 3.0 mm. Thus the parametric study is carried out to improve the antenna performance. The widths of the coupling slots increased from 3.0 mm to 4.5 mm with step size of 0.5 mm. It is noticed that by increasing the slots widths from 4.0 mm to 4.0 mm, the antenna bandwidth increased from 0.856 GHz to 1.023 GHz. For the slots widths of 4.5 mm, the bandwidth reduces to 0.870 GHz. It is depicted that the slots widths of 4.0 mm, gives the optimum improvement in the antenna performance with bandwidth of 1.023 GHz.

Table 4.6. Effects of changing the width of slots on central frequency and bandwidth.

Slot width (mm)	Central Frequency (GHz)	Bandwidth (GHz)
3.0	4.70	0.856
3.5	4.90	0.866
4.0	5.10	1.023
4.5	5.15	0.870

4.3.3 Antenna Radiation Pattern

The E-plane ($\phi = 0^\circ$) is the direction in which antenna radiates its maximum power and contains the E-field. This antenna array radiates its maximum power in z-direction. The simulated and measured E-plane radiation patterns of single band CDRA array at different frequencies 4.8 GHz, 5.1 GHz and 5.6 GHz are depicted in Figure 4.6. The corresponding magnitudes of the main lobes in E-plane are 8.6 dBi, 7.3 dBi and 9.0 dBi in direction of 1° , 0° and 0° respectively. Similarly, the H-plane consists of the H-field and is perpendicular to the E-plane. The corresponding H-plane radiation patterns of single band CDRA array are depicted in Figure 4.7. It is noticed that there is a spillover in the radiation patterns due to the small size ground plane. This kind of spillover in the radiation patterns is due to the electromagnetic scattering from the edges of the small size ground plane. However, simulated and measured results are in good agreement.

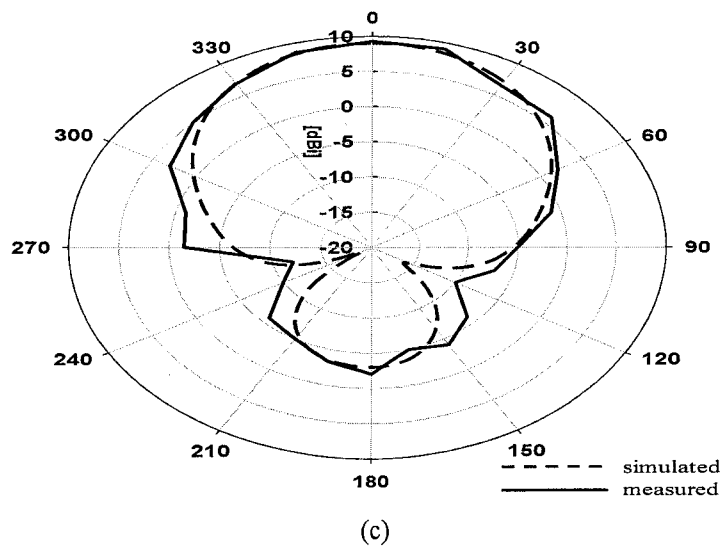
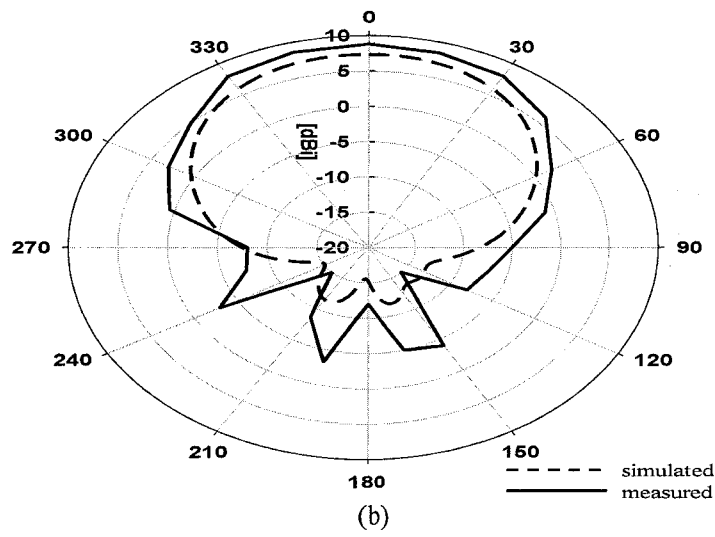
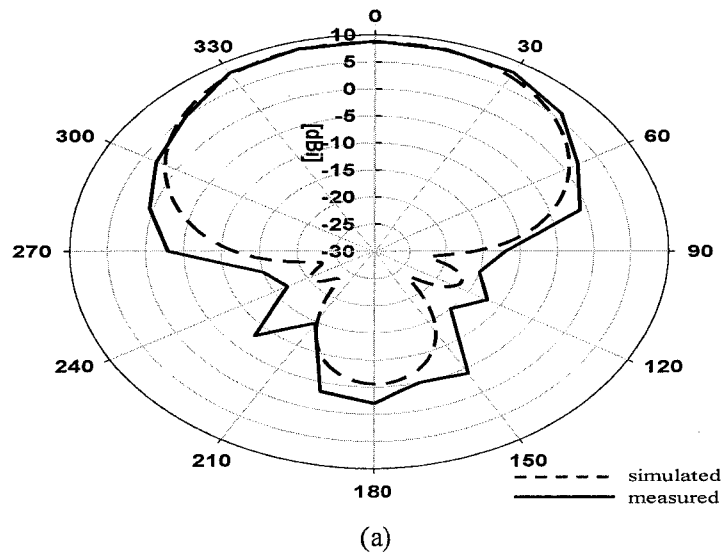
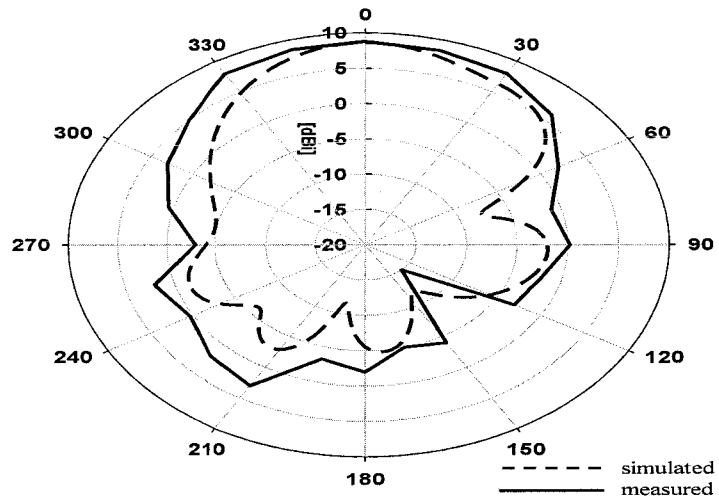
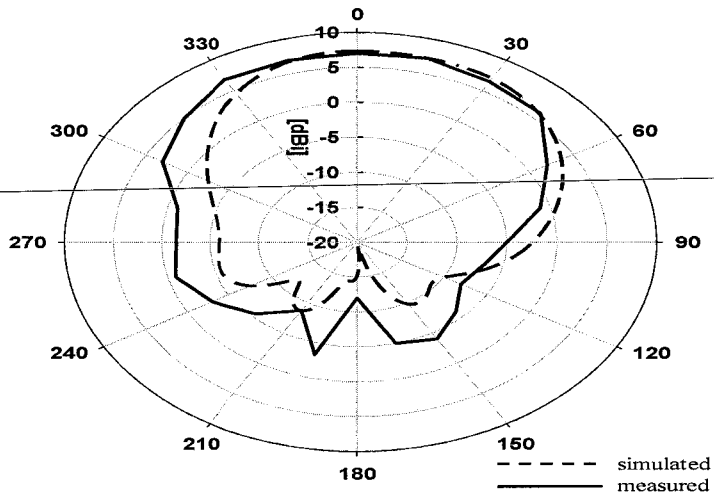


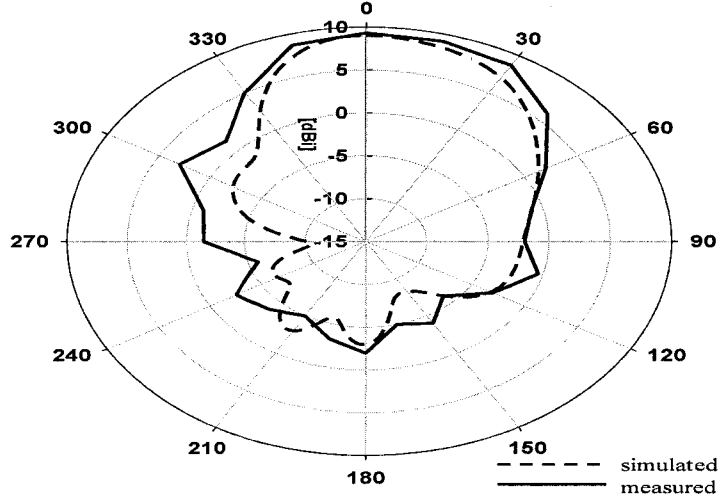
Figure 4.6. E-plane radiation patterns of single band CDRA array at (a) 4.8 GHz
(b) 5.1 GHz (c) 5.6 GHz.



(a)



(b)



(c)

Figure 4.7. H-plane radiation patterns of single band CDRA array at (a) 4.8 GHz (b) 5.1 GHz (c) 5.6 GHz.

The signal strength measurements of the single band CDRA array and the standard monopole antenna of 5.0 dBi gain are performed in open space at different distances. The

corresponding signal strength measurements at 5.5 GHz are depicted in Table 4.7. Initially the signal strength is measured at a distance of 2.0 m from the transmitter, then the distance between transmitter and receiver is increased from 5.0 m to 30.0 m with step size of 5.0 m. At 2.0 m, the signal strength of proposed antenna and the monopole antenna is -42.0 dBm and -45.0 dBm respectively. It is noticed that the by increasing distance from 5.0 m to 30.0 m, the signal strength of proposed antenna decreased from -42.0 dBm to -63.0 dBm, while the signal strength of monopole antenna decreased from -45.0 dBm to -70.0 dBm. From the open space measurements depicted in Table 4.7, it is clear that the performance of the proposed single band CDRA array is superior as compared to standard monopole antenna.

Table 4.7. Signal strength of single band CDRA array at different distances.

Distances (m)	Signal strength of single band CDRA array (dBm)	Signal Strength of monopole antenna (dBm)
2.0	-42.0	-45.0
5.0	-48.0	-55.0
10.0	-51.0	-60.0
15.0	-53.0	-65.0
20.0	-59.0	-68.0
25.0	-60.0	-69.0
30.0	-63.0	-70.0

4.3.4 Antenna Gain and Efficiency

The aperture slot radiates in the forward as well as in the backward direction [111]. By reducing the coupling slots, the backward radiations can be controlled. The proposed single band CDRA array radiates very small energy in the backward direction with front-to-rear ratio of 26 dB at 5.0 GHz. In general, the single element dielectric resonator gives a limited gain with broad radiation pattern. The single element CDRA gain can be increased by using in array configuration. The directivity of proposed single band array varied from

7.4 dBi to 9.6 dBi over the entire band from 4.6 GHz to 5.8 GHz. The simulated and measured gain of the proposed antenna is depicted in Table 4.8. The maximum directivity of 9.6 dBi is achieved at 5.5 GHz. It is shown that there is a good agreement between the simulated and measured results. The radiation efficiency of the single band CDRA array is also shown in Table 4.8. The radiation efficiency of single band CDRA array at different frequencies 4.8 GHz, 5.1 GHz and 5.5 GHz are 84.15%, 87.70% and 80.00% respectively. The impedance of the proposed antenna at resonance frequency is $51.75 + j9.02 \Omega$.

Table 4.8. The efficiency and gain of single band CDRA array antenna.

Frequency (GHz)	η %	$G_{\text{simulated}}$ (dBi)	G_{measured} (dBi)
4.8	84.15	8.6	8.3
5.1	87.70	7.3	7.2
5.5	80.00	9.6	9.3

4.4 Results and Discussion of Dual Band CDRA Array

The dual band CDRA array fed by microstrip transmission line is designed and fabricated for IEEE 802.11a/b WLAN application. With CST, the design is being simulated and finalized. The complete dimensions and the proposed geometry of dual band CDRA array are depicted in Table 3.4 and Figure 3.8 respectively. The fabricated prototype of the dual band CDRA array is depicted in Figure 3.9, which consists of CDRs made of CCTO ($\text{CaCu}_3\text{Ti}_4\text{O}_{12}$) dielectric material, whose dielectric constant; height and diameter are 55, 3.0 mm and 15.5 mm respectively. The top and bottom CDRs are placed on the coupling slots which are etched on the ground plane, while the 50Ω microstrip transmission line of the width 2.61 mm is used to excite the aperture slots. The middle CDR is excited through the mutual coupling of neighboring elements. The initial important step in the designing of dual band CRDA array is to design single band CDRA array antenna working for IEEE 802.11a WLAN, then by using metallic top-loaded mechanism resonance at lower band is achieved.

4.4.1 Design Verification

The comparison between the return loss results with and without top-loaded three elements CDRA array is depicted in Figure 4.8. It is noticed that antenna array without using top-loaded technique operates only for IEEE 802.11a WLAN band. Alternatively, the return loss response of metallic top loaded CDRA array operate for IEEE 802.11a/b WLAN application as depicted in Figure 4.8. It is shown that by using metallic top-loaded mechanism, resonance at lower frequencies can be achieved.

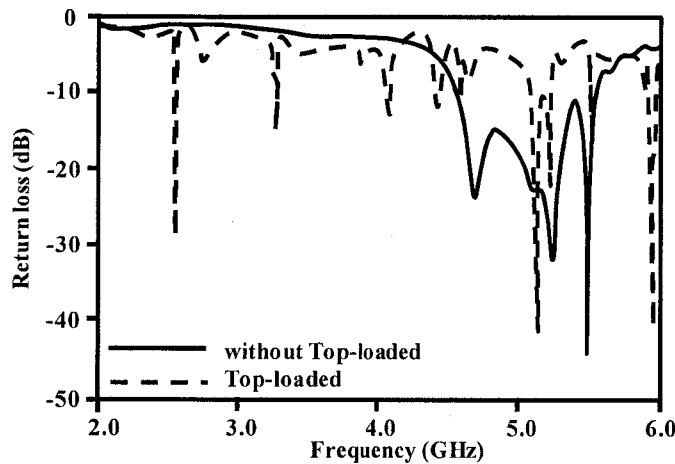


Figure 4.8. Return loss results of with and without top-loaded CDRA array.

The measured and simulated return loss of top-loaded array antenna is depicted in the Figure 4.9. The return loss of fabricated and simulated top-loaded antenna for both resonance frequencies are less than -10 dB. The fabricated top-loaded CDRA array design achieved a bandwidth of 4.0% (2.42-2.52 GHz) for lower frequency band and 21.14% (4.40-5.44 GHz) for upper frequency band. It is depicted that by using dual band operation can be achieved by using metallic top loaded mechanism and when one frequency band is not within the range, other frequency band can be tuned. The main causes of differences in the fabricated and simulated results are due to the fabrication error (high power loss due to the connector and surface of the CDR is not smooth which create the air gap between the CDR and the ground plane).

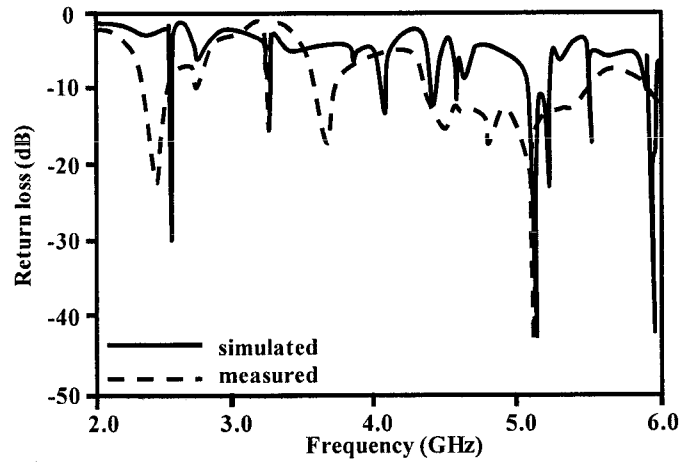


Figure 4.9. Comparison between fabricated and simulated return loss of top-loaded CDRA array.

4.4.2 Parametric Study

As the geometry of dual band CDRA array is same to the antenna array presented in section 4.3. The parametric study of antenna tuning parameters such as slot width and on the diameter of top-loaded metallic sheet is carried out and investigated to achieve the optimum results.

4.4.2.1 Effects of Diameter of Top-Loaded Metallic Sheet

The top-loaded metallic sheet mechanism is used to achieve the resonance at lower frequency band. The analysis on top-loaded metallic sheet is performed by changing its diameter from 0.5 mm to 15.5 mm with step size of 1.0 mm. It is shown that antenna gives no resonance at lower frequency band for top-loaded diameter form 0.5 mm to 4.5 mm as depicted in Table 4.9. For top-loaded diameter of 5.5 mm to 7.5 mm, the resonance frequency shift from 2.76 GHz to 2.47 GHz. The resonance at lower band is achieved when top-loaded metallic sheet diameter increased from 4.5 mm. It is depicted that the top-loaded diameter of 7.5 mm gives the required resonance at 2.47 GHz. It is observed that by changing the diameter of top loaded sheet resonance frequency can be controlled.

Table 4.9. Top-loaded sheet analysis on lower band.

Metallic sheet diameter (mm)	Resonance frequency f_o (GHz)
0.5	No resonance in 2.45 GHz band
1.5	No resonance in 2.45 GHz band
2.5	No resonance in 2.45 GHz band
3.5	No resonance in 2.45 GHz band
4.5	No resonance in 2.45 GHz band
5.5	2.76
6.5	2.58
7.5	2.47

4.4.2.2 Effects of Slot Width

The effects of changing the slots widths on the upper and lower resonance frequency are depicted in the Figure 4.10 and 4.11 respectively. The slot width increased from 3.8 mm to 4.2 mm with step size of 0.2 mm. It is noticed that by changing the slot width the resonance frequency down shifts towards the left for both lower and upper band. For the slot widths of 3.2 mm, 4.0 mm and 4.2 mm, the corresponding resonance frequency at lower frequency bands are 2.50 GHz, 2.47 GHz and 2.43 GHz respectively. It is depicted that the slot width of 4.0 mm gives the optimum performance for lower frequency band with return loss at required resonance of 2.47 GHz.

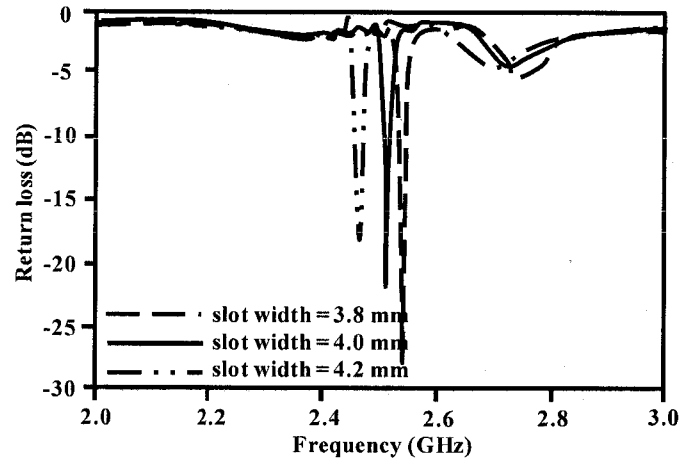


Figure 4.10. Effects of slot dimensions on lower frequency band.

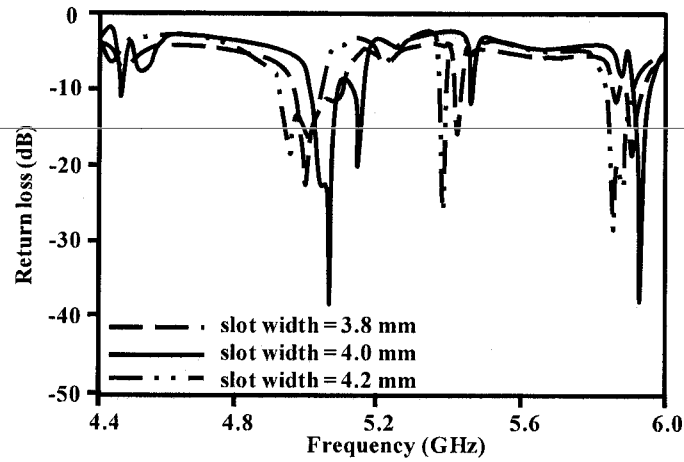


Figure 4.11. Effects of slot dimensions on upper frequency band.

4.4.3 Antenna Radiation Pattern

The simulated and measured E-plane ($\phi = 0^\circ$) and H-plane ($\phi = 90^\circ$) radiation patterns of dual band array at 2.47 GHz and 5.0 GHz are depicted in Figure 4.12 and 4.13 respectively. The magnitude of the main beam at 2.47 GHz is 5.6 dBi for both E- and H-plane. Similarly the corresponding magnitude at 5.0 GHz is 9.4 dBi for both E- and H- plane radiation patterns. It is noticed that there is a spillover in the radiation patterns due to the small size ground plane. This kind of spillover in the radiation patterns is due to the electromagnetic scattering from the edges of the small size ground plane. However, simulated and measured results are in good agreement.

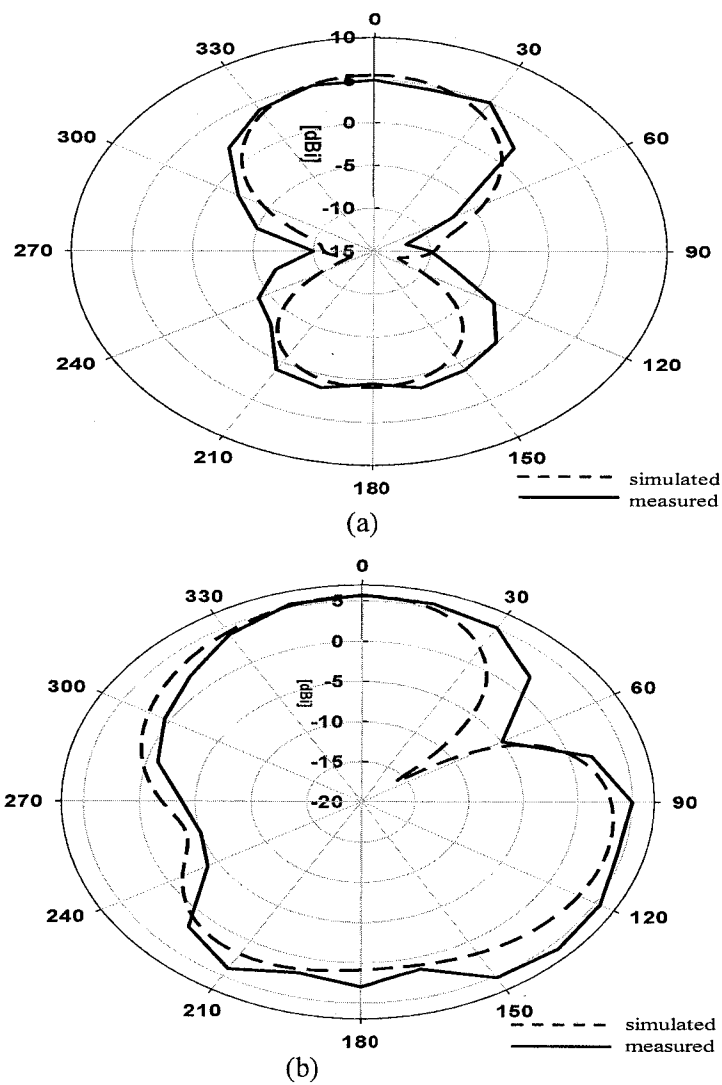


Figure 4.12. Radiation pattern of dual band CDRA array at 2.47 GHz (a) E-plane (b) H-plane.

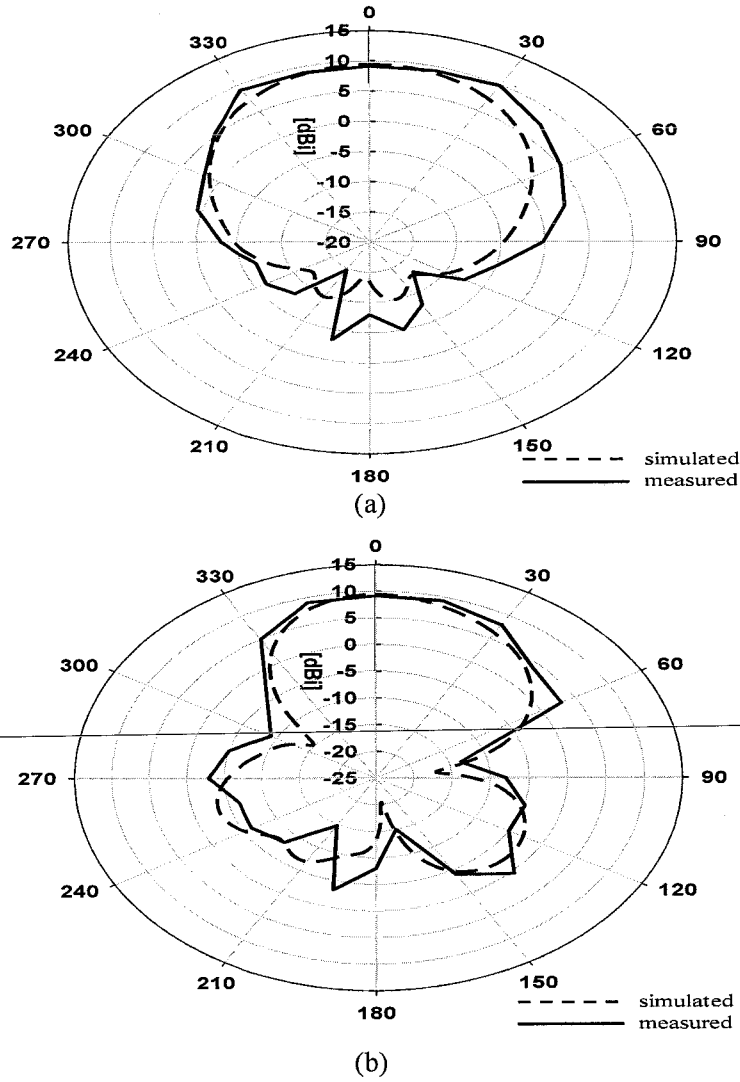


Figure 4.13. Radiation pattern dual band CDRA array at 5.0 GHz (a) E-plane ($\theta = 0^\circ$)
(b) H-plane ($\theta = 90^\circ$).

The signal strength measurements of the dual band CDRA array and the standard monopole antenna of 5.0 dBi gain are performed in open space at different distances. The corresponding signal strength measurements at 5.0 GHz are depicted in Table 4.10. Initially the signal strength is measured at a distance 2.0 m from the transmitter, then the distance between transmitter and receiver is increased from 5.0 m to 30.0 m with step size of 5.0 m. At 2.0 m, the signal strength of proposed antenna and the monopole antenna is -41.0 dBm and -45.0 dBm respectively. It is noticed that the by increasing distance from 5.0 m to 30.0 m, the signal strength of proposed antenna decreased from -41.0 dBm to -65.0 dBm, while the signal strength of monopole antenna decreased from -45.0 dBm to -70.0 dBm. From the open space measurements depicted in Table 4.10, it is clear that the

performance of the proposed dual band CDRA array is superior as compared to standard monopole antenna.

Table 4.10. Signal strength of dual band CDRA array at different distances.

Distances (m)	Signal strength of dual band CDRA array (dBm)	Signal Strength of monopole antenna (dBm)
2.0	-41.0	-45.0
5.0	-50.0	-55.0
10.0	-54.0	-60.0
15.0	-55.0	-65.0
20.0	-57.0	-68.0
25.0	-60.0	-69.0
30.0	-65.0	-70.0

4.4.4 Antenna Gain and Efficiency

In general, the dielectric resonator gives a unidirectional and broad radiation pattern. The single element CDRA gain can be increased by using in array configuration. The simulated and measured gain of the dual band CDRA array antenna at 2.47 GHz and 5.0 GHz is depicted in Table 4.11. The maximum achieved directivity for lower band is 5.7 dBi at 2.47 GHz and for upper band is 9.4 dBi at 5.0 GHz. The radiation efficiency of the dual band CDRA array at 2.45 GHz and 5.0 GHz is also shown in Table 4.11. The dual band array antenna achieved the radiation efficiency of 68% and 70% for lower and upper frequency band respectively. The impedance of the proposed antenna at resonance frequency is $49.62 - j0.16\Omega$.

Table 4.11. The efficiency and gain of dual band CDRA array.

Frequency (GHz)	η %	$G_{\text{simulated}}$ (dBi)	G_{measured} (dBi)
2.47	68	5.7	5.5
5.0	70	9.4	9.3

4.5 Results and Discussion of Small Size CDRA Array

The aperture and mutual coupled three elements small size CDRA array fed by stub loaded microstrip line is designed and fabricated to operate at 5.0 GHz band for 802.11a system applications. With CST the design of small size CDRA array is being simulated and finalized. The complete dimensions and the proposed geometry of small size CDRA array are depicted in Table 3.5 and Figure 3.10 respectively. The antenna array discussed in this section is small in size as compared to the antenna arrays reported in section 4.3 and section 4.4 respectively. The equivalent lumped element circuit of the proposed small size CDRA array is also modeled to validate the antenna's operation. With ADS the equivalent lumped element circuit is being designed and simulated. The equivalent lumped model of small size CDRA array is depicted in Figure 3.11. The Matlab programs of various equations (2.38) to (2.50) are used to determine the RLC values of the equivalent lumped element circuit. The results of equivalent lumped element circuit are confirmed by comparing against those obtained through the CST. The fabricated prototype of the small size CDRA array is depicted in Figure 3.12, which consists of three CDRs made of CCTO ($\text{CaCu}_3\text{Ti}_4\text{O}_{12}$) dielectric material, whose dielectric constant; height and diameter are 55, 3.0 mm and 15.5 mm respectively. The reliability of the fabricated prototype of small size CDRA array is verified by comparing its results against those obtained through the CST and ADS designs.

4.5.1 Design Verification

The return loss (S_{11}) results of small size CDRA array obtained through CST, ADS and fabricated prototype are depicted in Figure 4.14. Over the entire 5.0 GHz band the return loss (S_{11}) coefficients are below -10 dB for both the measured and simulated results. The

return loss of -51 dB is achieved through CST simulation at resonance frequency of 5.16 GHz with a bandwidth of 1.076 GHz. The ADS simulation provides the return loss of -51 dB at resonance frequency of 5.03 GHz with a bandwidth of 1.0 GHz and the fabricated design gives 1.2 GHz bandwidth and return loss of -42 dB at resonance frequencies of 5.0 GHz. It is noticed that the return losses results from the simulations and fabrication covered the frequency band (4.915-5.825 GHz), required for 802.11a application.

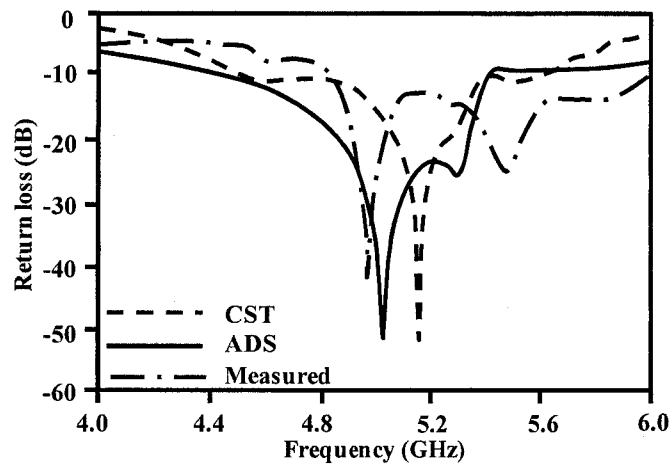


Figure 4.14. The comparison between the simulated and measured return loss (S_{11}) of small size CDRA array.

Figure 4.14, show that there is a frequency shift in the simulated and measured results as both simulators (CST and ADS) are based on different simulation techniques. CST microwave studio uses a finite integration technique (FIT) to simulate the 3D structure of proposed antenna, while ADS simulator uses finite element method (FEM) to simulate the 2D lumped element circuit. In addition to this, the main reason of shift in simulated results is due to rounding off the ADS parameters values that are numerically calculated. The shift in the measured results is due to the fabrication errors (the surface of the CDRs is not smooth which produces the air gap between the CDRs and ground plane).

4.5.2 Parametric study

The parametric study of antenna tuning parameters such as slot length, inter-slot distance and inter-element distance is carried out and investigated to achieve the optimum results. The effects of changing the slot length on resonance frequency f_o and R_r , L_r and C_r of the dielectric resonators are also studied and discussed. The equivalent lumped element circuit of small size CDRA array depicted in Figure 3.11 is used to analyze the effects of slot length on R_r , L_r and C_r of the dielectric resonator.

4.5.2.1 Effects of Aperture Slot Length on the Top Radiating Element of Small Size CDRA Array

The length of coupling slot used to excite the top CDR of small size CDRA array is varied to analyze its influence on resonance frequency f_o and R_r , L_r and C_r of top CDR. The effects of slot length on resonance frequency and R_r , L_r and C_r are studied by using CST and ADS designs respectively. Their corresponding results are compared to verify the calculated values used to obtain ADS result with 3D design results obtained through CST. The length of the coupling slot increased from 14.0 mm to 20.0 mm with step size of 1.2 GHz. The effects of changing the slot length on the resonance frequency of top radiating element of the CDRA array are depicted in Figure 4.15 and Table 4.12. It is noticed that by increasing slot length from 14.0 mm to 20.0 mm, the resonance frequency down shifts from 5.980 GHz to 5.524 GHz. As shown in the Figure 4.15, the returns loss results obtained through the CST and ADS are in good agreement for strong resonance which occurs at higher resonance frequency. The difference between the CST and ADS results at lower frequency is because of the ADS parameters are designed for strong resonance only, which is below -10 dB.

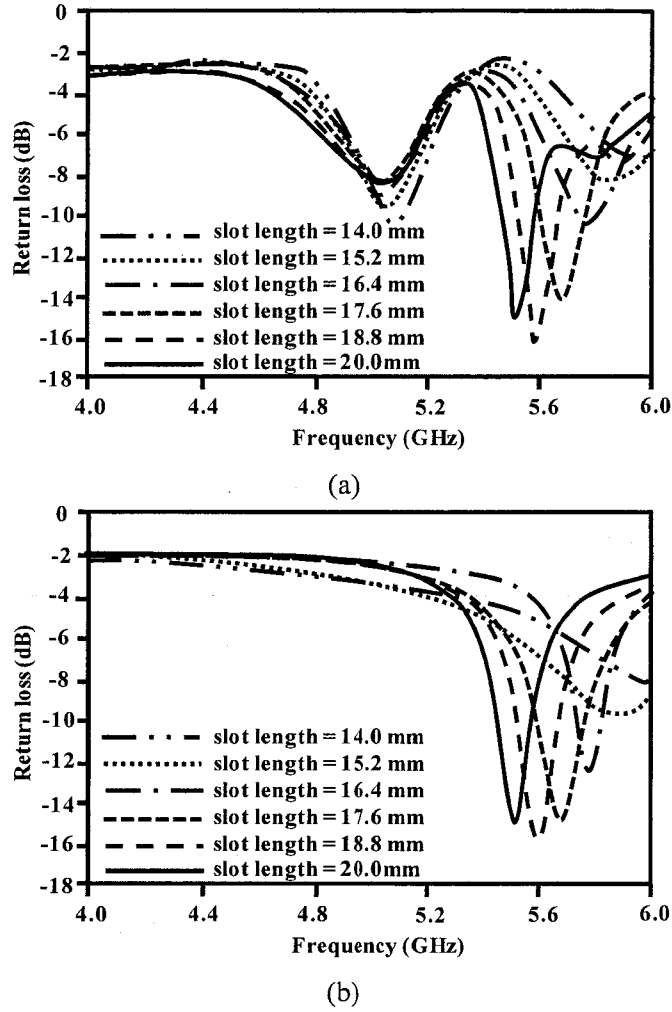


Figure 4.15. Slot length analysis on a first radiating element using (a) CST (b) ADS.

In addition to the effects of increasing slot length on resonance frequency, the slot length effects on the R_r , L_r and C_r of the top radiating element are also analyzed as depicted in Table 4.12. It is shown that by increasing the slot length from 14.0 mm to 20.0 mm, the value of resonance resistance R_r decreased from 170Ω to 70Ω . As there is an inverse relation between f_o and R_r with C_r , the value of C_r increased from 3.5468 pF to 17.6838 pF. Accordingly, the resonance inductance L_r is inversely related to C_r and the square to resonance frequency f_o ; hence an increase in the value of capacitance brings about a decrease in the value of inductance from 198.7030 pH to 46.9412 pH. The relation between the resonance frequency and antenna equivalent circuit parameters are determined by using equations from (2.38) to (2.40). The relation between the slot length, resonance frequency and R_r , L_r and C_r for top radiating element discussed in Table 4.12 is also depicted in Figure 4.16.

Table 4.12. Effect of slot length on the R_r , L_r and C_r of the first radiating element.

Slot length (mm)	Resonance frequency f_o (GHz)	R_r (Ω)	C_r (pF)	L_r (pH)
14.0	5.980	170	3.5648	198.7030
15.2	5.836	150	4.1398	179.6520
16.4	5.768	100	18.7315	40.6527
17.6	5.680	80	11.8501	66.2552
18.8	5.590	75	14.4668	56.0326
20.0	5.524	75	17.6838	46.9412

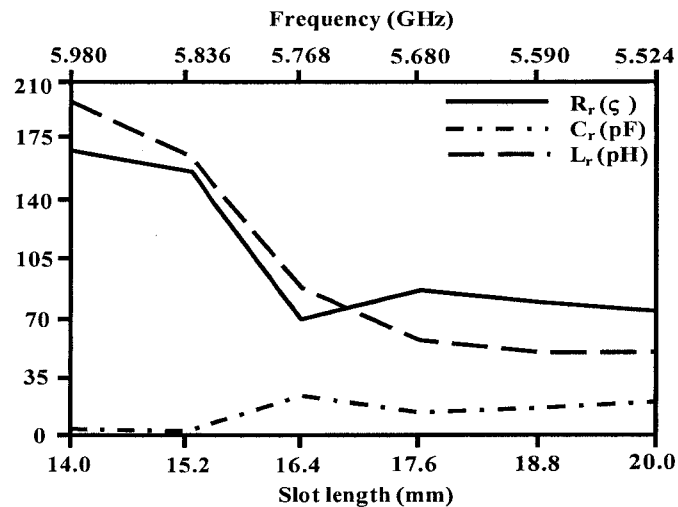


Figure 4.16. Relation between slot length, resonance frequency and R_r , C_r and L_r of top radiating element of small size CDRA array.

4.5.2.2 Effects of Aperture Slot Length on the Bottom Radiating Element of Small Size CDRA Array

The parametric study on coupling slot length used to excite the bottom CDR of small size CDRA array is also carried out to analyze its influence on resonance frequency f_o and R_r , L_r and C_r of bottom CDR. The effects of slot length on resonance frequency and R_r , L_r and C_r are studied by using CST and ADS designs respectively. Their corresponding results are

compared to verify the calculated values used to obtain ADS result with 3D design results obtained through CST. The length of the coupling slot increased from 14.0 mm to 20.0 mm with step size of 1.2 GHz. The effects of changing the slot length on the resonance frequency of bottom radiating element of the CDRA array are depicted in Figure 4.17 and Table 4.13. It is noticed that by increasing slot length from 14.0 mm to 20.0 mm, the resonance frequency down shifts from 5.80 GHz to 5.45 GHz. As shown in the Figure 4.17, the returns loss results obtained through the CST and ADS are in good agreement.

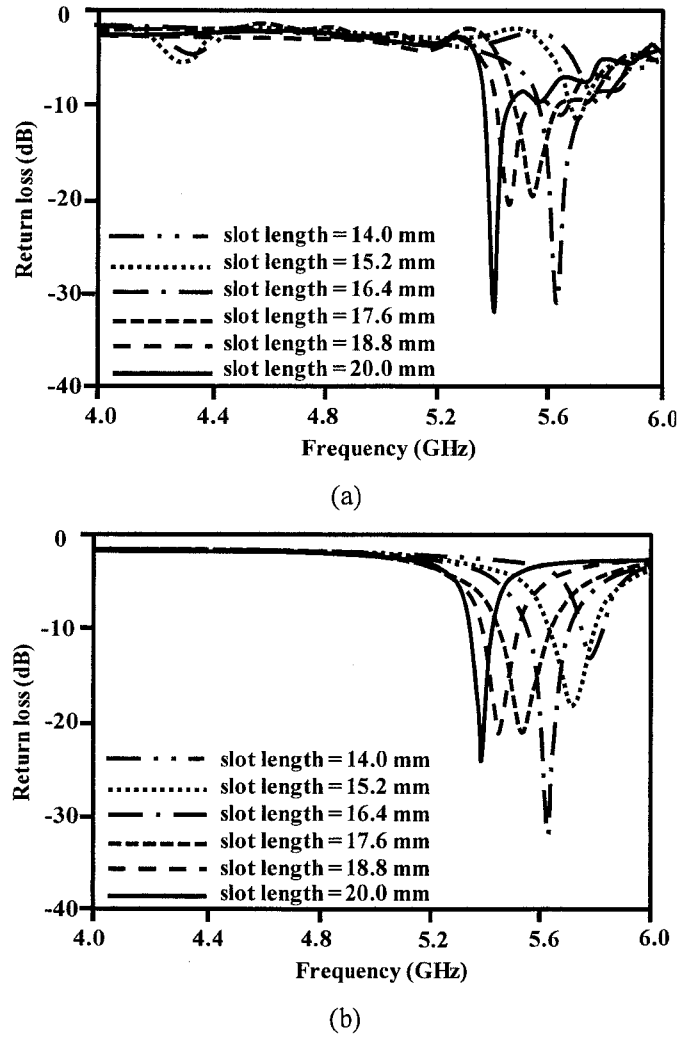


Figure 4.17. Slot length analysis on a last radiating element using (a) CST (b) ADS.

In addition to the effects of increasing slot length on resonance frequency, the slot length effects on the R_r , L_r and C_r of the bottom radiating element are also analyzed as depicted in Table 4.13. It is shown that by increasing the slot length from 14.0 mm to 20.0 mm, the value of resonance resistance R_r decreased from 100 Ω to 57 Ω . As there is

an inverse relation between f_o and R_r with C_r , the value of C_r increased from 24.2974 pF to 30.9956 pF. Accordingly, the resonance inductance L_r is inversely related to C_r and the square to resonance frequency f_o ; hence an increase in the value of capacitance brings about a decrease in the value of inductance from 31.3757 pH to 27.9735 pH. The relation between the resonance frequency and antenna equivalent circuit parameters are determined by using equations from (2.38) to (2.40). The relation between the slot length, resonance frequency and R_r , L_r and C_r for bottom radiating element discussed in Table 4.13 is also depicted in Figure 4.18.

Table 4.13. Effect of slot length on the R_r , L_r and C_r of the last radiating element.

Slot length (mm)	Resonance frequency f_o (GHz)	R_r (Ω)	C_r (pF)	L_r (pH)
14.0	5.80	100	24.2974	31.3757
15.2	5.72	70	17.7163	44.9476
16.4	5.64	53	23.0093	34.6081
17.6	5.56	65	28.6249	28.6249
18.8	5.47	65	29.0959	29.0959
20.0	5.45	57	30.9956	27.9735

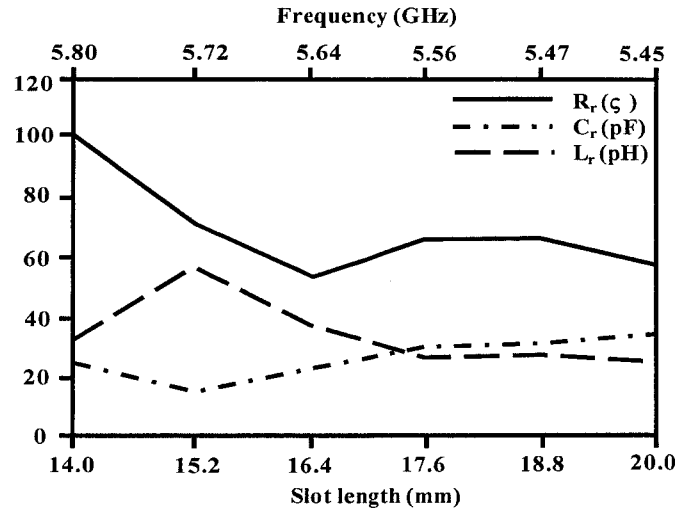


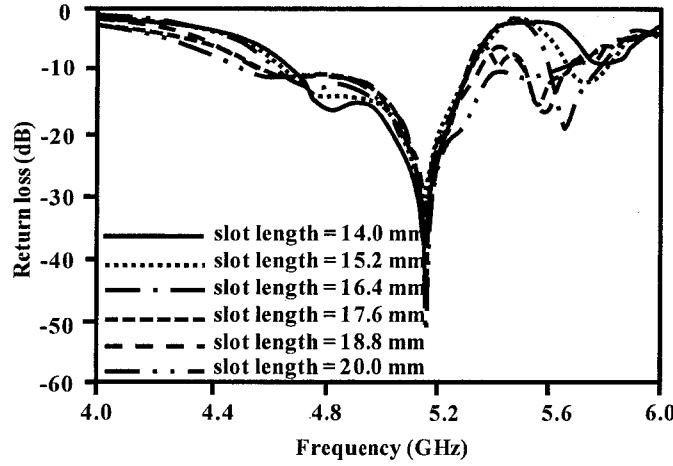
Figure 4.18. Relation between slot length, resonance frequency and R_r , C_r and L_r of bottom radiating element of small size CDRA array.

4.5.2.3 Effects of Two Slots Lengths on the Bandwidth of Small Size CDRA Array

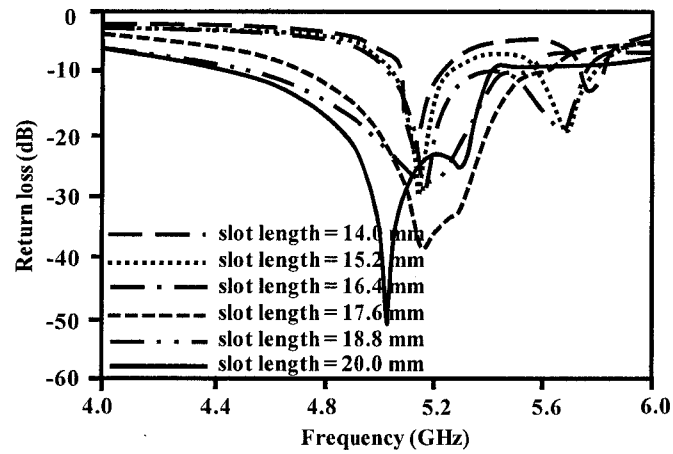
The effects of changing the two slots lengths used to excite the top and bottom radiating elements of small size CDRA array are also analyzed to find the optimum array bandwidth. The length of aperture slots is varied to improve the coupling to the CDRA and to analyze its influence on the antenna bandwidth. The initial slot length is chosen from equation 2.12 and slot width is chosen to be less than $\frac{\lambda_g}{4}$ to avoid back radiation. The slot length is electrically small in size, thus the parametric study is carried out to find the optimum bandwidth. As slot length is related to the feeding network, it has significant effects on antenna results. The length of the slots increased from 2.0 mm to 24.0 mm with step size of 2.0 mm as depicted in Table 4.14. It is shown that by increasing slots lengths from 4.0 mm till 20.0 mm, there is an improvement in antenna bandwidth from 0.048 GHz to 1.076 GHz. For the slots lengths of 22.0 mm to 24.0 mm, the bandwidth reduces to 0.594 GHz and 0.507 GHz respectively. It is depicted that the slots lengths of 20.0 mm, gives the optimum improvement in the antenna performance with maximum bandwidth of 1.076 GHz. The effects of changing the slot length from 14.0 mm to 20.0 mm are also depicted in Figure 4.19.

Table 4.14. Slot length analysis on the bandwidth.

Slot length (mm)	Bandwidth (GHz)
2.0	Null
4.0	0.048
6.0	0.513
8.0	0.465
10.0	0.518
12.0	0.588
14.0	0.636
16.0	0.688
18.0	0.742
20.0	1.076
22.0	0.594
24.0	0.507



(a)



(b)

Figure 4.19. Slot length analysis on three element array using (a) CST (b) ADS.

The effects of changing the two slots lengths on the bandwidth of small size CDRA arrays and on the R_r , L_r and C_r of middle CDR are depicted in Figure 4.19 and Table 4.15 respectively. It is noticed that by increasing the slots lengths, the value of the R_r of middle CDR is decreased from 58Ω to 55Ω as in the case of single elements. As there is an inverse relation between the f_o and R_r with C_r , the value of C_r increased from 71.5579 pF to 452.6030 pF. Similarly, the value of L_r decreased from 13.2948 pF to 2.2120 pF due to the inverse relation between the C_r and square of f_o with L_r . The relation between the slots lengths, resonance frequency and R_r , L_r and C_r for middle radiating element is also depicted in Figure 4.20.

Table 4.15. Effect of slot length on the R_r , L_r and C_r of the middle radiating element.

Slot length (mm)	Resonance frequency f_o (GHz)	R_r (Ω)	L_r (pH)	C_r (pF)
14.0	5.15	58	71.5579	13.2948
15.2	5.15	58	71.7804	13.3361
16.4	5.15	58	89.6558	10.6606
17.6	5.15	58	307.6990	3.2929
18.8	5.16	57	453.5910	2.2338
20.0	5.16	55	452.6030	2.2120

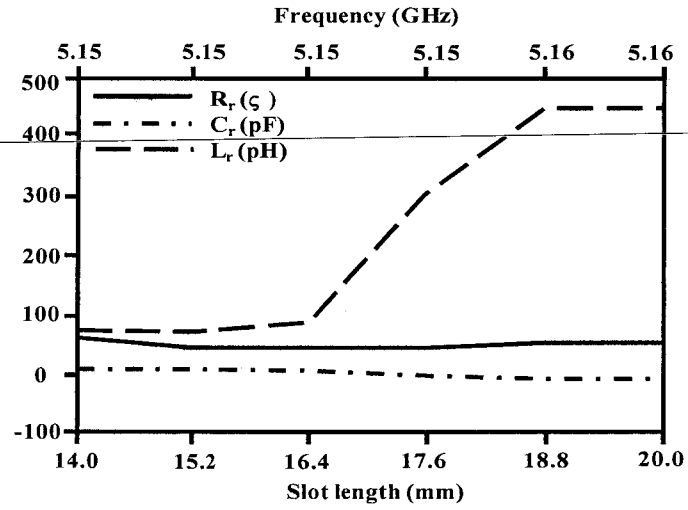


Figure 4.20. Relation between slots lengths, resonance frequency and R_r , C_r and L_r of middle radiating element of small size CDRA array

4.5.2.4 Effects of Inter-Slot Distance

The inter-slot distance is very critical factor. This distance should be between $0.5\lambda_g$ to λ_g to avoid the mutual coupling between the slots. The distance between the coupling slots increased from 23.5 mm to 25.5 mm with step size of 0.5 GHz as depicted in Table 4.16. It is noticed that by increasing inter-slot distance from 23.5 mm to 24.5 mm, antenna bandwidth reduced from 0.930 GHz to 0.920 GHz. For the inter-slot distance of 25.0 mm and 25.5 mm, the corresponding impedance bandwidths are 1.076 GHz and 0.822 GHz

respectively. It is depicted that the inter-slot distance of 25.0 mm gives the optimum improvement in the antenna performance with impedance bandwidth of 1.076 GHz.

Table 4.16. Effect of inter-slot distance on bandwidth.

Distance (mm)	Bandwidth (GHz)
23.5	0.930
24.0	0.924
24.5	0.920
25.0	1.076
25.5	0.822

4.5.2.5 Effects of Inter-element Distance

As the middle element of the small size CDRA array is exciting due to the mutual coupling of its neighboring elements. The parametric study on inter-element distance is carried out to find the optimum bandwidth and to study its influence on antenna performance. By setting the inter-slot distance of 25.0 mm, the distance between the top and bottom radiating element is $0.531\lambda_{air}$. Initially the middle CDRA is placed at the center of both radiating element at a distance of $0.265\lambda_{air}$, thus by changing its distance from top and bottom radiating element antenna performance is analyzed. The effects of changing the inter-element distance on the antenna bandwidth is depicted in Table 4.17. The middle CDR moved towards the top radiating element first and then towards the bottom radiating elements by $0.002\lambda_{air}$ respectively, with step size of $0.001\lambda_{air}$. It is noticed that for inter-element distance of $0.264\lambda_{air}$ and $0.263\lambda_{air}$ of middle CDR from top radiating element, the impedance bandwidths are 1.076 GHz and 0.822 GHz respectively. Alternatively, by moving middle CDR towards bottom radiating element, the corresponding impedance bandwidths are 0.940 GHz and 0.970 GHz respectively. It is depicted that the inter-element distance of $0.264\lambda_{air}$ and $0.266\lambda_{air}$ between the consecutive radiating elements, gives the optimum antenna performance with bandwidth of 1.076 GHz.

Table 4.17. Effect of inter-element distance on antenna array bandwidth.

Distance between top and middle CDR (λ_{air})	Distance between middle and bottom CDR (λ_{air})	Bandwidth (GHz)
0.263	0.267	0.822
0.264	0.266	1.076
0.265	0.265	1.000
0.266	0.264	0.940
0.267	0.263	0.970

4.5.3 Antenna Radiation Patterns

The simulated and measured E-plane ($\theta = 0^\circ$) and H-plane ($\theta = 90^\circ$) radiation patterns of the proposed array antenna at different frequencies 5.0 GHz, 5.6 GHz and 5.8 GHz are depicted in the Figure 4.21 and 4.22 respectively. The corresponding directions of the main lobes in E-plane are 0° , 0° and 0° with a magnitude of 8.3 dBi, 10.5 dBi and 10.1 dBi respectively. The corresponding H-plane radiation patterns at 5.0 GHz, 5.6 GHz and 5.8 GHz respectively are depicted in Figure 4.22. It is noticed that there is a spillover in the radiation patterns due to the small size ground plane. This kind of spillover in the radiation patterns is due to the electromagnetic scattering from the edges of the ground plane. However, simulated and measured results are in good agreement.

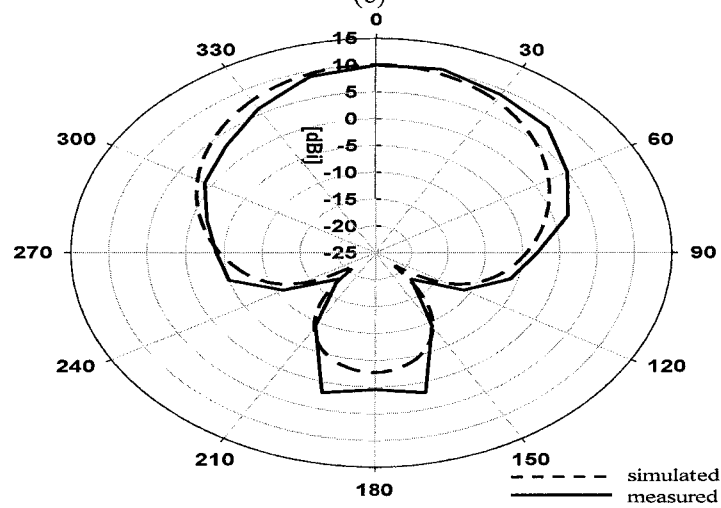
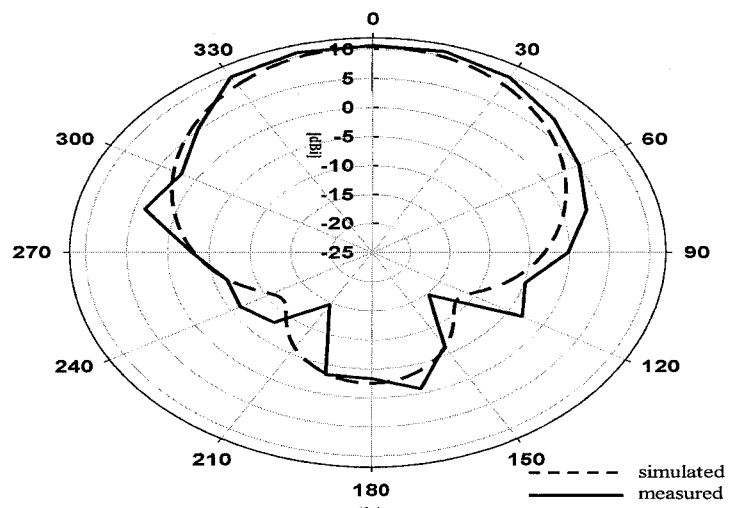
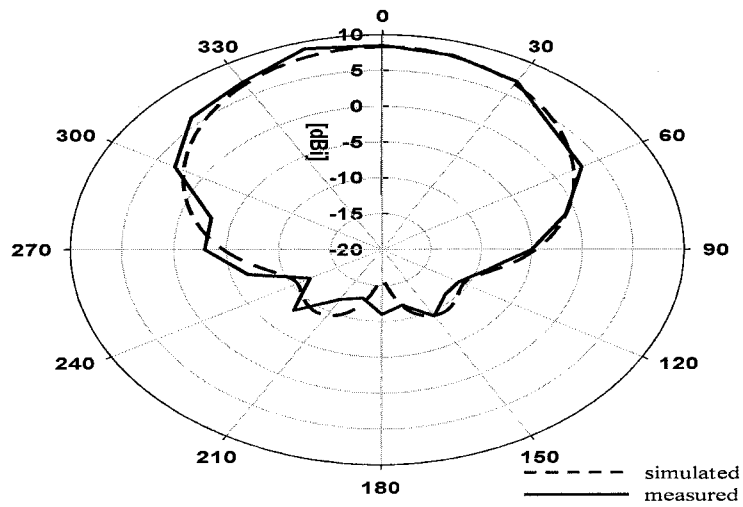


Figure 4.21. E-plane radiation patterns of small size CDRA array at (a) 5.0 GHz
(b) 5.6 GHz (c) 5.8 GHz.

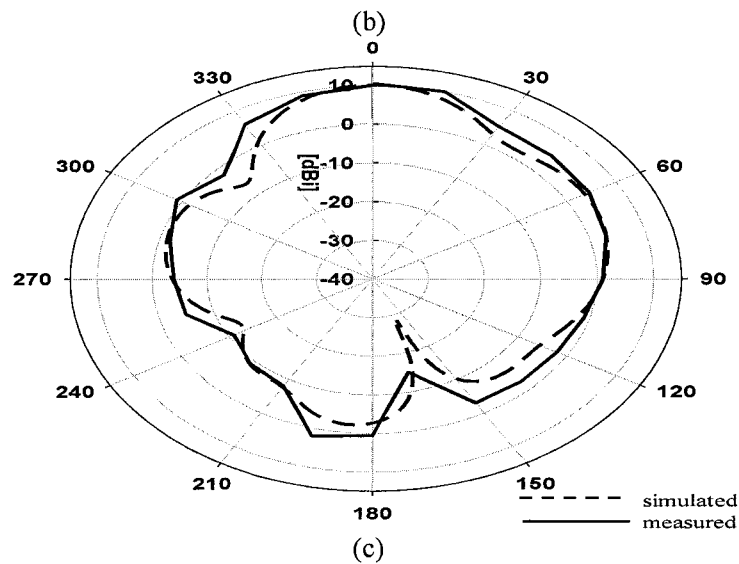
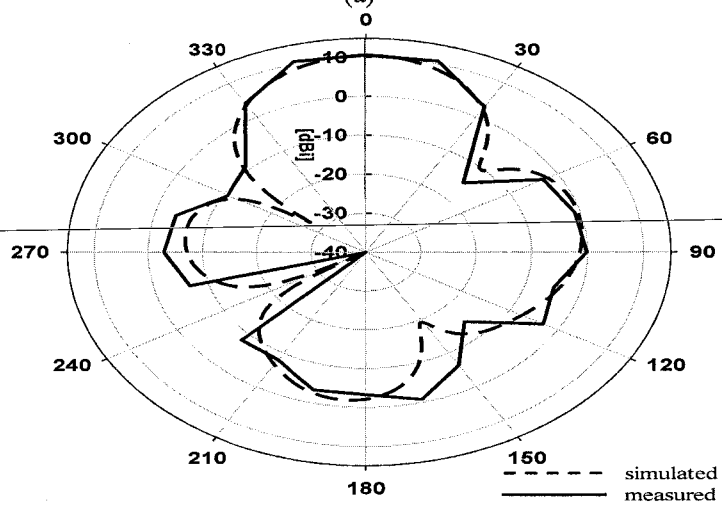
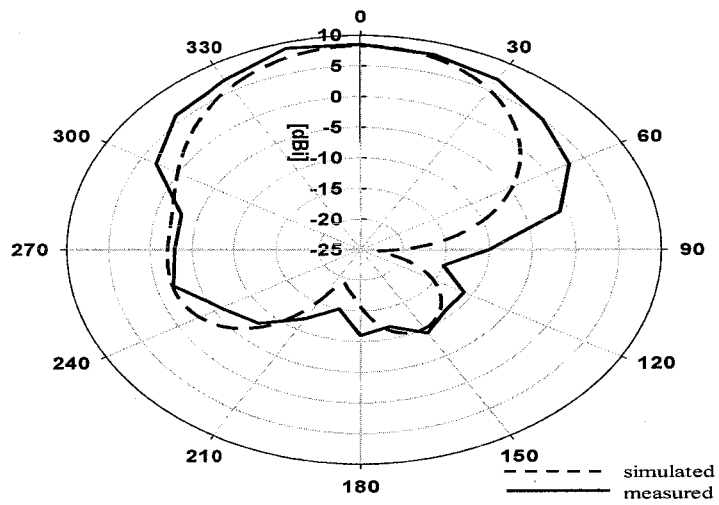


Figure 4.22. H-plane radiation patterns of small size CDRA array at (a) 5.0 GHz
(b) 5.6 GHz (c) 5.8 GHz.

The signal strength measurements of the small size high gain CDRA array and the standard monopole antenna of 5.0 dBi gain is performed in open space at different distances. The corresponding signal strength measurements at 5.6 GHz are depicted in Table 4.18. Initially the signal strength is measured at a distance of 2.0 m from the transmitter, then the distance between transmitter and receiver is increased from 5.0 m to 30.0 m with step size of 5.0 m. At 2.0 m, the signal strength of proposed antenna and the monopole antenna is -40.0 dBm and -45.0 dBm respectively. It is noticed that the by increasing distance from 5.0 m to 30.0 m, the signal strength of proposed antenna decreased from -40.0 dBm to -60.0 dBm, while the signal strength of monopole antenna decreased from -45.0 dBm to -70.0 dBm. From the open space measurements depicted in Table 4.18, it is clear that the performance of the proposed small size high gain CDRA array is superior as compared to standard monopole antenna.

Table 4.18. Signal strength of small size CDRA array at different distances.

Distances (m)	Signal strength of small size CDRA array (dBm)	Signal Strength of monopole antenna (dBm)
2.0	-40.0	-45.0
5.0	-44.0	-55.0
10.0	-49.0	-60.0
15.0	-54.0	-65.0
20.0	-56.0	-68.0
25.0	-59.0	-69.0
30.0	-60.0	-70.0

4.5.4 Antenna Gain and Efficiency

In general, the dielectric resonator gives a unidirectional and broad radiation pattern. The single element CDRA gain can be increased by using in array configuration. The achieved directivity of the proposed array antenna varied from 7.33 dBi to 10.5 dBi over the entire band from 4.6 GHz to 6.0 GHz. The simulated and measured gain of the small size CDRA array at different frequencies 5.0 GHz, 5.6 GHz and 5.8 GHz is depicted in Table 4.19. It is shown that the maximum directivity of 10.8 dBi is achieved at operating frequencies of 5.6 GHz. The proposed array radiates very small energy in the backward direction with front-to-rear ratio of 26 dB at resonance frequency of 5.0 GHz. The radiation efficiency of the small size CDRA array at different frequencies is also shown in Table 4.19. The radiation efficiency at different frequencies 5.0 GHz, 5.6 GHz and 5.8 GHz are 94.30%, 92.48% and 88.13% respectively. The impedance of the proposed antenna at resonance frequency is $52.97 + j2.99 \Omega$.

Table 4.19. The efficiency and gain of the small size CDRA array.

Frequency (GHz)	η %	$G_{simulated}$ (dBi)	$G_{measured}$ (dBi)
5.0	94.30	8.3	8.5
5.6	92.48	10.5	10.8
5.8	88.13	10.1	10.4

4.5.5 Advantages and Comparison of Proposed Technique with Literature Work

The aperture slot radiates in the forward as well as in the backward direction [111]. The backward radiation can be minimized by reducing the number of coupling slots in antenna design. In the proposed design, energy radiate by the coupling slots is used to excite the top and bottom radiating elements. The middle CDR is excited due to the mutual coupling of its neighboring elements instead of using another slot. By using mutual coupling in the proposed design, significant improvement in the antenna performance is achieved with impedance bandwidth of 1.2 GHz as depicted in Figure 4.14. Another advantage of using

two slots instead of three slots, back side radiation of proposed design is minimized. The back side radiation of the proposed small size CDRA array by using two and three aperture slots are depicted in Figure 4.23. The back side radiation with two and three aperture slots are -17.6 dB and -12.5 dB respectively at 5.0 GHz, which shows that by using the mutual coupling instead of using third slot to excite the middle CDRA not only increase the bandwidth but also reduces the back side radiation over the entire frequency band.

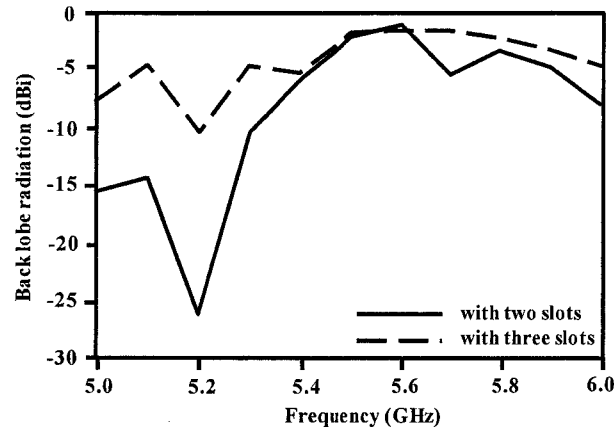


Figure 4.23. Back side radiation comparison using two and three aperture slots.

The comparison between the previous literatures on aperture coupled technique and the proposed work using aperture and mutual coupling is depicted in Table 4.20. In [36], four elements RDRA array using aperture coupled microstrip transmission line has been presented. It is noticed that there is significant improvement in DRA gain by using in array configuration but with limited bandwidth of about 0.042 GHz. The 4 x 2 elements microstrip patch antenna array designed for 802.11a WLAN application also has been introduced [1]. The corresponding array achieved a bandwidth of 0.6 GHz with 13.0 dBi gain. The nine elements aperture coupled RDRA array has been presented in [45]. It achieved a bandwidth and gain of 0.080 GHz and 10 dBi respectively at 5.8 GHz. The proposed design shows that by utilizing aperture and mutual coupling, significant improvement in the antenna performance is achieved with impedance band and gain of 1.2 GHz and 10.8 dBi respectively. It is also observed that by using mutual coupling with aperture coupling technique, not only enhance the bandwidth but also reduce the number of element as compared to the literature work. Overall it reduces the size as well as the cost of the proposed antenna.

Table 4.20. Comparison between the previous literatures on aperture coupled array antenna and the proposed array antenna.

Author and year	Frequency band (GHz)	Number of elements	Bandwidth (GHz)	Maximum Gain (dBi)
M. F. Ain, Y. M. Qasaymeh, Z. A. Ahmad, M. A. Zakariya et. al., 2012	X - band	1 x 4	0.042	9.0
Dau-Chyrh Chang and Shao-Hsiang Yen 2011	5.0	4 x 2	0.600	13.0
M. F. Ain, Y. M. Qasaymeh, Z. A. Ahmad, M. A. Zakariya et. al., 2010	5.8	3 x 3	0.080	10.0
Proposed work	5.0	1 x 3	1.200	10.8

4.6 Summary

The results of single element cylindrical dielectric resonator antenna (CDRA) and three single band, dual band and small size high gain CDRA arrays designed for IEEE 802.11a/b are discussed. The aperture coupled single element CDRA achieved an impedance bandwidth of 0.2 GHz with 7.0 dBi gain. It is noticed that the proposed single element CDRA is suitable for IEEE 802.11a WLAN application for frequency range of 5.15 GHz to 5.35 GHz. The results of electrical model and fabricated prototype of single element CDRA are in good agreement with the simulated results.

To overcome the limited gain of single element CDRA, three CDRA arrays are proposed. The mutual coupling mechanism is used along with aperture coupling technique to excite the array elements, which enhances the limited bandwidth of aperture coupled DRA array. By using mutual and aperture coupling mechanisms, the proposed three single band, dual band and small size CDRA array designs achieved the impedance bandwidth of 1.08 GHz, 1.04 GHz and 1.2 GHz respectively. The dual band CDRA array achieved the resonance at lower frequency band of 2.45 GHz by utilizing the top loaded mechanism. The fabricated prototypes of proposed three array designs are also studied. The equivalent

lumped element circuit of the small size high gain CDRA array is also modeled, which gives the good agreement with the simulated and measured results.

The advantages of using mutual coupling in terms of bandwidth and back side radiation are also discussed. It is noticed that by using mutual coupling instead of three slots, not only enhance the impedance bandwidth but also reduces the back side radiation. The comparison between the proposed array designs and literature work showed that, the proposed array not only achieved the 93.3% improvement in the impedance bandwidth but also reduced the less number of radiating elements used as compared to literature work.

CHAPTER 5

CONCLUSION AND CONTRIBUTION

5.1 Conclusion

This thesis reviewed several techniques to enhance the gain of the antenna such as linear array, planar array and reflect array antenna. The linear DR antenna array has established itself in various applications at high and low frequencies. The aperture coupled linear arrays with large number of elements has been reported, but with limitations in bandwidth for WLAN and X band applications as presented in section 2.4.2. The main objective of this thesis is to design a wide band and high gain CDRA array for IEEE 802.11a WLAN applications. The operating frequency for IEEE 802.11a WLAN band is 4.915 to 5.875 GHz.

In this research work, a high permittivity dielectric material $\epsilon_r = 55$ is used to fabricate the CDRs; which makes them compact in size. However, the bandwidth is expected to be narrow due to high permittivity material, and it is challenging to enhance the bandwidth. A combination of aperture and mutual coupling techniques is used to enhance the array antenna bandwidth using high permittivity CDRs.

The proposed research work, presented all aspects of successful single element aperture coupled CDRA before designing the three aperture and mutual coupled high gain and wide band CDRA array designs. Fundamental concepts of DRA and use of DRA in different array configurations are reported in order to explore the foundation of DRA and its array structure. Based on the literature, the design of single element aperture coupled CDRA was initially developed before designing the high gain and wideband CDRA array using CST. The single element aperture coupled CDRA achieved an impedance bandwidth of 0.2 GHz with 6.9 dB gain. From the parametric study on the antenna tuning parameters, it is revealed that single element CDRA produces the optimum bandwidth

of 0.2 GHz from 5.15 GHz to 5.35 GHz, when the slot length, width and slot offset distance are 14.0 mm 4.0 mm and 4.0 mm respectively.

The 1 x 3 element single band CDRA array designed to enhance the performance of single element CDRA for IEEE 802.11a WLAN application. The single band CDRA array achieved an impedance bandwidth of 1.08 GHz with 9.6 dBi gain. From the parametric study performed on the antenna tuning parameters, it is depicted that the antenna gives the optimum bandwidth of 1.08 GHz when slot length, width and inter-slot distance are 14.0 mm, 4.0 mm and 25.0 mm respectively.

The dual band CDRA array designed for IEEE 802.11a/b WLAN application achieved impedance bandwidths of 0.1 GHz and 1.04 GHz respectively for lower and upper band. It is clear that resonance at lower frequency can be achieved by using metallic top-loaded mechanism. It is analyzed that the dual band antenna gives the optimum bandwidth of 0.1 GHz and 1.04 GHz for lower and upper resonance frequencies when slot length, width, inter-slot distance and the radius of top-loaded metallic sheets are 14.0 mm, 4.0 mm, 25.0 mm and 7.75 mm respectively.

The small size high gain CDRA array designed for IEEE 802.11a WLAN application achieved impedance bandwidths of 1.076 GHz. The parametric study performed on the antenna tuning parameters, depicted that the antenna gives the optimum bandwidth of 1.076 GHz when slot length, width and inter-slot distance are 20.0 mm, 4.0 mm and 25.0 mm respectively.

The equivalent lumped element circuits of single element CDRA and small size high gain antenna array are also designed to verify the antennas feasibility. The corresponding achieved impedance bandwidths are 0.2 GHz and 1.0 GHz respectively. The parametric study performed on the position of coupling slot under single element CDRA design showed that the resonance frequency shifted from 4.70 GHz to 5.35 GHz by moving slot from the CDR centre to 5.0 mm towards its edge. It is shown the antenna give no resonance below -10 dB until slot offset of 3.0 mm. For the slot offset of 4.0 mm and 5.0 mm the resonance frequencies are 5.25 GHz and 5.34 GHz respectively. It is analyzed that the values of lumped parameters changed accordingly with slot position under CDR namely R_r (300 Ω to 83 Ω), C_r (432.289 pF to 53.655 pF) and L_r (2.650 pH to 16.556 pH). While the parametric study performed on the slots lengths of small size high gain antenna array from 2.0 mm to 24.0 mm showed that the antenna gives the optimum results with impedance bandwidth of 1.076 GHz when slots lengths are 20.0 mm. It is observed that the

value of resonance resistance R_r decreased by increasing the slot length. The value of R_r decreased from $170\ \Omega$ to $75\ \Omega$ for top radiating element, $100\ \Omega$ to $58\ \Omega$ for bottom radiating element and $58\ \Omega$ to $55\ \Omega$ for middle radiating element. The value of C_r and L_r changed accordingly due to the inverse relation between the R_r with C_r and L_r with C_r .

Fabrication of the single element CDRA and three high gain and wide band 1×3 element CDRA arrays (single band, dual band and small size) are reported. The aperture coupled technique is used for single element CDRA while the aperture and mutual coupled mechanisms are used to excite the array elements. The single element CDRA and three 1×3 element CDRA arrays produces the impedance bandwidth of 0.23 GHz, 1.08 GHz, 1.076 GHz and 1.2 GHz respectively. The corresponding achieved gain is 7.0 dBi, 9.3 dBi, 9.3 dBi and 10.8 dBi respectively. The small size high gain and wide band CDRA array showed good impedance bandwidth of 1.2 GHz with 10.8 dBi gain and covers the entire frequency band of IEEE 802.11a WLAN application. The measured results of the all designs showed good agreement between the simulated (CST and ADS) results.

There has been various attempts to develop a high gain DRA array but the reported band width achieved is limited [36, 45]. In [36], four elements RDRA array using aperture coupled microstrip transmission line has been presented. It is noticed that there is significant improvement in DRA gain by using in array configuration but with limited bandwidth of about 0.042 GHz. Similarly, the nine elements aperture coupled RDRA array has been presented in [45]. It achieved a bandwidth and gain of 0.080 GHz and 10 dBi respectively at 5.8 GHz. In the proposed aperture and mutual coupled technique, an improvement of 93.3 % in bandwidth has been achieved as compared to the literature work. The improvement in the bandwidth is due to the utilization of mutual coupling mechanism while the improvement in the gain is achieved by using CDR in array configuration. Back side radiation is also significantly improved by adopting a combination of aperture and mutual coupled mechanism instead of relying on aperture coupled slot only.

5.2 Contribution

In this thesis, four antenna designs (single element CDRA, single band CDRA array, dual band CDRA array and small size, high gain and wide band CDRA array) are proposed. The equivalent lumped models of single element CDRA and small size, high gain CDRA array

are also designed and reported. The fabricated prototypes of all four designs are also investigated.

The single element aperture coupled CDRA 3D structure, its electrical model and fabricated prototype are proposed for IEEE 802.11a WLAN application. The *TE* mode of single element CDR is tuned to operate for required application. The parametric study on antenna tuning parameters such as aperture slot dimensions (length and width) and slot position are carried out to achieve the optimum antenna performance. It is depicted that the *TE* mode in CDR is excited by placing aperture slot close to the edge of the CDR.

The major contribution in this thesis is wide band and high gain (single band, dual band and small size) CDRA arrays. The bandwidth of DRA array is enhanced by using mutual coupling with aperture coupling mechanism. From the analysis, it is depicted that 93.3% improvement in the bandwidth is achieved as compared to literature work on aperture coupled technique. By using aperture and mutual coupling mechanism, three proposed arrays achieved an impedance band width of 1.08 GHz, 1.04 GHz and 1.20 GHz respectively. The maximum gains of the proposed array antennas for IEEE 802.11a WLAN application are 9.6 dBi, 9.4 dBi and 10.5 dBi respectively.

The equivalent lumped element model of small size and high gain CDRA array is also designed to verify the antenna feasibility. The equivalent model is designed by transforming each antenna component into its equivalent lumped model circuit. The mutual coupling between the top and bottom radiating elements is represented by coupling capacitors. The equivalent circuit parameters are determined by using equation (2.38) to (2.50). The result shows that the electrical model return loss response is in good accordance with CST results. The performance of fabricated prototype is verified by comparing its results against those obtained through the simulated (CST and ADS) results. In conclusion, by using mutual coupling with aperture coupling mechanism, significant improvement in the bandwidth is achieved.

5.3 Recommendation and Future Work

Since the discussed work in this thesis is all about exploring the mutual coupling technique with aperture coupling and cylindrical shape dielectric resonators. It will be great experience to apply the mutual coupling with probe feed and other shapes of dielectric

resonators. The mutual and aperture coupling antenna array can be designed using probe feed to evaluate the performance of proposed technique with different feeding structure.

REFERENCES

- [1] D. C. Chang and S. H. Yen, "High Gain Antenna Array for the Application of IEEE802.11a Access Point", IEEE International Workshop on Electromagnetic, Applications and Student Innovation (iWEM), p.p 125-129, 2011.
- [2] A. Petosa, "Dielectric resonator antennas Handbook", Artech House Inc., 2007.
- [3] G. Almpanis, C. Fumeaux and R. Vahldieck, "Pyramidal Dielectric Resonator Antenna for Wideband Applications", The Second European Conference on Antennas and Propagation, p.p 1-4, 2007.
- [4] Y. Huang and K. Boyle, "Antennas From Theory to Practice", John Wiley and Sons Ltd., 2008.
- [5] M. S. Aras, M. K. A. Rahim, et. al., "An array of a dielectric resonator antenna for wireless application", IEEE international conference on RF and Microwave, p.p 459-463, 2008.
- [6] S. A. Long, M. W. McAllister and L. C. Shen, "The resonant cylindrical dielectric cavity antenna", IEEE Transactions on Antennas and Propagation, Vol. 31, p.p 406-412, 1983.
- [7] M. A. Saed and R. Yadla, "Microstrip - FED low profile and compact dielectric resonator antennas", Progress In Electromagnetic Research, Vol. 56, p.p 151-162, 2006.
- [8] K. P. Esselle, "A dielectric-resonator-on-patch (DROP) antenna for broadband wireless applications: concept and results", IEEE Antennas and Propagation Society International Symposium, Vol. 2, p.p 22-25, 2001.
- [9] S. M. Deng, C. L. Tsai, et. al., "CPW-fed rectangular ceramic dielectric resonator antennas with high profile", IEEE Antennas and Propagation Society International Symposium, Vol. 1, p.p 1098-1101, 2004.
- [10] Y. Coulibaly, T. A. Denidni and H. Boutayeb, "Broadband Microstrip-Fed Dielectric Resonator Antenna for X-Band Applications", IEEE Antennas and Wireless Propagation Letters, Vol. 7, p.p 341-345, 2008.
- [11] A. Petosa, S. Thirakoune and A. Ittipiboon, "Higher-order modes in rectangular DRAs for gain enhancement", 13th International Symposium on Antenna Technology and Applied Electromagnetics and the Canadian Radio Sciences Meeting, p.p 1-4, 2009.

- [12] J. George, C. K. Aanandan, et. al., "Dielectric-resonator-loaded microstrip antenna for enhanced impedance bandwidth and efficiency". *Microw. Opt. Technol. Lett.*, Vol. 17, p.p 205–207, 1998.
- [13] C. H. Lin, J. S. Sun, et. al., "Cylindrical DR Antenna Design", *Progress In Electromagnetics Research Symposium*, Beijing, China, March 23-27, 2009.
- [14] Y. Coulibaly, M. Nedil, et. al., "High gain cylindrical dielectric resonator with superstrate for broadband millimeter-wave underground mining communications", *14th International Symposium on Antenna Technology and Applied Electromagnetics & the American Electromagnetics Conference (ANTEM-AMEREM)*, p.p 1-4, 2010.
- [15] A. V. P. Kumar, V. Hamsakutty, et. al., "Microstrip fed cylindrical dielectric resonator antenna with a coplanar parasitic strip", *Progress In Electromagnetic Research*, PIER, Vol. 60, p.p 143-152, 2006.
- [16] R. A. Kranenburg, S. A. Long and J. T. Williams, "Coplanar waveguide excitation of dielectric resonator antennas", *IEEE Transactions on Antennas and Propagation*, Vol. 39, p.p 119-122, 1991.
- [17] K. Pliakostathis, "A novel enclosed cylindrical dielectric resonator antenna", *7th IEEE High Frequency Postgraduate Student Colloquium*, Vol. 4, p.p 474-477, 2002.
- [18] G. Drossos, Z. Wu and L. E. Davis, "Circular polarised cylindrical dielectric resonator antenna," *Electronics Letters*, Vol. 32, p.p 281-283, 1996.
- [19] D. Guha and Y. M. M. Antar, "Four-Element Cylindrical Dielectric Resonator Antenna for Wideband Monopole-Like Radiation", *IEEE Transactions on Antennas and Propagation*, Vol. 54, p.p 2657-2662, 2006.
- [20] S. H. Zainud-Deen, H. A. Hend, et. al., "Investigation of cylindrical dielectric resonator antenna mounted on a circular cylindrical ground plane", *IEEE Antennas and Propagation Society International Symposium (APSURSI)*, p.p 1-4, 2010.
- [21] S. Sreekantan, Y. K. Ling, et. al., "Simulation and experimental investigations on rectangular, circular and cylindrical dielectric resonator antenna", *Progress In Electromagnetics Research C*, Vol. 7, p. p 151-166, 2009.
- [22] L. C. Y. Chu, D. Guha, et. al., "Conformal Strip-Fed Shaped Cylindrical Dielectric Resonator: Improved Design of a Wideband Wireless Antenna", *IEEE Antennas and Wireless Propagation Letters*, Vol. 8, p.p 482-485, 2009.
- [23] K. M. Luk and K. W. Leung, "Dielectric Resonator Antennas", *Research Studies Press*, Hertfordshire, U.K, 2003.

- [24] D. Yau and M. V. Shuley, "Numerical analysis of an aperture coupled rectangular dielectric resonator antenna using a surface formulation and the method of moments", IEEE proceeding on Microwaves, Antennas and Propagation, Vol. 146, p.p 105-110, 1999.
- [25] R. K. Mongia and P. Bhartia, "Dielectric resonator antennas - a review and general design relations for resonant frequency and bandwidth", International Journal of Microwave and Millimeter-Wave Computer-Aided Engineering, Vol. 4, Issue 3, p.p 230-247, 1994.
- [26] P. M. Hadalgi, R. G. Madhuri and S. L. Mallikarjun, "Slot fed wideband dielectric resonator antenna for wireless applications", Indian Journal of Radio & Space Physics, Vol. 39, p.p 372-375, 2010.
- [27] R. K. Gangwar, S. P. Singh and D. Kumar, " Comparative Studies of Rectangular Dielectric Resonator Antenna with Probe and Microstrip line Feeds", Scholar research library, Vol. 2(3), p.p 1-10, 2010.
- [28] M. T. Lee, K. M. Luk, et. al., "A small dielectric resonator antenna", IEEE transaction on Antennas and Propagation, Vol. 50, p.p 1485-1487, 2002.
- [29] A. Ittipiboon, A. Petosa, et. al., "An investigation of a novel broadband dielectric resonator antenna", Antennas and Propagation Society International Symposium, Vol. 3, p.p 2038-2041, 1996.
- [30] J. Carrie, K. P. Esselle, et. al., "A K-band circularly polarized cavity backed dielectric resonator", Antennas and Propagation Society International Symposium, Vol. 1, p.p 734-737, 1996.
- [31] A. Buerkle, K. Sarabandi, et. al., "A novel approach to enhance the bandwidth of miniaturized dielectric resonator antennas", IEEE Antennas and Propagation Society International Symposium, Vol. 2, p.p 1359-1362, 2004.
- [32] H. Raggad, M. Latrach, et. al., "Cylindrical dielectric resonator antenna fed by a stair slot in the ground plane of a microstripline", General Assembly and Scientific Symposium, p.p 1-4, 2011.
- [33] Z. Aijaz and S. C. Shrivastava, "Effect of the Different Shapes:Aperture Coupled Microstrip Slot Antenna", International Journal of Eletronics Engineering, p.p 103-105, 2010.
- [34] M. F. Ain, Y. M. Qasaymeh, et al., "An Equivalent Circuit of Microstrip Slot Coupled Rectangular Dielectric Resonator Antenna", Progress In Electromagnetics Research Symposium Proceedings, 2012.

- [35] J. J. Adz, H. M. Md Khir, et. al., "A compact dual band directional cylindrical dielectric resonator antenna", 4th International Conference on Intelligent and Advanced Systems, p.p 265-268, 2012.
- [36] M. F. Ain, Y. M. Qasaymeh, et. al., "Novel modeling and design of circularly polarized dielectric resonator antenna array", Progress In Electromagnetic Research, Vol. 28, p.p 165-179, 2012.
- [37] P. V. Bijumon, S. K. Menon, et. al., "Broadband cylindrical dielectric resonator antenna excited by modified microstrip line", Electronics Letters, Vol. 41, Issue 7, p.p 385-387, 2005.
- [38] A. Petosa, A. Ittipiboon, et. al., "Dielectric resonator antenna technology for wireless applications," IEEE Antennas and Propagation for Wireless Communications, p.p 117-120, 1998.
- [39] A. A. H. Azremi, N. A. Saidatul, et. al., "A cylindrical barium strontium titanate (BST) dielectric resonator antenna for 5.0 GHz wireless LAN application", Asia-Pacific Symposium on Electromagnetic Compatibility, p.p 327-330, 2008.
- [40] Rezaei and Pejman, "Dielectric resonator antenna for wireless LAN applications", IEEE Antennas and Propagation Society International Symposium , p.p 1005-1008, 2006.
- [41] M. F. Ain, S. I. S. Hassan, et. al., "2.5 GHz batio3 dielectric resonator antenna", Progress In Electromagnetics Research, Vol. 76, p.p 201-210, 2007.
- [42] A. Petosa, A. Ittipiboon, et. al., "Recent advances in dielectric-resonator antenna technology", IEEE Antennas and Propagation Magazine, Vol. 40, p.p 35-48, 1998.
- [43] J. J. Adz, M. H. Md Khir, et. al., "Frequency tuning for compact cylindrical dielectric resonator antenna (CDRA)", National Postgraduate Conference (NPC), p.p 1-5, 2011.
- [44] A. Laisne, R. Gillard and G. Piton, "Circularly polarised dielectric resonator antenna with metallic strip", Electronics letters, Vol. 38 No.3, 2002.
- [45] M. F. Ain, Y. M. Qasaymeh, et. al., "A novel 5.8 GHz high gain array dielectric resonator antenna", Progress In Electromagnetics Research C, Vol. 15, p.p 201-210, 2010.
- [46] A. Petosa, R. K. Mongia, et. al., "Investigation of various feed structures for linear arrays of dielectric resonator antennas", IEEE Antennas and Propagation Society International Symposium, Vol. 4, p.p 1982-1985, 1995.

- [47] R. Kumari, S. K. Behera and R. K. Mishra, "Log Periodic Dielectric Resonator Antenna for K and Ka-band Applications", International Conference on Electronic Systems India, 2011.
- [48] A. S. Al-Zoubi, A. A. Kishk and A. W. Glisson, "A Linear Rectangular Dielectric Resonator Antenna Array Fed by Dielectric Image Guide With Low Cross Polarization", IEEE Transactions on Antennas and Propagation, Vol. 58, p.p 697-705, 2010.
- [49] H. Dashti, M. H. Neshati and F. Mohanna, "RDRA Array Fed by Dielectric Image Line with Improved Gain & Low Back Radiation", First International Conference on Communication Engineering, p.p 44-44, 2010.
- [50] H. Dashti, M. H. Neshati and F. Mohanna, "Design investigation of DRA array fed by Dielectric Image Line", IEEE 19th Iranian Conference in Electrical Engineering (ICEE), p.p 1-4, 2011.
- [51] E. M. Kejani and M. H. Neshati, " Design investigation of circularly polarized Dielectric Resonator Antenna array excited by Dielectric Image Line ", IEEE 18th Iranian Conference in Electrical Engineering (ICEE), p.p 75-79, 2010.
- [52] M. T. Birand and R. V. Gelsthorpe, "Experimental millimetric array using dielectric radiators fed by means of dielectric waveguide", Electronics Letters, Vol. 17, p.p 633-635, 1981.
- [53] G. D. Loos and Y. M. M. Antar, "Investigation of a novel aperture-coupled dielectric resonator antenna subarray," IEEE Antennas and Propagation Society International Symposium, Vol. 3, p.p 1510-1513, 1994.
- [54] K. Y. Chow, K. W. Leung, et. al., "Cylindrical dielectric resonator antenna array," Electronics Letters, Vol. 31, p.p 1536-1537, 1995.
- [55] A. Petosa, R. K. Mongia, et. al., "Design of microstrip-fed series array of dielectric resonator antennas", Electronics Letters, Vol. 31, p.p 1306-1307, 1995.
- [56] A. Petosa, A. Ittipiboon, et. al., "Bandwidth improvement for a microstrip-fed series array of dielectric resonator antennas," Electronics Letters, Vol. 32, p.p 608-609, 1996.
- [57] A. Petosa, R. Larose, et. al., "Microstrip-fed array of multisegment dielectric resonator antennas", IEE Proceedings Microwaves, Antennas and Propagation, Vol. 144, p.p 472-476, 1997.
- [58] A. Petosa and S. Thirakoune, "Linear array of dielectric resonator antennas optimized using a genetic algorithm for low-sidelobe applications", IEEE Asia-Pacific Microwave Conference, p.p 21-24, 2000.

- [59] A. Lambrecht, O. Oestreich, et. al., "Dielectric Resonator Antennas for Polarization Diversity in Base Station Array Applications", IEEE International Conference on Electromagnetics in Advanced Applications, p.p 527-530, 2007.
- [60] T. Ueda, N. Michishita, et. al., "Dielectric-Resonator-Based Composite Right/Left-Handed Transmission Lines and Their Application to Leaky Wave Antenna", IEEE Transactions on Microwave Theory and Techniques, Vol. 56, p.p 2259-2269, 2008.
- [61] W. M. A. Wahab and S. S. Naeini, "High efficiency millimeter wave planar waveguide fed dielectric resonator antenna (DRA)," IEEE Antennas and Propagation Society International Symposium, p.p 1-4, 2009.
- [62] T. Ruiyuan, V. plcanic, et. al., "A Compact Six-Port Dielectric Resonator Antenna Array: MIMO Channel Measurements and Performance Analysis", IEEE Transactions on Antennas and Propagation, Vol. 58, p.p 1369-1379, 2010.
- [63] V. Plicanic, Z. Meifang and B. K. lau, "Diversity mechanisms and MIMO throughput performance of a compact six-port dielectric resonator antenna array", IEEE International Workshop on Antenna Technology (iWAT), p.p 1-4, 2010.
- [64] A. Motevasselian, A. Ellgardt and B. L. G. Jonsson, "A comparison of a finite and an infinite antenna array with cylindrical dielectric resonator elements," IEEE General Assembly and Scientific Symposium, p.p 1-4, 2011.
- [65] S. H. Zainud-Deen, H. A. Malhat and K. H. Awadalla, "Near-Field Focusing Dielectric Resonator Antenna Array for Fixed RFID Readers", International Journal of Radio Frequency Identification and Wireless Sensor Networks, Vol. 1 No. 2, p.p 1-12, 2011.
- [66] W. M. Abdel-Wahab, D. Busuioc and S. Safavi-Naeini, "Millimeter-Wave High Radiation Efficiency Planar Waveguide Series-Fed Dielectric Resonator Antenna (DRA) Array: Analysis, Design, and Measurements," IEEE Transactions on Antennas and Propagation, Vol. 59, p.p 2834-2843, 2011.
- [67] W. M. Abdel-Wahab, S. Safavi-Naeini and D. Busuioc, "High gain/ efficiency 2D-dielectric resonator antenna array for low cost mm-wave systems", IEEE International Symposium on Antennas and Propagation (APSURSI), p.p. 1682-1684, 2011.
- [68] S. H. Zainud-Deen, S. M. Gaber, et. al., "Multilayer dielectric resonator antenna transmitarray for near-field and far-field fixed RFID reader," Progress In Electriomagnetic Research, Vol. 27, p.p 129-142, 2012.

- [69] A. Al-Zoubi, A. Kishk and A. W. Glisson, "Analysis of Aperture Coupled Dielectric Resonator Antenna Fed by Dielectric Image Line", IEEE Antennas and Propagation Society International Symposium, p.p 2519-2522, 2006.
- [70] S. Kanamaluru, L. Ming-yi and Kai Chang, "Analysis and design of aperture-coupled microstrip patch antennas and arrays fed by dielectric image line", IEEE Transactions on Antennas and Propagation, Vol. 44, p.p 964-974, 1996.
- [71] Z. Wu, L. E. Davis and G. Drossos, "Cylindrical dielectric resonator antenna arrays", IEEE Eleventh International Conference on Antennas and Propagation, Vol. 2, p.p 668-671, 2001.
- [72] A. Derneryd, U. M. Khan, et. al., "Dual-polarized dielectric resonator antennas for base station applications", IEEE Proceedings of the 5th European Conference on Antennas and Propagation, p.p 606-610, 2011.
- [73] L. Song, S. Gigoyan, et. al., "Dielectric Resonator Antennas fed by Image Guide Lines", IEEE Antennas and Propagation Society International Symposium, p.p 2205-2208, 2006.
- [74] Thomas A. Milligan, "Modern antenna design", 2nd Edition, John Wiley & sons, 2005.
- [75] Y. Huang and K. Boyle, "Antennas: From Theory to Practice", John Wiley & sons, 2008.
- [76] A. Petosa and A. Ittipiboon, "Dielectric Resonator Antennas: A Historical Review and the Current State of the Art", IEEE Antennas and Propagation Magazine, Vol. 52, p.p 91-116, 2010.
- [77] R. Kumari, K. Parmar, et. al., "A dual band triangular shaped DRA array for WLAN/WiMAX applications", Annual IEEE India Conference (INDICON), p.p 1-4, 2011.
- [78] A. Buerkle, K. F. Brakora and K. Sarabandi, "Fabrication of a DRA Array Using Ceramic Stereolithography", IEEE Antennas and Wireless Propagation Letters, Vol. 5, p.p 479-482, 2006.
- [79] A. Petosa, S. Thirakoun, et. al., "Comparison between planar arrays of perforated DRAs and microstrip patches", IEEE Antennas and Propagation Society International Symposium, Vol. 2A, p.p 168-175, 2005.
- [80] M. Haneishi and W. Bing, "Array antenna composed of circularly polarized dielectric resonator antennas", IEEE Antennas and Propagation Society International Symposium, Vol. 1, p.p 252-255, 1999.

- [81] A. Petosa, R. Larose, et. al., "Active phased array of dielectric resonator antennas", IEEE Antennas and Propagation Society International Symposium, Vol. 2, p.p 690-693, 1997.
 - [82] K. W. Leung, H. Y. Lo, et. al., "Two-dimensional cylindrical dielectric resonator antenna array", Electronics Letters, Vol. 34, p.p 1283-1285, 1998.
 - [83] H. Y. Lo, K. W. Leung, et. al., "Square arrays of cylindrical dielectric resonator antennas", IEEE Antennas and Propagation Society International Symposium, Vol. 4, p.p 2816-2819, 1999.
 - [84] S. L. S. Yang, R. Chair, et. al., "Circular Polarized Elliptical Dielectric Resonator Antenna Sub Array Fed by Hybrid-Ring Feeding Network", IEEE Antennas and Propagation Society International Symposium, p.p 2221-2224, 2006.
 - [85] Z. Yizhe, A. A. Kishk, et. al., "Analysis of Wideband Dielectric Resonator Antenna Arrays for Waveguide-Based Spatial Power Combining", IEEE Transactions on, Microwave Theory and Techniques, Vol. 55, p.p 1332-1340, 2007.
-
- [86] J. Svedin, L. G. Huss, et. al., "A Micromachined 94 GHz Dielectric Resonator Antenna for Focal Plane Array Applications", IEEE/MTT-S International Microwave Symposium, p.p 1375-1378, 2007.
 - [87] R. Kazemi, A. E. Fathy and R. A. Sadeghzadeh, "Dielectric Rod Antenna Array With Substrate Integrated Waveguide Planar Feed Network for Wideband Applications", IEEE Transactions on Antennas and Propagation, Vol. 60, p.p 1312-1319, 2012.
 - [88] S. H. Zainud-Deen, M. A. Abd-Elhady, et. al., "Dielectric resonator reflectarray with two DRA sizes and varying slot loading", IEEE Antennas and Propagation Society International Symposium (APSURSI), p.p 1-4, 2010.
 - [89] L. Qin-Yi, J. Yong-Chang and Z. Gang, "A Novel Microstrip Rectangular-Patch/Ring- Combination Reflectarray Element and Its Application", IEEE Antennas and Wireless Propagation Letters, Vol. 8, p.p 1119-1122, 2009.
 - [90] N. chang, "Gain enhancement for reflect array", Progress In Electromagnetic Research S , Vol. 2, No. 6, 2006.
 - [91] L. Naragani and P. H. Rao, "Stub loaded microstrip reflect array", Proceedings of the 9th International Conference on ElectroMagnetic Interference and Compatibility (INCEMIC), p.p 486-489, 2006.
 - [92] M. H. Jamaluddin, R. Gillard, et. al., "A Dielectric Resonator Antenna (DRA) Reflectarray", 39th European Microwave Conference, Italy, 2009.

- [93] C. Tienda, M. Arrebola, et. al., "Analysis of a dual-reflect array antenna", *IET Microwaves, Antennas & Propagation*, Vol. 5, p.p 1636-1645, 2011.
- [94] M. G. Keller, J. Shaker, et. al., "A Ka-Band Dielectric Resonator Antenna Reflectarray", 30th European Microwave Conference, p.p 1-4, 2000.
- [95] A. M. Abd-Elhady, S. H. Zainud-Deen, et. al., "X-band linear polarized aperture-coupled DRA reflectarray," *International Conference on Microwave and Millimeter Wave Technology (ICMMT)*, p.p 1042-1044, 2010.
- [96] M. Abd-Elhady, S. H. Zainud-Deens, et. al., "Slot-loading rectangular dielectric resonator elements reflectarray," *IEEE Middle East Conference on Antennas and Propagation (MECAP)*, p.p 1-3, 2010.
- [97] S. H. Zainud-Deen, E. Abd, et. al., "Design of dielectric resonator reflectarray using full-wave analysis", *NRSC National Radio Science Conference*, p.p 1-9, 2009.
- [98] M. Moeini-Fard and M. Khalaj-Amirhosseini, "Uneven dielectric reflect-array antennas", 5th International Symposium on Telecommunications (IST), p.p 82-86, 2010.
- [99] M. Moeini-Fard and M. Khalaj-Amirhosseini, "Inhomogeneous Perforated Reflect-Array Antennas", *Wireless Engineering and Technology*, Vol. 2, No. 2, 2011.
- [100] C. A. Balanis, "Antenna Theory Analysis and Design", 3rd Edition, John Wiley & sons, 2005.
- [101] H. G. Akhavan and D. Mirshekar-Syahkal, "A simple technique for evaluation of input impedance of microstrip-fed slot antennas", *Ninth International Conference on Antennas and Propagation*, Vol. 1, p.p 265-268, 1995.
- [102] H. G. Akhavan and D. Mirshekar-Syahkal, "Approximate model for microstrip fed slot antennas", *Electronics Letters*, Vol. 30, p.p 1902-1903, 1994.
- [103] F. Abboud, J. P. Damiano and A. Papiernik, "A new model for calculating the input impedance of coax-fed circular microstrip antennas with and without air gaps", *IEEE Transactions on Antennas and Propagation*, , Vol. 38, p.p 1882-1885, 1990.
- [104] F. T. Ladani and A. Z. Nejzhad, "Modeling of the conical dielectric resonator by simulation at 10 GHz and comparing with the cylindrical dielectric resonator", *International Symposium on Telecommunication*, 2008.
- [105] S. Simion, "Dielectric resonator equivalent circuit", *IEEE 7th Mediterranean Electrotechnical Conference Proceedings*, Vol. 2, p.p 488-491, 1994.
- [106] S. H. Zainud-Deen, S. I. El-Doda, et. al., "The relation between lumped element circuit models for cylindrical dielectric resonator and antenna parameters using MBPE", *Progress In Electromagnetics Research M*, Vol. 1, p.p 79-93, 2008.

- [107] A. Ferchichi, N. Fadlallah and A. Gharssallah, "A novel electrical model to an antenna array", Journal of engineering and technology, Vol. 3(12), p.p 321-329, 2011.
 - [108] R. E. Collin, "Foundations for Microwave Engineering", 2nd Edition, Wiley - IEEE Press, 2001.
 - [109] A. K. Verma and Nasimuddin, "Analysis of circular microstrip antenna on thick substrate", Journal of Microwaves and Optoelectronics, Vol. 2, 2002.
 - [110] P. D. M. Pozar, "A Review of Aperture Coupled Microstrip Antennas: History, Operation, Development, and Applications," 1996.
 - [111] O. Ahmed and A. Sebak, "Mutual coupling effect on ultrawidebandlinear antenna array performance", International Journal of Antenna and Propagation, Vol. 2011, 2011.
-

ACHIVEMENTS

Publications:

Journals:

- 1) A. A. Baba, M. A. Zakariya, Z. Baharudin, M. H. M. Khir, M. Z. Rehman, Z. A. Ahmad, and Y. M. A. Qasaymeh, "Aperture and mutual coupled cylindrical dielectric resonator antenna array", Progress In Electromagnetic Research C, Vol. 37, 223-233, 2013.
- 2) A. A. Baba, M. A. Zakariya, Z. Baharudin, M. Z. Rehman, F. A. Ain and Z. A. Ahmad, " Analysis of equivalent lumped element circuit of aperture and mutual coupled cylindrical dielectric resonator antenna array", Progress In Electromagnetic Research. (*Submitted*).

Conferences:

- 1) A. A. Baba, M. A. Zakariya, and Z. Baharudin, "Cylindrical Dielectric Resonator Antenna with TE 011 + δ Mode", IEEE Symposium on Wireless Technology & Applications (ISWATA 2013), 22-25 Sep, 2013.
- 2) A. A. Baba, M. A. Zakariya, and Z. Baharudin, "Electrical Model of Two Elements Aperture Coupled Cylindrical Dielectric Resonator Antenna Array", The 5th International Conference on Information Technology and Electrical Engineering (IEEE ICITEE 2013), 7-8, Oct, 2013.
- 3) A. A. Baba, M. A. Zakariya, Z. Baharudin, M. F. Ain and Z. A. Ahmad, "Wideband and High gain Cylindrical Dielectric Resonator Antenna Array", International conference on Ubiquitous Information Management and Communication (ICUMIC 2013), 17-19 Jan, 2013.
- 4) A. A. Baba, M. A. Zakariya, Z. Baharudin, M. H. M. Khir, S. M. Ali and J. J. Adz, "Dual Band Aperture Coupled Cylindrical Dielectric Resonator Antenna Array", IEEE Business Engineering and Industrial Applications Colloquium (IEEE BEIAC 2013), 7-9 April, 2013.
- 5) A. A. Baba, M. A. Zakariya, and Z. Baharudin, "Small Size and High Gain Cylindrical Dielectric Resonator Antenna Array", IEEE Conference on Sustainable

Utilization and Development in Engineering and Technology (IEEE CSUDET),
30-31 May, 2013.

Awards

- 1) Gold Medal in 24th International Invention Innovation & Technology Exhibition (ITEX) 2013, “Cylindrical Dielectric Resonator Antenna Array for IEEE 802.11a WiFi applications”, 9-11 May, 2013, Kuala Lumpur Convention Centre, Malaysia.

Research Grants

1) STIRF

STIRF Code Number: 15/2012

Amount: RM 25,000.

Title: “Gain Enhancement of Compact DRA Array Using Dielectric Image Line and Defected Ground Structures (DGS) tuning structure”.

Duration: June 2012 – June 2013.

2) URIF

URIF Code Number: 34 / 2011

Amount: RM 50,000.

Title: “Frequency Tuning For Compact Cylindrical Dielectric Resonator Antenna (CDRA)”.

Duration: June 2011 – June 2012.

APPENDIX A

CODES FOR DETERMINING THE LUMPED ELEMENT CIRCUIT PARAMETERS

The equivalent lumped element circuits of proposed single element CDRA and small size high gain CDRA array are model to verify the antennas feasibility. The Matlab programs of the various equations (2.38) to (2.50) are used to determine the RLC parameters of the equivalent circuits.

The resonant resistance R_r , inductance L_r and capacitance C_r for the dielectric resonators are determine by using equations (2.38) to (2.40). The Matlab program used to calculates the dielectric resonator RLC parameters are given as

$$R_r = (2 \cdot (n^2) \cdot Z \cdot S_{11}) / (1 - S_{11}); \quad \backslash \text{Resonant resistance of DR}$$

$$C_r = \{Q / (w \cdot R_r)\}; \quad \backslash \text{capacitance of DR}$$

$$L_r = \{1 / (C_r \cdot (w^2))\}; \quad \backslash \text{Inductance of DR}$$

The input impedance Z_{slot} of coupling slot is determined by using equation (2.41). The Matlab equation for Z_{slot} is given as

$$Z_{slot} = Z_c \cdot ((2 \cdot R) / (1 - r)) + j Z_c \cdot \cot(B \cdot L_t)$$

The input impedance of microstrip line is determined by using equations (2.42) and (2.43). The Matlab program used to determine the radiation conductance G_{rm} and susceptance of the fringing field capacitance B_m of microstrip line are given as

$$G_{rm} = \{(160 \cdot (\pi \cdot \pi \cdot (h^2))) / ((Z^2) \cdot (\lambda^2) \cdot (E_{cm}))\}; \quad \backslash \text{Radiation conductance of microstrip line.}$$

$$C_l = ((l_{eq} \cdot C \cdot \sqrt{E_{cm}}) / Z);$$

$$B_m = w \cdot C_l; \quad \backslash \text{Susceptance of microstrip line.}$$

The mutual coupling between radiating elements of small size high gain CDRA array are determine by using equations (2.44) to (2.50). The Matlab program for the mutual coupling between the radiating elements is given as

$C_c = C_{air} + C_{fring} + C_{overlapped}$; \ Coupling capacitor

$C_{air} = (E_o/\pi) * \ln\{2*((1 + \sqrt{K}))/ (1 - \sqrt{K})\}$; \ Capacitance between DRAs through the air.

$C_{fring} = K_{av} * \epsilon_o * [(d + at) * \pi * r^2 / (2 * d)]$; \ Capacitance from the edges of the DRs.

$C_{overlapped} = K * \epsilon_o * (A/d)$; \ Capacitance between the DR and ground plane.

APPENDIX B

PROCEDURE TO MEASURE THE ANTENNA RETURN LOSS USING VOLTAGE NETWORK ANALYZER

Introduction

In practice, the most commonly quoted parameter in regards to antennas is return loss S_{11} . Antenna return loss S_{11} represents how much power is reflected from the antenna, and hence is known as the reflection coefficient. If $S_{11} = 0$ dB, then all the power is reflected from the antenna and nothing is radiated. If $S_{11} = -10$ dB, this implies that if 3 dB of power is delivered to the antenna, -7 dB is the reflected power. The remainder of the power was "accepted by" or delivered to the antenna. This accepted power is either radiated or absorbed as losses within the antenna. It is usually expressed as a ratio in decibels (dB). Antenna resonance frequency and bandwidth can be determined from return loss graph.

The procedure follow to measure the return loss using Voltage Network Analyzer (VNA) is given as:

1. Calibrate the VNA for required frequency band (4.0 GHz – 6.0 GHz).
2. Connect the device (designed antenna prototype) using one of the two ports through RF cable (Megaphase TM18-S1S2-40) as shown in the Figure B1.
3. Place the CDRA at the required position on the PCB board.
4. Record the measurements.

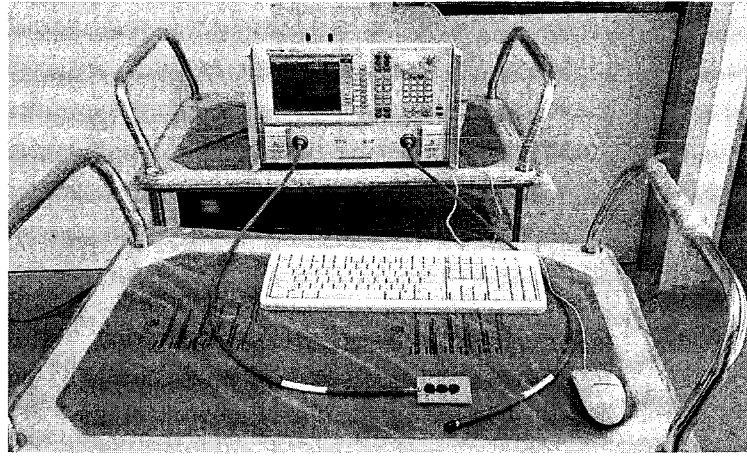


Figure B1. Antenna setup to measure the S_{11} using network analyzer.

5. The example of return loss S_{11} of small size CDRA array presented in section 3.6, measured by using above procedure is depicted in Figure B2. The return loss of -42 dB is achieved through fabricated prototype of small size CDRA array at resonance frequency of 5.0 GHz with a bandwidth of 1.2 GHz. The comparison between the measured and simulated return losses of small size CDRA array is depicted in Figure 4.14.

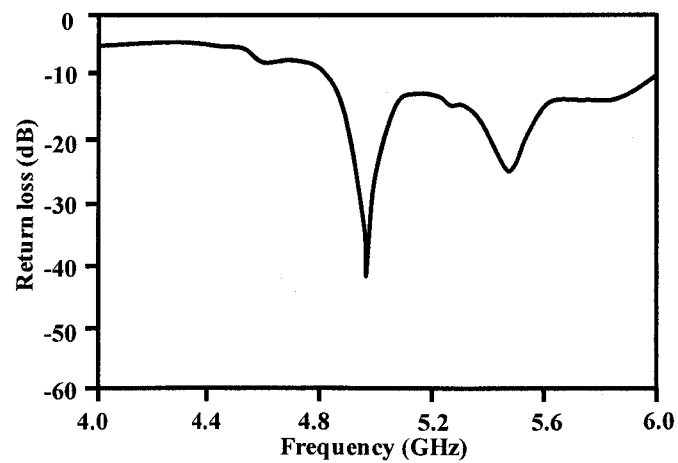


Figure B2. Return loss of small size CDRA array measured by using network analyzer.

APPENDIX C

PROCEDURE TO MEASURE THE ANTENNA GAIN USING GAIN TRANSFER

METHOD

Introduction

Gain is one of the key specifications in antenna datasheets. It is defined as the ratio of the intensity of an antenna (usually in direction of peak radiation) relative to an isotropic antenna. This is the reason why the antenna gain is specified as “**dBi**” in antenna datasheets - “**dB**” refers the ratio or gain and “**i**” signifies relative comparison to an isotropic antenna. An isotropic antenna is a hypothetical antenna that radiates with equal intensity in every direction without any losses.

According to IEEE Standard Test Procedures for antennas, ANSI/IEEE Std 149-1979, gain-transfer method is the most commonly employed method for antenna power-gain measurement.

The gain-transfer method requires 3 antennas - 1 AUT, 1 reference and 1 unknown gain antenna. The AUT or antenna under test is the one which we are interested in finding out the gain (the designed antenna). The reference antenna is the one which the gain (G_{Ref}) is accurately known. It is used as a benchmark. The unknown gain antenna is basically an antenna which we do not need to know the gain exactly, but it must at least have sufficient dynamic range to transmit all the way to the AUT.

S- parameters have earned a prominent position in RF circuit design. S-parameters describe the input-output relationship between ports in an electrical system. Modern network analyzers are well suited for measuring S-parameters. Because the networks being analyzed are often employed by insertion in a transmission medium with common characteristic reference impedance, S-parameters have the advantage that they relate directly to commonly specified performance parameters such as insertion gain and return loss. The gain of AUT is calculated by using insertion loss S_{21} value. The S_{21} represents the power transfer from Port 1 to Port 2.

The procedure follow to measure the antenna gain using Voltage Network Analyzer (VNA) as shown in Figure C1 is given as

1. Mount the “unknown gain antenna” and the reference antenna (antenna with known gain) on two stands.
2. The distance between the two antennas: unknown gain antenna and the reference antenna is represented by R . The equation used to calculate the distance R is given as

$$R = \frac{2D^2}{\lambda} \quad (1C)$$

$$R \gg D$$

where

R is the separation between the antennas.

D is the linear maximum dimension of antenna.

3. Connect the “unknown gain antenna” to port 1 (transmitter) of the network analyser and reference antenna to port 2 (receiver).
-
4. Aligned the antennas to get the maximum gain.
 5. Activate the S_{21} measurement.
 6. Set the frequency range of interest on the network analyzer (4.0 GHz to 6.0 GHz).
 7. Optimize the dynamic range.
 8. Perform response/normalize calibration to produce a flat S_{21} response at 0 dB across the selected frequency range. This means that the gain is now normalized to the reference antenna.

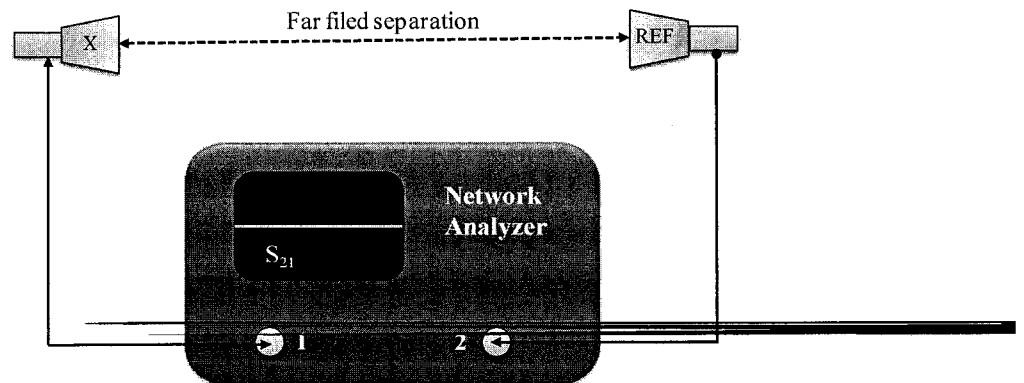


Figure C1: Setup for normalization to a reference antenna

9. Replace the reference antenna with the AUT (the designed antenna) at the exact position and alignment.

10. Record the new S_{21} values. This is the gain/loss $G_{relative}$ of the AUT relative to the reference antenna.
11. The equation used to calculate the gain of AUT, is given as

$$G_{aut} = G_{ref} + G_{relative} \quad (2C)$$

Example of measuring the antenna gain using gain transfer method.

The example of measuring the antenna gain at 5.6 GHz by using steps (1) to (11) of gain transfer method is given below.

Three antennas are required to measure the antenna gain by using gain transfer method. Three antennas used for gain transfer method are: 1 AUT (small size high gain CDRA array presented in section 3.6), 1 reference antenna (microstrip patch antenna with 2 dB gain) and 1 unknown gain antenna (microstrip patch antenna).

The procedure used to measure the antenna gain is given as

1. Mount the “unknown gain antenna” and the reference antenna on two stands as shown in Figure C2.
2. The distance between two antennas is set to be 182.94 mm as shown in Figure C2. The equation 1C is used to calculate the distance between the two antennas as given below

$$R = \frac{2D^2}{\lambda} = 182.94 \text{ mm}$$

Where

D = Maximum dimension of antenna = 70.0 mm

$\lambda = 53.57 \times 10^{-3}$.

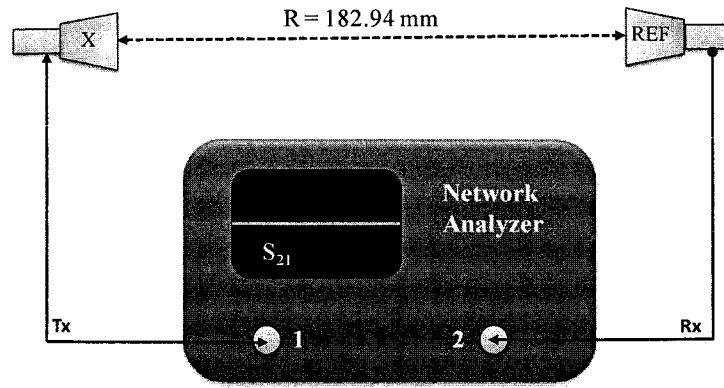


Figure C2. Experimental setup to show distance between unknown and reference antenna.

3. The experiment setup is performed by using steps (3) – (9) of gain transfer method presented in Appendix C.
4. The S_{21} value is recorded and the gain of reference antenna is added to determine the gain of AUT (small size CDRA array). The gain of AUT antenna is calculated by using equation (2C) which is 10.66 dBi.
5. The radiation pattern of small size high gain CDRA array is determined by rotating the AUT antenna (small size CDRA array) 360° with step size of 15° . The gain of antenna at 5.6 GHz for different angles is depicted in Table C1.
6. The radiation pattern of small size CDRA array at 5.6 GHz is found out by plotting the values of Table IC using sigma plot software as depicted in Figure C3.

Table 1C. Gain of small size CDRA array at different angles.

Angle (degree)	Gain (dBi)
0.0	10.6600
15.0	10.8000
30.0	9.8000
45.0	7.5000
60.0	5.1600
75.0	3.0000
90.0	-0.2000
105.0	-4.8800
120.0	-3.0000
135.0	-14.7000
150.0	-6.3500
165.0	-0.7600
180.0	-3.3000
195.0	-3.3000
210.0	-14.7000
225.0	-8.0000
240.0	-6.3500
255.0	-6.6000
270.0	-2.9400
285.0	3.7500
300.0	2.0000
315.0	5.2000
330.0	9.9000
345.0	10.6600
360.0	10.6600

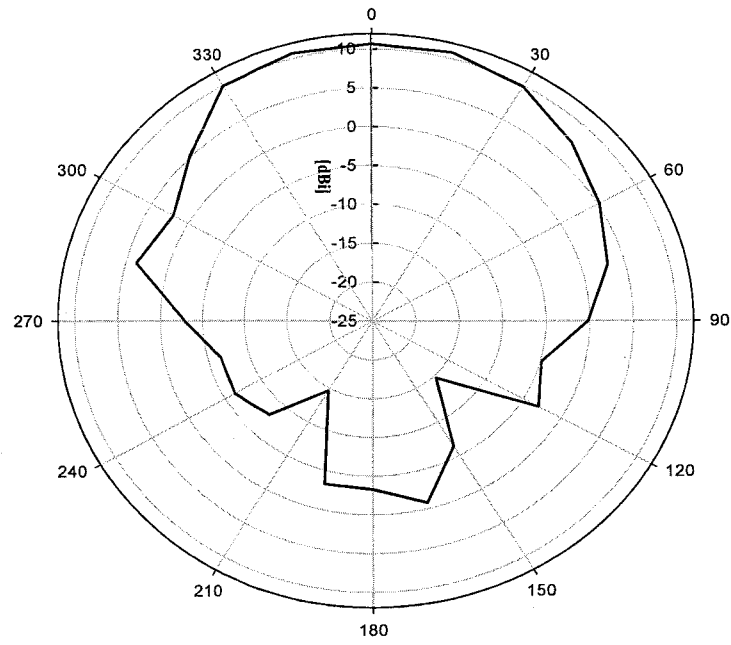


Figure C3. Example of radiation pattern at 5.6 GHz measured by using gain transfer method.

APPENDIX D

OPEN SPACE ANTENNA MEASUREMENTS

Introduction

The antenna is an important element of radio-communication, remote sensing and radio-localisation systems. The measurement of the antenna signal strength characteristics allows one to verify the conformity of the antenna. Antenna measurement techniques refer to the testing of antennas to ensure that the antenna meets specifications or simply to characterize it. The simplest measurement method consists in the direct far-field measurement.

The main objective of open space measurements is to measure the signal strength of the designed antenna and compared with the standard monopole antenna signal strength. The equipment required to measure the antenna signal strength are given below

1. Power system (UPS/ Battery).
2. Field Fox Handheld Microwave Spectrum Analyzer.
3. Signal Generator.
4. Two Antenna Stands
5. Monopole antenna with known gain.
6. Designed antenna.

The procedure follow to measure the antenna signal strength in open space as shown in Figure D1 is given as

1. Mount the “monopole” and the designed antenna on two stands.
2. The distance between the two antennas: monopole and the designed antenna is represented by R . The distance between two antennas is determined by using equation C1.
3. Connect the “monopole antenna” to the signal generator and designed antenna with the spectrum analyzer.
4. Aligned the antennas to get the maximum signals.
5. Set the frequency of interest on the network analyzer (from 5.0 GHz to 6.0 GHz).
6. Note the signal strength from spectrum analyzer at different distance.
7. Replace the designed antenna with monopole antenna and repeat the step 6.

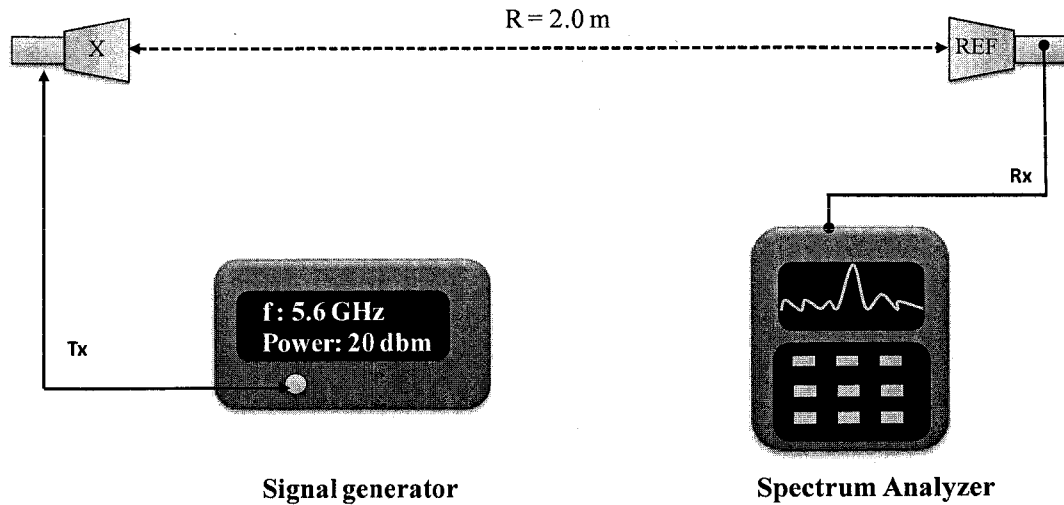


Figure D1. Experimental setup for open space antenna signal strength measurements.

Example of measuring the antenna signal strength in open space

The example of measuring the antenna signal strength at 5.6 GHz is given below.

Three antennas are required to measure the antenna signal strength in open space. Three antennas used for open space measurements are: 2 monopole antennas and one designed antenna.

The procedure used to measure the antenna signal strength is given as

1. Mount the “monopole antenna” and the designed antenna on two stands.
2. The distance between two antennas is set to be 2.0 as shown in Figure D2. The equation 1C is used to calculate the distance between the two antennas as given below

$$R = \frac{2D^2}{\lambda} \approx 0.2 \text{ m}$$

where

D = Maximum dimension of antenna = 70.0 mm

$\lambda = 53.57 \times 10^{-3}$.

where

R is the separation between the antennas.

D is the linear maximum dimension of antenna.

3. Connect the “monopole antenna” to the signal generator and designed antenna with the spectrum analyzer.
4. Aligned the antennas to get the maximum signal strength.
5. Set the frequency of interest on the network analyzer (let's say 5.6 GHz).
6. Note the signal strength from spectrum analyzer at different distance as shown in Table D1.
7. Replace the designed antenna with monopole antenna and repeat step 6.

Table D1. Signal strength of small size CDRA array and monopole antenna at different distances.

Distance (m)	Small size CDRA array signal strength (dBm)	Monopole antenna signal strength (dBm)
2.0	-40.0	-45.0
5.0	-44.0	-55.0
10.0	-49.0	-60.0
15.0	-54.0	-65.0
20.0	-56.0	-68.0
25.0	-59.0	-69.0
30.0	-60.0	-70.0